UVA-mediated iron release in skin cells

Zhong, Li Julia

Award date:
2001

Awarding institution:
University of Bath

UVA-MEDIATED IRON RELEASE IN SKIN CELLS

Submitted by **Li (Julia) Zhong**

for the degree of PhD
of the University of Bath
2001

COPYRIGHT

ProQuest LLC
789 East Eisenhower Parkway
P.O. Box 1346
Ann Arbor, MI 48106-1346

ACKNOWLEDGMENTS

I wish to express my sincere thanks to my supervisors, Prof Rex M Tyrrell and Dr Charareh Pourzand for their tireless supervision and constant encouragement over these years.

I would also like to thank my dear husband Rui Lin Wang for his love and support.

My thanks are extended to all the members of the photobiology group.

The University of Bath is acknowledged for the award of a postgraduate scholarship.

My thanks are also extended to ORS committee.

SUMMARY

The ultraviolet A (UVA) radiation component of sunlight has been shown to be a source of oxidative stress to skin *via* generation of reactive oxygen species. Recently it has been shown that the exposure of human primary foreskin fibroblast cell line, FEK4, to UVA radiation causes immediate release of 'free' iron in the cells *via* proteolytic degradation of ferritin. Since the rapid release of potentially harmful 'free' iron to the cytosol could be a major factor in UVA-induced damage to the skin, this phenomenon was investigated in more detail in both cultured human skin fibroblasts and keratinocytes following single or repeated exposure to UVA radiation at natural exposure levels. The results demonstrated that immediately following single or repeated UVA irradiation of both fibroblast and keratinocyte cells, the intracellular labile iron pool (LIP) concentration increases in a dose-dependent manner. The level of LIP returns to basal level only 6 h after a single irradiation and does not change further for the next 48 h. Furthermore, the basal and UVA-induced level of LIP was 2-4 fold higher in fibroblasts when compared to keratinocytes. The low level of LIP in keratinocytes is likely to be an important factor for their higher resistance to UVA-induced membrane damage. Indeed, it appears that there is a direct relationship between the basal level of LIP in cells and the extent of UVA-induced LIP release and lysosomal and plasma membrane damage. Overall these findings indicate that UVA-mediated immediate release of LIP plays a key role in the increased susceptibility of cells to UVA-induced damage.

CONTENTS

page

1. Introduction 1

1.1 Ultraviolet (UV)-General introduction 1

1.2 Oxidative stress and reactive oxygen species (ROS) 3

1.3 Human skin 4

1.4 Cellular defence against UVA 8

1.4.1 Non-enzymatic defence 8

1.4.2 Enzymatic defence 13

1.4.3 The inducible defence pathway in FEK4 cells 17

1.5 Iron 19

1.5.1 General introduction 19

1.5.2 Ferritin 23

1.5.3 Iron Homeostasis 25

1.5.4 New genes in iron metabolism 28

1.5.5 Labile iron pool (LIP) 31

1.5.6 Determination of LIP 33

1.6 UVB 37

1.7 UVA 39

1.7.1 General introduction 39

1.7.2 UVA-induced oxidative stress 40

1.7.3 UVA-induced DNA damage and skin cancer 44

1.7.4 UVA activation of genes in skin cells 45

1.7.5 UVA-induced lipid peroxidation and membrane damage 47

1.7.6 UVA and FEK4 fibroblasts 51

1.8 Objectives of the study 54

2. Materials and Methods 55

2.1 Chemicals 55

2.2 Cell culture 56

2.3 Treatments 58

2.3.1 Chemical treatments 58
2.3.2 UVA irradiation 60
2.4 Fluorescence Calcein assay and LIP calibration 63
2.4.1 Calcein (CA) assay 63
2.4.2 LIP calibration 69
2.5 Ferritin ELISA 85
2.6 Epifluorescence microscopy studies 87
2.7 Cathepsin B ELISA 88
2.8 Cathepsin B immunohistochemistry 91
2.9 LDH assay 92
2.10 Survival assay 93
2.11 Neutral red assay 94
2.12 Explanations of the experimental design and symbols 95

3. Results 101
3.1 Characterisation of LIP release in human skin cells following single or repeated exposures to UVA irradiation 101
3.1.1 Fibroblasts 102
3.1.2 Keratinocytes 111
3.1.3 Range of other cell types 119
3.2 The role of ROS on the UVA-mediated LIP release in FEK4 cells 123
3.2.1 Hydrogen peroxide 123
3.2.2 Singlet oxygen ($^1O_2$) 123
3.2.3 Antioxidant vitamin E 124
3.3 The role of ferritin on UVA-mediated LIP release in skin cells 126
3.3.1 Comparison of the basal level of ferritin in fibroblasts and keratinocytes 127
3.3.2 Modulation of ferritin levels in FEK4 and HaCaT cells 128
3.3.3 Effect of iron loading on UVA-mediated LIP release in FEK4 cells 130
3.3.4 Effect of protease inhibitors on UVA-mediated LIP release in FEK4 cells 131
3.4 The correlation between the level of UVA-induced iron release and the extent of lysosomal membrane damage 133
3.4.1 Epifluorescence microscope studies 133
3.4.2 Cathepsin B ELISA 141

3.4.3 Cathepsin B immunocytochemistry 146
3.4.4 Neutral red assay 149
3.5 The correlation between the level of UVA-induced iron release and the extent of plasma membrane damage in FEK4 and HaCaT cells 151
3.6 Determination of colony-forming ability of skin cells 157

4. Discussion 159
4.1 The significance of UVA-mediated LIP release in skin cells 159
4.2 The source of UVA-induced iron release in skin cells 162
4.3 The origin of UVA-induced iron release in skin cells 164
4.4 The link between intracellular LIP and the susceptibility of skin cells to the UVA-mediated oxidative damage 166

5. Future projects 169

6. References 170

ABBREVIATION

AA	Arachidonic acid
Ac	Aconitase
ATP	Adenosine 5'-triphosphate
ATZ	3-amino-1, 2, 4-triazole
BHT	Butylated hydroxytoluene
BIP	2, 2'-bipyridyl
BSA	Bovine serum albumin
BSO	DL-buthionine-[S,R]-sulfoximine
CA	Calcein
CA-AM	Calcein-acetoxymethyl ester
CA-assay	Fluorescence calcein assay
CA-Fe	Calcein bound iron
CO	Carbon monoxide
CSF	Colony-stimulating factors
Cu-Zn-SOD	Copper-zinc superoxide dismutase
DFO	Desferrioxamine or desferrioxamine mesylate or Desferal
DMSO	Dimethyl sulphoxide
D_2O	Deuterium oxide
DTPA	Diethylenetriamine pentaacetic acid
EDTA	Ethylenediaminetetracetic acid
ELISA	Enzyme-linked immunosorbent assay
EMEM	Earle's modified minimal essential medium
EthD-1	Ethidium homodimer-1
FAS	Ferrous ammonium sulphate
FCS	Foetal calf serum
Fe^{2+}	Ferrous iron
Fe^{3+}	Ferric iron
FITC	Fluorescein Isothiocyanate
GPX	Glutathione peroxidase
GSH	(reduced) glutathione
GSSG	Glutathione disulphide (oxidised glutathione)
GR	Glutathione reductase
Hepes	N-[2-hydroxyethyl]piperazine-N'-[2-ethanessulphonic acid]
HO1/2	Heme oxygenase1/2
H_2O_2	Hydrogen peroxide
ICAM-1	Intercellular adhesion molecule –1
IL	Interleukin
kDa	Kilo Dalton
kJ/m^2	KiloJoules per meter square
IRE	Iron response element
IRP	Iron-regulatory protein
LDH	Lactate dehydrogenase
LIP	Labile iron pool
$LO^{\bullet}$ or $RO^{\bullet}$	(Lipid) alkoxyl radical
$LOO^{\bullet}$ or $ROO^{\bullet}$	(Lipid) peroxyl radical
LOOH or ROOH	(Lipid) hydroperoxide

LMW-Fe	Low molecular weight iron
MAPK	Mitogen-activated protein kinases
MDA	Malondialdehyde
MMP1	Matrix metalloprotenase-1
Mn-SOD	Manganese–superoxide dismutase
mRNA	Messenger RNA
MTT	3-(4,5-dimethylthiazol-2-ye)-2,5-diphenyltetrazolium bromide
NAC	N-acetyl cysteine
NADH	Nicotine adenine dinucleotide
NADP	Nicotine adeninedinucleotide phosphate
NO	Nitric oxide
NP-40	(octylphenoxy)-polyethoxyethanol or Nonidet P-40
8-oxo-dG	7,8-dihydro-8-oxo-2'-deoxyguanosine
$^1O_2$	Singlet oxygen
$O_2^{\bullet-}$	Superoxide anion
$OH^{\bullet}$	Hydroxyl radical
PPIX	Protoporphyrin IX
PBS	Phosphate buffered saline
PUFA	Polyunsaturated fatty acid
ROS	Reactive oxygen species
RT	Room temperature
SFM	Serum free medium
SIH	Salicylaldehyde isonicotinoyl hydrazone
SOD	Superoxide dismutase
TBARs	Thiobarbituric acid reactive species
Tf	Transferrin
TGF	Transforming growth factors
TfR	Transferrin receptor
TNFα	Tumor necrosis factor alpha
Tris	Tris[hydroxymethyl]-aminomethane
UVA(B)	Ultraviolet A(B)
UTR	Untranslated region
W/V	Weight per volume
α-Toco	α-Tocopherol succinate

1. Introduction

1.1 Ultraviolet (UV)-General introduction

The electromagnetic spectrum includes wavelengths that range from very short (10^{-15} m), high energetic to longer (10^{3} m), less energetic radiowaves. Ultraviolet (UV) is a part of non-ionising electromagnetic radiation, including wavelengths from 10 nm to 400 nm. Exposure to UV occurs from both natural and artificial sources. The sun is the major source of UV radiation. The sun emits radiation extending from infrared (760-3000 nm), visible (400-760 nm) to UVA band (320-400 nm, near-UV) through UVB (290-320 nm, mid-UV) down to the high energy UVC band (190-290 nm) and vacuum UV (10-190 nm). UV undergoes absorption and scattering as it passes through the Earth's atmosphere with absorption by ozone, molecular oxygen and other molecules. Variation in UV intensity reaching the Earth depends on solar zenith angle, atmospheric ozone, cloudiness and aerosol load etc. Due to the absorption of the wavelengths below 310 nm by ozone, only infrared, visible, UVA and a part of UVB can reach the Earth's surface. Therefore the effects of solar UV radiation on biological systems concern only UVA and UVB wavebands. Only UVA will be investigated in this thesis. UVA comprises the major part (90%) of solar UV at noon (Pathak et al., 1997). It can be further divided into the UVA-II (320-340 nm) and UVA-I (340-400 nm) regions. UVA-II and UVB radiations have similar effects. Classification of the solar spectrum reaching the Earth's surface is shown in the Table 1.1.

Table 1.1 Classification of the solar spectrums that reach the Earth's surface

Type	UVB	UVA	Visible	Infrared
Wavelength/nm	290-320	320-400	400-760	760-3000

UV radiation must be absorbed by biomolecules to produce damage. The interaction of UV with biological material changes as a function of wavelength. At short wavelengths, the UVB region overlaps with the tail of DNA absorption so that direct absorption by molecules such as nucleic acid (e. g. DNA) dominates. At longer wavelengths including the UVA region, different chromophores absorb and this can lead to oxidative stress. Hence, organisms on the Earth's surface have to be well adapted, e.g. by forming UV-absorbing surface layers (skin or fur), by antioxidant defences to quench UV-generated reactive oxygen species (ROS) or by efficiently repairing damaged DNA (reviewed by de Grujil, 2000).

In recent decades, there has been a substantial decrease in the ozone layer and a consequence is that the earth is exposed to more UV radiation. Furthermore life styles have been changed leading to increased personal sunlight exposure: e. g. changes such as holidays in the sun, cosmetic tanning, minimal clothing outdoors, insufficient use of sunscreens and photo therapy used for medical reasons.

In humans, the major targets for UV are the skin and the eyes and it is important to emphasise that the transmission of UV through these tissues and cells increases with increase in wavelength, so that longer wavelengths penetrate much deeper and can cause effects on targets which differ from those of short wavelengths. Both acute and chronic exposure to sunlight are associated with various physiological and pathological states. The acute response involves immediate effects including erythema, heat, swelling, sunburn, pigmentation, hyperplasia, immune suppression and vitamin D synthesis (Gasparro et al., 1998). The chronic response involves delayed effects such as cataract and skin ageing (also called photo-ageing), which is the result of morphological

changes such as wrinkling, elasticity loss, uneven pigmentation due to general alteration of all the epidermal and dermal components of skin. Chronic exposure of skin to UV radiation may lead to skin cancer (reviewed by Tyrrell, 1994).

1.2 Oxidative stress and reactive oxygen species (ROS)

Oxygen is the most abundant element in the Earth's crust. All animals and plants require oxygen for the efficient production of energy, except those organisms that are especially adapted to live under anaerobic conditions. Although oxygen is essential to life, it can give rise to a variety of ROS as a part of normal metabolism.

The term "oxidative stress" describes a situation in cells in which the equilibrium between prooxidant and antioxidant species is broken in favour of prooxidant state, due to ROS. Toxicities and pathologies associated with the oxidation of nucleic acids, proteins, lipids and carbohydrates have been collectively termed 'oxidative stress'. ROS, referred to as oxidative stress, can be generated both exogenously (e. g. xenobiotics, pesticides, ozone, photochemical smog, ultraviolet light, ionising radiation) and endogenously (e. g. mitochondrial respiration, microsomal and nuclear membrane electron transfer and phagocytic oxidative burst).

ROS is a collective term that includes not only oxygen-based radicals (see below) but also non-radical derivatives of oxygen such as singlet oxygen ($^1O_2$) and hydrogen peroxide (H_2O_2), which are capable of forming radicals. ROS have been implicated in inflammation, ageing, some diseases (including cancer), drug action, drug toxicity and recently apoptosis.

Free radicals are species capable of independent existence and contain one or more unpaired electrons in an orbital in the outermost electron shell. They are able to take an electron from or donate an unpaired electron to another molecule. Free radicals are very active intermediates and are potentially powerful damaging agents *in vivo*. Organic free radical species are numerous, but oxygen-based free radicals that occur in biological systems are limited. Here, discussion will be restricted to oxygen-based free radicals included superoxide anion ($O_2^{\bullet-}$), hydroxyl radical ($OH^{\bullet}$), peroxyl radical ($ROO^{\bullet}$) and alkoxyl radical ($RO^{\bullet}$), which can oxidise protein, lipid and carbohydrate. The primary target of free radicals is the lipid bilayer of the membrane. Free radicals may be involved in the initiation and propagation of free radical chain reactions which potentially damage cells (Riley, 1994). Free radicals can kill bacteria, damage biomolecules, modify genomic and cellular structures, provoke immune responses, activate oncogenes, cause artherogenesis and enhance the ageing process.

UVA radiation generates ROS in cultured skin cells (see section **1.7**). Free radicals are generated in skin exposed to UVA (Black, 1987; Trenam et al., 1992; Yasui et al., 2000). Uncontrolled production of ROS leads to damage to biomolecules and may cause diseases because ROS have been implicated in many inflammatory skin disorders (Trenam et al., 1992).

1.3 Human skin

Skin, the largest organ of the body, keeps internal systems intact. It is not only a barrier to protect the body from chemical and physical (e. g. ultraviolet light) agents and micro organisms, but is also involved in defence mechanisms and other important functions. The skin thickness varies according to the site of the human body, but the average is

0.3-0.4 mm. The skin composes two layers - the upper epidermis and inner dermis (see **Fig. 1A** and **1B**). The epidermis is beginning at the outer surface and working inwards. There are four clear layers that can be observed in the epidermis under a light microscope. They are defined as:

1) Cornified layer - stratum corneum

2) Granular layer – the zone where epidermal nuclei disintegrate

3) Germinative or prickle cell layer- the bulk of the living epidermal keratinocytes

4) Basal layer- the only keratinocytes in normal epidermis that undergo cell division

The epidermis is mainly composed of keratinocytes with some Langerhans cells and melanocytes. Keratinocytes produce the protein keratin (which provides a strength and flexibility to the epidermis) and a low level of a wide range of cytokines so that keratinocytes can influence immunologic function. These cytokines include interleukins (ILs), chemokines, tumour necrosis factors (TNF), colony-stimulating factors (CSF), transforming growth factors and growth factors. Keratinocytes in the basal layer divide (on average every 4 weeks) and the daughter cells undergo changes as they move upward to the skin surface. At the final stage, these cells lose their nuclei and then die, dehydrate and flatten out to form a cornified external layer (stratum corneum). Dead cells are constantly being shed, while new cells are continuously being produced in the basal layer. Langerhans cells are antigen-presenting cells and play a major role in the immune surveillance system of the skin. Melanocytes synthesise melanin, which matures into melanosomes and are delivered to the keratinocytes in the outermost layer of the epidermis. They are uniformly distributed to form an UV-absorbing barrier, which reduces the amount of radiation that can penetrate the skin.

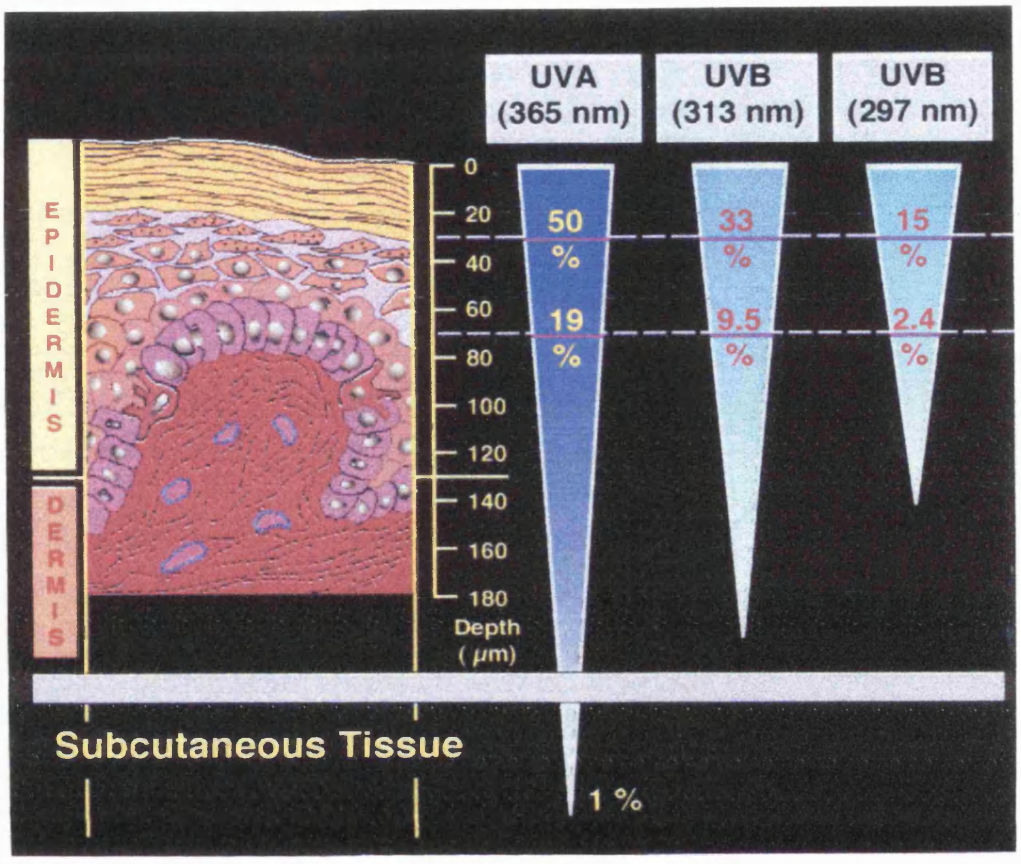

Fig. 1A Penetration of solar UV radiation into the skin (reproduced with the permission of Prof. Rex Tyrrell)

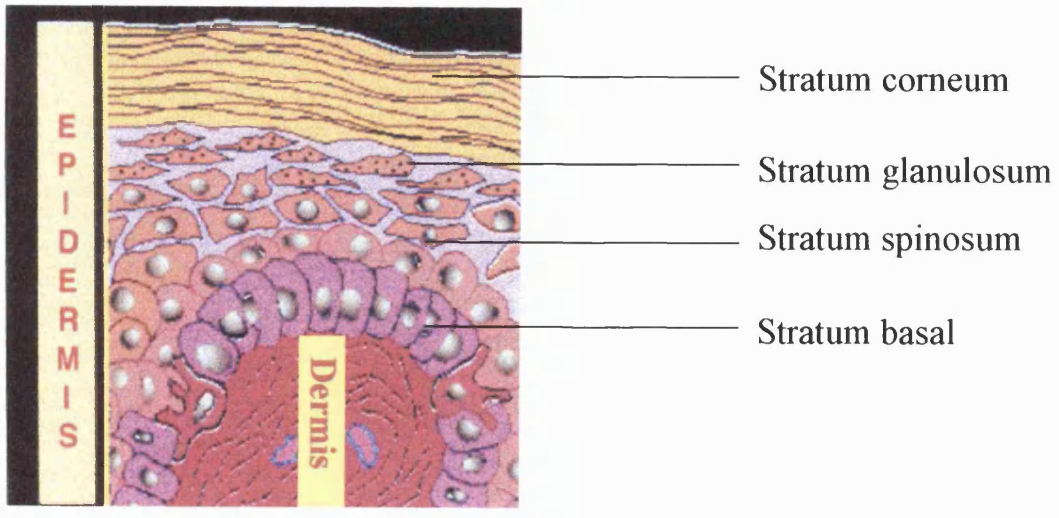

Fig. 1B Epidermis

The dermis is a connective tissue matrix that is between the epidermis and the subcutaneous layer. The upper dermis contains capillaries to nourish the epidermis. The lower thicker layer is reticular dermis. Fibroblasts are the major cells in the dermis. They synthesise collagen, elastin and glycosaminoglycans (GAG). Collagen fibres provide strength and resilience while elastin fibres provide elasticity to the skin. GAG provides viscosity, hydration and allows the dermis limited movement. Other cells embedded in the reticular layer including fat cells and dermal dendrocytes, mast cells, macrophages and lymphocytes as well as many blood and lymphatic vessels, nerves and nerves endings, oil glands and hair roots.

The solar energy reaching the skin is quite different for the epidermis and dermis so that damage to epidermal and dermal cells is very different. The epidermis is the primary target for oxidative stress generated not only by solar radiation, but also by other physical and chemical agents in the environment. When the two major skin cells, the epidermal keratinocytes and the dermal fibroblasts are exposed to UVA radiation, they receive different amounts of radiation. The epidermal keratinocytes are exposed to both UVA and UVB radiation while the dermal fibroblasts are shielded from UV radiation to a considerable extent by the overlying epidermis and will be mostly received by UVA radiation. A major part of UVA can penetrate quite deeply into the skin. Indeed, 35-50% of UVA radiation may reach the dermis of Caucasian skin (Bruls et al., 1984. see **Fig. 1A**). A small amount of UVA radiation can reach below the surface of the skin and penetrate blood vessels.

1.4 Cellular defence against UVA

The epidermal keratinocytes and underlying fibroblasts are protected to some extent by the stratum corneum, a physical absorption barrier. It reflects, scatters and absorbs incident UV radiation. Melanin can act as an additional defence of the epidermis. It provides some physical protection and attenuates UV radiation by scattering and dissipation of absorbed energy. Since most cellular components are susceptible to potentially deleterious oxidation, the cellular antioxidant systems are crucial to the prevention or removal of the damage caused by the oxidising component of UV radiation. Cellular antioxidant defence mechanisms include non-enzymatic and enzymatic systems, which sometimes act in synergy. DNA repair and inducible protection pathways also contribute to cellular defence.

1.4.1 Non-enzymatic defence-antioxidant molecules

Glutathione (GSH): GSH is an endogenous tripeptide (γ-glutamyl-cysteinyl-glycine) that is the most abundant thiol found in most tissues. The ubiquitous non-protein free thiol is present at high concentration (3-5 mM) in most the cell types and therefore is considered as a major constitutive component in the maintenance of cellular reducing equivalents (reviewed by Tyrrell, 1991). It is an effective reductant, and a powerful radical scavenger. GSH reacts with LOOH or quenches ROS (such as H_2O_2, $O_2^{\bullet -}$ and $OH^{\bullet}$) by hydrogen atom donation resulting in the formation of GSH disulphide (GSSG or oxidised glutathione).

$$LOOH + 2GSH \xrightarrow{GPX} LOH + GSSG + H_2O$$

$$2GSH + H_2O_2 \xrightarrow{GPX} GSSG + 2H_2O$$

So GSH acts as a radical scavenger itself and also as a cofactor (hydrogen donor) for protective enzymes such as GSH peroxidase (GPX), GSH transferases, trans-hydrogenases and also for several other antioxidants such as ascorbate, which in turn regenerate α-tocopherol (reviewed by Tyrrell, 1994). GSSG is reduced to GSH by glutathione reductase (GR) in the presence of NADPH as the hydrogen donor.

$$GSSG + H^+ + NADPH \xrightarrow{GR} 2\,GSH + NADP^+$$

The populations of cultured human skin fibroblasts or epidermal keratinocytes that have been depleted of GSH by treatment with low concentration of BSO (buthionine sulfoximine: a specific inhibitor of γ-glutamyl-cystein synthesis) are strongly sensitised to the lethal action of both UVA and UVB radiation and visible light, so GSH provides a major line of defence against the cytotoxic effects of both UVA and UVB radiation (Tyrrell and Pidoux, 1986 and 1988).

Pre-mutagenic damage induced by UVA radiation in human lymphoblastoid cell (TK6) is lower in the presence of GSH when compared with cells depleted of GSH (Applegate et al., 1992). GSH has also been shown to protect calf thymus DNA and Chinese hamster ovary cell (CHO) against 7,8-dihydro-8-oxo-2'deoxyguanosine (8-oxo-dG) formation after UVA exposure (Fischer-Neilsen et al., 1992 and 1993). UVA radiation

decreased GSH and GSH depletion strongly enhanced both basal levels and UVA/peroxide enhanced expression of (and threshold of UVA-induced) HO-1. It may lead to enhance gene expression either as a result of the potential accumulation of ROS or as a result of the direct influence of GSH on a critical target involved in signal transduction (Lautier et al., 1992). GSH depletion by BSO in HaCaT cells also leads to enhance UVA-induced damage (Tobi et al., 2000). Experiments with murine skin have demonstrated that glutathione levels in both dermis and epidermis are depleted by UVA or UVA plus UVB treatment (Connor and Wheeler, 1987; Shindo et al., 1993).

Vitamin E: Vitamin E refers to at least eight isomers of tocopherol. Among these, α-tocopherol (TOC-OH) is the best-known isomer and possesses the most potent antioxidant activity. High levels of tocopherol are found in selected mammalian tissues. It is a major lipophilic antioxidant, which acts as a scavenger and chain breaking antioxidant during lipid peroxidation by donating labile hydrogen to terminate propagating $LO^{\bullet}$ and $LOO^{\bullet}$ groups and other radicals $O_2^{\bullet-}$, $OH^{\bullet}$, in turn producing α-tocopheryl radical (TOC-$O^{\bullet}$) which is insufficiently reactive to abstract hydrogen atoms. This process can be written as:

$$\mathbf{LOO^{\bullet} + TCO\text{-}OH \longrightarrow LOOH + TOC\text{-}O^{\bullet}}$$

α-tocopherol has been shown to be a physical quencher and chemical scavenger of $^1O_2$, with the irreversible oxidation of α-tocopherol to its α-tocopheryl quinone (reviewed by Fryer, 1993). Tocopherol can be regenerated by reduction of the tocopheryl radical by GSH or vitamin C (ascorbic acid) (Niki et al., 1987). Vitamin C and vitamin E (α-

tocopherol) have complementary roles in preventing lipid peroxidation induced by oxidative stress (reviewed by Tyrrell, 1994).

There are reports that α-tocopherol protects against UVA-induced lipid peroxidation in cultured human fibroblasts (Morliere et al., 1991; Gaboriau et al., 1993; Coulomb et al., 1996; Clement-Lacroix et al., 1996; Skoog et al., 1997) and keratinocytes (Djavaheri-Megny et al., 1996). The main *in vivo* function of α-tocopherol is to prevent lipid peroxidation. There is evidence that vitamin E, at least when applied topically to skin, is able to protect particularly against ozone-mediated lipid peroxidation (Thiele, 1997). UVA-induced cytotoxicity could be inhibited in the case of fibroblasts derived from the patient with photosensitive disease using the water-soluble vitamin E analogy, Trolox C (Kralli and Moss, 1987).

Vitamin C (ascorbate): Vitamin C is a hydrophilic antioxidant and reacts with a wide range of ROS (Halliwell and Gutteridge, 1999). It is able to quench $^1O_2$ (Chou and Khan, 1983), which could be an important mode of protection of biological systems where $^1O_2$ is generated in aqueous-phase. In addition, it has a strong reduction potential and therefore has the ability to restore the antioxidant properties of α-tocopherol (Niki et al., 1987; Njus and Kelley, 1991). Such a reduction can be expressed as follows:

$$\mathbf{TOC\text{-}O^{\bullet} + AH^{-} \longrightarrow TOC\text{-}OH + A^{\bullet -}}$$

AH^- is the ascorbate anion and $A^{\bullet -}$ is its product. Vitamin C therefore may prevent oxidative damage in skin by acting synergistically with vitamin E. Tebbe and co-workers in 1997 found that vitamin C inhibited UVA-induced lipid peroxidation in cultured human keratinocytes. A dietary antioxidant mixture (vitamin E, vitamin C and

glutathione) clearly reduced the UVB-induced tumour multiplicity and increased the tumour latent period in mouse studies (Black et al., 1985). Using vitamin C topically also protected porcine skin from ultraviolet radiation-induced damage (Darr et al., 1992). Vitamin C was reported to increase ferritin mRNA translation in cultured cells in response to iron (Toth et al., 1995), which may increase storage of harmful iron inside cells. However, ascorbate (> 1mM) may also act as a prooxidant since it can efficiently reduce Fe^{3+} to Fe^{2+}, marking it available for Fenton-type reactions. For example, ascorbate stimulates iron-dependent peroxidation of membrane lipids in cultured skin fibroblasts (Basu-Modak et al., 1996) and release iron from ferritin thus induced DNA damage in neuroblastoma cells (Badder et al., 1994).

Carotenoids: Carotenoids such as vitamin A can protect against photosensitised reactions in several ways including quenching $^1O_2$ (Krinsky et al., 1982). β-carotene itself is a precursor of vitamin A and is a member of the carotenoid family of antioxidants. β-carotene has been shown to inhibit UV-induced epidermal damage and tumour formation in mouse models (Mathews-Roth and Krinsky, 1987). In humans, high doses of β-carotene are effective in certain photosensitivity diseases (Epstein, 1977; Mathews-Roth et al., 1982). However, there is still a controversy about β-carotene as a photoprotectant. It may be reasonable to suggest that β-carotene itself is limited in its protection unless it co-operates with other antioxidants.

1.4.2 Enzymatic defence-antioxidant enzymes

The enzymatic system of the skin functions by catalysing the decomposition of oxidants and free radicals into less reactive species. The major antioxidant enzymes are catalase (which destroys H_2O_2), superoxide dismutase (SOD, which converts $O_2^{\bullet -}$ to H_2O_2), GPX and associated enzymes (which in addition to metabolising H_2O_2, also reduce LOOH such as those that result from lipid peroxidation).

Glutathione peroxidase (GPX) is a selenium dependent enzyme, located in the cytosol and mitochondrial matrix. It acts on H_2O_2 and lipid peroxides by coupling the reduction of these compounds with the oxidation of GSH, forming water and an alcohol respectively (see **1.4.1**). This is important because the central role of glutathione in protection of cells against damage by UVA radiation (Tyrrell and Pidoux, 1986 and 1988; Lautier et al., 1992). Selenium deficient cultured human fibroblasts were found to have a lower GPX activity and were sensitive to UVA and H_2O_2 cytotoxicity and lipid peroxidation (Moysan et al., 1993 and 1996; Bertling et al., 1996). Selenium supplementation increased GPX and decreased UVA-induced lipid peroxidation in human skin fibroblasts (Leccia et al., 1993). Emonet (1997) also found that thiols and selenium protected human skin fibroblasts against UVA-induced toxicity. Recently, it has been shown that single or repetitive low dose UVA radiation (200 kJ/m^2) to human skin fibroblasts led to a substantial up-regulation of GPX activity, which protects cells against subsequent challenge with high dose of UVA radiation (Meewes et al., 2001). Previously, the same group reported that Mn-SOD was induced by UVA radiation (Poswig et al., 1999). The adaptive responsive involving GPX protection clearly depended on the irradiation interval and a sufficient selenium concentration. Normally

no changes or only a slight decrease in GPX activity has been observed upon UVA radiation in fibroblasts (Shindo et al., 1997; Moysan et al., 1993)

Catalase: Catalase locates in peroxisomes. The catalase (a heme protein) is an enzyme that primarily scavenges H_2O_2 (another is GPX). Unlike other peroxidases, catalase catalyses the direct decomposition of H_2O_2 to ground state oxygen and water without the use of another substrate as GPX does. In cultured human fibroblasts and keratinocytes, catalase activity is strongly reduced after UVA exposure (Punnonen et al., 1991; Moysan et al., 1993; Tirache et al., 1995; Shindo et al., 1997). This is probably due to oxidative damage to the enzyme (Giordani et al., 1997). Comparing the protection of GSH against UVA, catalase is less important because catalase deficient (cells treated with amino-triazole, a catalase inhibitor) fibroblasts did not show decreased survival after UVA radiation (Tyrrell and Pidoux, 1989; Peak et al., 1990a), although they were more sensitive to H_2O_2 induced cytotoxcity. On the contrary, Bertling in 1996 found that H_2O_2 played a major role in broad-spectrum (310-400 nm) cytotoxicity of selenium deficient murine cells. Although catalase may not be a major protective enzyme of fibroblasts following UVA radiation, it may reduce the damage of other antioxidant enzymes (GPX and SOD) (Tirache et al., 1995).

Superoxide dismutases (SODs): SODs include Cu/Zn-SOD, Mn-SOD and Cu-SOD, located in cytosol, mitochondria and plasma membranes, respectively. They catalyse the reduction of $O_2^{\bullet -}$ to less reactive H_2O_2. The trace element zinc (Zn) is thought to maintain the configuration of SOD whereas Cu is involved in the catalytic activity for Cu/Zn SOD. Zn, like selenium (Se), when added to cultured human skin fibroblasts, resulted in a reduction in UVA-induced lipid peroxidation and an increase in cell

survival, but no increase in Zn-SOD activity (Leccia et al., 1993). Richard in 1993 observed the same phenomenon and also found that the Zn protection was not mediated by antioxidant activity. Similarly, the addition of manganese (Mn, the metal in the active site of Mn-SOD) into cultured human fibroblasts protected these cells from oxidative injury by UVA radiation but this was not accompanied by an increase in Mn-SOD activity (Parat et al., 1995). Zn supplementation can protect against both DNA strand breakage and apoptosis in human skin fibroblasts (Leccia et al., 1999). It was found that SOD activity was decreased by solar simulated UV radiation in human skin fibroblasts (Shindo et al., 1997) and human skin keratinocytes (Punnonen et al., 1991). However, inactivation of this enzyme was considered to occur indirectly by ROS rather than directly as has been found with catalase (Shindo et al., 1997).

Recently, cultured fibroblasts repetitively exposed to UVA radiation (200 kJ/m^2 per day for three days) actually developed an adaptive response marked by an increase in Mn-SOD mRNA levels and Mn-SOD activity after the third exposure (Poswig et al., 1999). Since SOD dismutates $O_2^{\bullet -}$ to H_2O_2, the increase in SOD activity is accompanied with an increase in catalase and/or GPX (Amstad et al., 1991; Yohn et al., 1991) to prevent H_2O_2 toxicity. Studying SOD and catalase content of human fibroblasts from different normal cell lines and the efficiency of lipid peroxidation after UVA radiation, it was found that the extent of lipid peroxidation was correlated with the ratio of SOD to catalase. Furthermore when this ratio increased, by increasing SOD or decreasing catalase before UVA radiation, the peroxidation of lipid increased (Leccia et al., 1993). If SOD activity exceeded that of H_2O_2 scavenger, accumulation of H_2O_2 by SOD could lead to toxicity.

It was shown that both enzymatic (catalase, GR, SOD, GPX, HO-2) and non-enzymatic (GSH, vitamin E and ascorbate) antioxidant capacities of the epidermis are higher than those of the dermis, when measured *in vivo* in mouse and human skin and *in vitro* in fibroblasts and keratinocytes (Shindo et al., 1993 and 1994; Applegate et al., 1995).

Immediately after UV radiation (UVB and UVA), some of the enzymatic and non-enzymatic antioxidant of the mouse and human skin or cultured cells decreased (Fuchs et al., 1989; Shindo et al., 1993 and 1997; Lautier et al., 1992), especially catalase (Moysan et al., 1993). However, there is still no clear relationship established between higher antioxidant level and cellular resistance to UVA radiation.

Thioredoxin/thioredoxin reductase: Thioredoxin/thioredoxin reductase may also play a role in the defence of skin against oxidative stress including UV radiation. Thioredoxin is a small protein that, in its reduced form, has a protein disulfide reductase activity as a consequence of its two reactive thiol groups. The protein reacts with free radicals in human keratinocytes *in vivo* (Schallreuter and Wood, 1986).

Repair processes, such as excision of damaged DNA bases, can prevent the effects of UVA-mediated oxidative processes. DNA enzymes responsible for excision, repair of the damaged DNA strand, all aid in reducing the carcinogenic action of UV radiation (de Laat et al., 1996). If this antioxidant defence is not enough, cells can no longer divide and will die (either by apoptosis or necrosis) or may be left with apparently mutagenic /carcinogenic persistent lesions (reviewed by Tyrrell, 1994).

1.4.3 The inducible defence pathway in FEK4 cells-The role of HO in UVA-mediated oxidative stress

Heme oxygenase (HO) catalyses the initial steps of heme degradation in eukaryotic cells, leading mainly to the formation of biliverdin (biliverdin is reduced to bilirubin by biliverdin reductase) and carbon monoxide (CO), with the release of iron. Three isoforms of HO have been identified in mammalian cells: HO-1, HO-2, HO-3. They are the products of separate genes. HO-1 is widely distributed in tissues (highest in livers and spleens) and highly inducible in virtually all cells. HO-2 is expressed constitutively but is unresponsive to any of the inducers of HO-1. HO-2 levels are the highest in the brain and testes of mammals. HO-3 is nearly devoid of catalytic activity and may act mainly as a heme-sensing or heme-binding protein or both (Elbirt and Bonkovsky, 1999).

HO-1 gene expression is inducible both *in vivo* and *in vitro* by numerous chemicals and oxidative stress including UVA (Keyse et al., 1989 and 1990; Applegate et al., 1991). It was found that the induction of expression of the HO-1 occurs at the transcriptional level. The induction of HO-1 is a general response to oxidative stress in cells cultured from a variety of human tissue and mammalian species. Induction of HO-1 leads to a reduction in the cellular pool of heme and heme-containing proteins and thereby removes potential pro-oxidant catalysts. The liberated iron acts as an inducer of ferritin (Vile et al., 1994). *In vivo* and *in vitro* studies demonstrated that biliverdin/bilirubin act as antioxidants (Stocker et al., 1987). The other product of HO is CO, appears as a potential regulator of neural processes and vascular tone (reviewed by Ryter and Tyrrell, 2000). Since high levels of HO-1 are induced in cells from a tissue (skin) which are clearly not important in haemoglobin metabolism, a second function of HO-1 has

been proposed. Its induction may protect cells against oxidative stress (Keyse et al, 1990; Balla et al., 1992; Elbirt and Bonkovsky, 1999).

Poss and Tonegawa (1997) proposed that HO-1 is required for mammalian iron reutilization: mice lacking the functional HO-1 developed an anaemia associated with abnormally low serum iron levels, yet accumulated hepatic and renal iron that contributed to macromolecular oxidative damage, tissue injury and chronic inflammation because they lack the functional HO-1 to metabolise heme iron to extracellular spaces. Ferris et al (1999) showed that in murine fibroblast cells, HO-1 activity regulated iron accumulation and efflux. In experiments where ^{55}Fe was added to cells over-expressing HO-activity, iron uptake was reduced and iron efflux was increased compared to normal cells or HO-1 deficient cells. This preventing of cell death by regulation of cellular iron, suggested another possible cytoprotective role for HO-1, attributed to the augmentation of iron efflux. However, there is also evidence to suggest that HO can act as prooxidant (reviewed by Ryter and Tyrrell, 2000). Human Hela (HtTA-1) cells which overexpress HO-2 protein actually displayed a lower intracellular heme concentration and a higher level of chelatable iron than the parent strain HtTA cells shortly after hemin treatment and are more sensitive to high doses of UVA radiation (500 kJ/m^2). This hypersensitivity does not occur 24 h after removal of hemin (Kvam et al., 1999) and was reversed by Desferrioxamine (DFO) treatment.

1.5 Iron

1.5.1 General introduction

Iron is the second most abundant metal, after aluminium and the fourth most abundant element in the Earth's crust (5%). It is the most abundant transition metal in living organisms. An adult human has a total 4g of iron present in the body. One percent of tissue iron (i.e. 40mg) is mobilised by macrophages of the reticuto-endothelial system to the erythroid bone marrow for hemoglobin synthesis per day. Humans absorb 1-2 mg from the diet and excrete 1-2 mg of iron per day to maintain the balance of body iron. Living organisms such as mammals appear to have selected iron for achieving a large number of essential biological processes, since it is involved as a part of, or as a cofactor of many protein and enzymes. Its bioavailability is generally limited and higher species often exhibit deficiency, such as anaemia. Although iron is essential to all the cells because of its role in catalysing reactions of oxidation and reduction by virtue of its ability to change valence states, it could be potentially toxic. Iron overload conditions also occur, such as genetic or acquired iron overload (Hemochromatosis) or the delocalisation of intracellular iron such as the inflammatory response (some skin conditions: psoriasis, venous ulceration, atopic eczema) or atherosclerosis (Trenam et al., 1992). Another danger of iron is its ability to favour neoplastic cell growth. The metal is carcinogenic due to its catalytic effects on the formation of $OH^{\bullet}$, suppression of the activity of host defence cells and promotion of cancer cell multiplication (Weinberg et al., 1996). Iron may have a role in the carcinogenic process of other transition metals such as copper and nickels, or other kinds of carcinogens (Toyokuni et al., 1996). Iron also contributes to the skin inflammation by ROS in the rat (Trenam et al., 1992).

Iron in the form of ferrous (Fe^{2+}) is readily soluble at neutral pH but the polymeric oxides and hydroxides of ferric (Fe^{3+}) precipitate at neutral pH as $Fe(OH)_3$ unless the metal is suitably chelated (Crichton et al., 1987). Iron's biochemical activity reflects its dual ability to co-ordinate electron donors and to participate in redox processes (capacity to reduce or to oxidise a molecule). Most of the iron in organisms is found in a complex in proteins (reviewed by Richardson and Ponka, 1997) because of the low solubility of the metal in biological milieu. Of the proteins, ferritin allows the cells to deposit a pool of bio-available iron in a form which is soluble under physiological conditions and is non-toxic (see section **1.5.3 Iron homeostatasis**).

The largest pool of iron (about 75%) presents in heme of hemoglobin and myoglobin where they transport oxygen. Other iron-containing proteins comprise cytochromes and iron-sulphur proteins transferring electrons in the respiratory chain, and various enzymes involved in oxygen-dependent reactions like oxygenases, hydroxylases, peroxidases and catalase, among them are the detoxifying P450 cytochromes, iron regulatory proteins and aconitase. Finally the enzymatic activity of ribonucleotide reductase requires iron. All of these together may account for no more than 10% of the total iron pool. The other 15% of body iron is present in ferritin, the iron storage compartment (reviewed by Kuhn, 1994). There is also a small part (0.1-1 %) of labile iron pool (LIP) (see section **1.5.5**) that can catalyse the formation of ROS, if not appropriately shielded due to its extreme reactivity towards oxygen.

Under normal physiological conditions, $O_2^{\bullet-}$ and H_2O_2 interact with organic substrate slowly. However, in the presence of transition metals such as iron or copper, the reaction will be accelerated. It is generally assumed that there is a small intracellular pool of free iron that can react with $O_2^{\bullet-}$ and H_2O_2, giving rise to the reactive $OH^{\bullet}$ via

the Haber-Weiss reaction (1) or Fenton reaction (2). Much of the biological damage attributed to those species (O_2^-, H_2O_2 and $OH^\bullet$) is dependent on the presence of iron (Aust, 1985; Halliwell and Gutteridge, 1999). These processes can be expressed as follows:

$$O_2^{\bullet -} + Fe^{3+} \longrightarrow Fe^{2+} + O_2 \quad (1)$$ **(Haber-Weiss reaction)**

$$H_2O_2 + Fe^{2+} \longrightarrow OH^\bullet + OH^- + Fe^{3+} \quad (2)$$ **(Fenton reaction)**

Net:

$$O_2^{\bullet -} + H_2O_2 \xrightarrow{\text{Iron}} OH^\bullet + OH^- + O_2 \quad (3)$$

(Source: Halliwell and Gutteridge, 1999)

The net effects are DNA damage; impaired synthesis of proteins, membrane lipids and carbohydrates; induction of proteases; and altered cell proliferation. Iron is an essential component in redox-driven lipid peroxidation systems. Iron plays an important role in damage to lipids, by catalysing lipid peroxidation, to produce ROOH, which split to form of $RO^\bullet$ and $ROO^\bullet$ radicals (Aust et al, 1995). These reactions can be described as follows:

$$ROOH + Fe^{2+}\ complex \longrightarrow RO^{\bullet} + OH^{-} + Fe^{3+}\ complex \quad (4)$$

$$ROOH + Fe^{3+}\ complex \longrightarrow ROO^{\bullet} + H^{+} + Fe^{2+}\ complex \quad (5)$$

$$ROOH \longrightarrow RO^{\bullet} + OH^{\bullet} \quad (6)$$

Transition metals other than iron, notably copper, are also able to catalyse the above reactions, but the best candidate *in vivo* is iron. Several iron complexes can also catalyse the Haber-Weiss reaction in cell-free systems, including Fe^{2+}-EDTA (McCord and Day, 1978; Halliwell and Gutteridge, 1999). In cells, however, the true catalyst in Fenton chemistry is more likely to be the low-molecular weight (LMW) free iron pool, or iron made available from other cellular sources under conditions of oxidative stress. This pool provides the cell with a relatively accessible form of iron for incorporation into cytosolic enzymes and proteins. The iron which can be extracted from proteins by ligands into a LMW form has been termed the 'labile iron pool' (LIP) by Jacobs (1977); White et al. (1976) (see section **1.5.5**).

Iron has been involved in UVA-mediated damage to biomolecules, both *in vitro* and in cell cultures. UVA-mediated cytotoxicity in primary human fibroblasts was significantly reduced by pre-treatment of the cells with iron chelators, e. g. DFO, which chelated both Fe^{2+} and Fe^{3+}, preferentially Fe^{3+} (Keyse and Tyrrell, 1989). Similarly, UVA-mediated protein oxidation measured by sulfhydryl loss was strongly reduced by pre-treatment of cells with iron chelators (Vile and Tyrrell, 1995). UVA-induced lipid peroxidation in membranes of cultured human primary fibroblasts was shown to occur via pathways involving iron and $^1O_2$ (Vile and Tyrrell, 1995). Solar UV radiation-

mediated generation of $LO^{\bullet}$ in mouse and human skin is significantly decreased by topical application of the iron chelator DFO (Jurkiewwicz and Buettner, 1996), also indicating a role for iron in lipid peroxidation. Iron treatment significantly increased lipid peroxidation, while DFO significantly decreases lipid peroxidation in human fibroblasts irradiated with UVA (Morliere et al., 1997). Fe^{2+}, in conjunction with H_2O_2, can also catalyse the oxidation of protein sulphydryl group and cause the inactivation of protein function *in vitro* (Hu et al., 1992; Vile and Tyrrell, 1995). Because of the dangerous nature of 'free' or 'catalytic' iron, the free iron level is tightly maintained within cells by feed-back mechanisms that lead to ''iron homeostasis'' (see section **1.5.3**).

1.5.2 Ferritin

Ferritin is the iron storage protein. The protein must maintain its iron in a soluble, bio-available and non-toxic form. The ubiquitous protein ferritin (450 kDa) is a cytosolic, hollow protein and consists of 24 subunits of polypeptides. The heteropolymeric components (light chain, L, 19 kDa; and heavy chain, H, 21 kDa) form a shell around an inorganic iron oxyhydroxide core [FeOOH]x. The sequestered iron is maintained in an oxidised Fe^{3+} state by the ferritin H-chain, which has ferroxidase activity which is necessary for iron uptake by the ferritin molecule. The L-chain facilitates iron core formation within the protein shell and has more iron storage capacity. The proportion of H to L varies depending upon the tissue source as well as the level of iron loading. The mammalian H-ferritin and L-ferritin polypeptide show 50% homology and have the same ancestral gene (Ponka et al., 1998).

A ferritin molecule can sequester up to 4500 iron atoms. Normally, ferritin is only about 20% iron-saturated (Reif, 1992) and as much as one third of ferritin iron may turn over daily as a result of degradation and synthesis. Ferritin is slowly degraded to a non-specific complex containing iron, which becomes the component of hemosiderin. Hemosiderin is lipoprotein found in lysosomes, which appears to be a dead end in the metabolism of iron and ferritin (reviewed by Bridges, 1996).

In cells, most of the iron is sequestered in ferritin as a crystalline core of ferric Fe^{3+} ions. Ferritin has high capacity to chelate iron and convert it to the ferric state in which it is relatively safer. Thus ferritin is able to restrict the availability of Fe^{2+} to participate in the Fenton reaction. Ferritin therefore appears to play an important role as a cytoprotective protein. In this way iron is limited in its capacity to catalyse oxidative reactions in the presence of H_2O_2 (Ollinger and Roberg, 1997). It is generally considered that the chelation of the intracellular iron with exogenous chelators or increased levels of the endogenous iron storage ferritin will protect mammalian cells in culture against oxidative stress generated by a variety of agents such as H_2O_2 and UVA radiation (Balla et al., 1992; Vile et al., 1993 and 1994).

Although ferritin's iron-scavenging property is well known, it may also be a potentially hazardous molecule under pathological conditions or in cells exposed to oxidative stress (Reif, 1992; Pourzand et al., 1999). Ferritin photoreduction could trigger peroxidation of lipoproteins such as low density lipoprotein LDL (Aubailly et al., 1994). Reductive release of iron from ferritin may catalyse cytotoxic radical reactions like the Haber-Weiss reaction. $O_2^{\bullet-}$ may mobilise iron from ferritin, although the ability of $O_2^{\bullet-}$ to do this is very limited (Bolann et al., 1990). Ferritin may also exert a prooxidant role

because of ferrous ions released from the ferritin protein by a variety of reducing agents (Reif, 1992).

1.5.3 Iron Homeostasis

Because of the ambivalent role of iron in cells, it is essential for living organisms to maintain iron homeostasis in order to ensure the iron supply but prevent accumulation of excess iron. Cellular iron metabolism which comprises pathways of iron uptake *via* transferrin receptor (TfR) and storage in ferritin is co-ordinately regulated through a feedback control mechanism mediated at the post-transcriptional level by cytoplasmic factors known as iron regulatory proteins (IRPs). In response to fluctuations in the level of LIP, IRPs act as major regulators of these pathways (see below).

Transferrin (Tf): Tf, the plasma iron-binding glycoprotein which is the major vehicle for transfer of iron in the body, provides most of the iron for the physiological needs of iron-requiring cells, and is normally the only source of iron for hemoglobin synthesis. It binds and transports iron, hence reduce the toxic side effect of iron. The 80 kDa Tf has high affinity for Fe^{3+}. Each Tf molecule consists of two globular domains and each domain contains a high-affinity binding site for one iron molecule. Fe^{3+} attaches to these sites extremely tight at physiological pH. Although Tf can also bind to other metals such as aluminium, manganese, copper and cadmium, the affinity is much lower than iron. Tf exists as a mixture of iron-free (apo Tf), one iron (mono Tf) and two iron (diferric Tf) forms of the molecule. The primary function of Tf is to bind iron in plasma and to transport iron into various cells and tissues. Tf is bound to membrane receptors and that are found in many cells. The Tf is then internalised by endocytosis and releases its iron at acidic pH in late endosomes.

Transferrin receptor (TfR): TfR is a homodimeric glycoprotein with a molecular weight of approximately 180 kDa. Its two identical subunits are joined by two disulfide bonds. Because each domain contains a binding site for the Tf molecule, a homodimer of TfR can bind up to two molecules of Tf simultaneously. TfR is expressed in all cells except mature erythrocytes and other terminally differentiated cells. There are two forms of TfR, TfR1 and TfR2 which have distinct cell-and tissue-specific expression pattern. TfR is expressed at high levels in rapidly dividing cells. Expression of TfR in non-erythroid cells is regulated at the post-transcriptional level by the interaction of IRPs and 5 x iron responsive element (IREs) in 3'-untranslated regions (UTR) of TfR mRNA. TfR linked to the cell surface and binds diferric iron-loaded Tf with high affinity. TfR complex is formed that is then endocytosed within an acidic endosomal compartment where the TfR iron is released from Tf in a pH dependent manner. The TfR complex is subsequently cycled back to the cell surface and Tf is released from the receptor to the plasma as apotransferrin (reviewed by Eisenstein, 1998). Dissociation of apotransferrin from its receptor takes place at neutral pH at the cell surface, making both the ligand and receptor available for further rounds of iron absorption. Apart from this Tf dependent pathway, several cell types also have other efficient mechanisms of iron uptake that includes a process consistent with non-specific uptaken, pinocytosis and a mechanism that is stimulated by a LMW-Fe complex (see section **1.5.5**).

Iron regulatory proteins (IRPs): IRPs include IRP1 (90 kDa) and IRP2 (105 kDa), which are cytosolic mRNA-binding proteins that bind to a stem loop (hairpin) RNA structure known as the IRE. IREs are located in either the 5'or 3'-UTRs of specific mRNAs encoding proteins involved in iron and energy homeostasis. IRPs expressed in

all tissue but in most cells IRP2 has less abundant expression than IRP1. IRP1 was shown to be the cytosolic counterpart of aconitase (Ac), which is a (4Fe-4S)-containing Krebs cycle enzyme that catalyzes the isomerization of citrate to isocitrate. Although IRP1 and Ac are only 30% identical, IRP1 contains all the Ac active sites. A (4Fe-4S) cluster assembly/disassembly leads to the switch between the forms. High iron levels convert apo-IRP into the active (4Fe-4S) Ac, non RNA-binding form. RNA binding and Ac activities are mutually exclusive and the switch between these activities occurs without changes in the IRP1 protein level. IRP2 shares about 60% identity with IRP1. Despite sequence similarities, IRP2 is thought not to form a (4Fe-4S) cluster and consequently lacks Ac activity. IRP2 is controlled at the level of protein stability and the regulation involves proteolysis by the proteasome (reviewed by Hentze and Kuhn, 1996).

When cellular iron is high, it will cause inactivation of IRP-1, which has an intact [4Fe-4S] cluster (holo-protein) and high Ac activity and cannot bind IRE of 5'-UTR or ferritin mRNA so that ferritin is translated freely, and can sequester excess iron in the newly formed ferritin shell. It also leads to degradation TfR mRNA that inhibits iron uptake. Both bring down the level of intracellular 'free' iron. When cellular iron is low, the IRPs is in the form of the apo-protein without the Fe-S cluster, and no Ac activity. It binds IREs with high affinity leading to the inhibition of ferritin mRNA translation and also binds to the 3'-UTR of TfR mRNA, thus stabilises of TfR mRNA and induces of TfR protein synthesis (Ponka et al., 1998). The net result is an increase in iron uptake and availability within the cell. Iron can therefore be considered as a feed-back regulator of its own metabolism.

Although iron is the major regulator of IRP activity, other factors such as UVA, H_2O_2, nitric oxide (NO), protein kinase C phosphorylation and hypoxia/reoxygenation modulate the RNA binding activity of IRP1 and/or IRP2 besides iron (reviewed by Cairo et al., 2000). IRP1 is up-regulated by NO and H_2O_2, IRP2 is up-regulated by NO but not H_2O_2, thereby may limit the pro-oxidant challenge of iron (Pantopoulos and Hentze, 1998, Lieu et al, 2001).

1.5.4 New genes contribute to iron homeostasis.

Recent identification and characterisation of the hemochromatosis protein HFE, the iron exporter ferroprotin 1 and the transferrin-independent transporter Nramp2 and SFT also been demonstrated to have important roles in maintaining iron homeostasis in the body.

The hemochromatosis gene and its product

Hereditary hemochromatosis (HH) is a common autosomal-recessive disorder of iron metabolism, with an inherited disorder that results from an accumulation of excess iron in many organs, which is manifested by liver, heart and skin dysfunction. More than 80% of HH patients have mutation in a major histocompatibility complex (MHC) class I type protein (HFE). HFE has been identified, cloned and expressed. The missense mutation of HFE is responsible for most cases of hemochromatosis. HFE is a glycoprotein, which associates with β_2-microglobulin at the cell surface. Lack of HFE expression may be associated with iron over-loading. HFE forms specific complexs with the TfR to decrease the affinity for Tf (the negative regulator of TfR; Feder et al., 1998). Expression of HFE leads to activation of IRPs and results in decreased ferritin and iron uptake from diferric Tf in HeLa cells (Riedel et al., 1999).

Nramp (natural resistance associated macrophage protein), comprises include Nramp1 and Nramp2. Nramp2 was first identified as a divalent metal transporter1 (DMT1) or divalent cation transporter1 (DCT1). The mRNA of the protein has IREs at its 3'-UTR, and is expressed in many different tissues with high expression levels at the duodenum brush border, is consistent with its role in intestinal iron absorption and iron acquisition. Nramp2 is located on the plasma membrane as well as on subcellular compartments characterised as late endosomes or lysosomes. It stimulates divalent metal (such as Fe^{2+} and Zn^{2+}, Mn^{2+}, Ni^{2+}, Co^{+2}, Cu^{+2}, Cd^{+2}) uptake and its function is pH dependent at an optimum at low pH (pH < 6). Nramp2 is subcellularly colocalised with Tf, and may play a role in transporting Tf-bound iron exits from the endosome membrane, thus it is named iron importer also (reviewed by Lieu et al., 2001). Nramp1, regulates macrophage activation in infectious and auto-immune disease. It is located in late endosomes/lysosomes and delivers divalent cations from the cytosol to phagolysosomes (reviewed by Lieu et al., 2001).

SFT (stimulator of iron (Fe) transporter) is a transmembrane protein that enhances uptake of both Tf-bound and non-Tf-bound iron in cultured cells. Its activity appears relatively selective for Fe^{2+} and Fe^{3+} transport, which is energy dependent and at neutral pH. Expression of SFT seems to be inversely regulated by cellular iron levels. SFT is localised to endosomes and its expression stimulates iron assimilation from Tf, however, the relationship between SFT and Nramp1 is still not clear (reviewed by Lieu et al., 2001).

IMP (integrin mobilferrin pathway): Fe^{3+} is bound to a cell surface β_3-integrin and transferred to a calreticulin-like chaperone protein called mobilferrin in intestinal cells

of normal rodents and non-intestinal K562 (human erythroleukemia) cells. This pathway is not shared by other metals (Conrad et al., 2000).

Paraferritin: The 520 kDa membrane complex called paraferritin contains β-integrin, mobilferrin, flavin mono-oxygenase and β-microglobulin. It participates in the mucin-mediated Fe^{3+} uptake in the gut lumen. Following internalisation, ferric iron may reduce to ferrous iron, then available for incorporation into compounds such as ferritin and heme (Conrad et al., 1999).

The iron exporter: ferroprotin1. Ferroprotin1 was identified recently in man. It has IREs at its 5'-UTR, which can bind IRP1 and IRP2, indicating ferroprotin1 is regulated by intracellular iron levels. It resides at the basolateral surface of duodenal enterocytes and may mediate iron efflux across membranes to plasma by a mechanism that requires ferroxidase activity (reviewed by Lieu et al., 2001)

1.5.5 The Labile iron pool (LIP)

It is generally accepted that there is a small amount (<1%) of iron not bound to iron proteins or loosely bound to ligands present in the cytosol. This cytosolic iron pool is often referred as the transit iron pool, based on the assumption that it represents iron in transit between Tf and ferritin (Crichton et al., 1987). It has been named LMW-Fe or LIP, which serves to provide the cell with a relatively accessible form of iron for incorporation into cytosolic enzymes or proteins (Breuer et al., 1996). Although the nature of the LIP is not fully understood, it probably consists of both Fe^{2+} or/and Fe^{3+} ligands, existing in dynamic equilibrium as Fe^{2+} and Fe^{3+} forms. The Fe^{2+} becomes oxidised and deposited within ferritin (reviewed by Harrison and Arosio, 1996). In cells, where the environment becomes even more reducing than plasma, one may expect Fe^{2+} LMW species to be predominant. Ligands such as pyrophosphates, phosphate ester, ATP, ADP, GTP, nucleic acids, lipids, glycogen, riboflavin, ascorbate, sugars, amino acids, polypeptides and uncharged growth factors have been proposed, but none of these ligands have been universally accepted as the major ligand for iron in the LMW-Fe pool (reviewed by Crichton and Ward, 1992). Evidence confirming the importance of nucleotides as ligands for the LMW-Fe pool was presented by the discovering of receptors for ATP-Fe^{2+} or/and ATP-Fe^{3+} in mitochondria or ferric citrate in the cells (Weaver and Pollock, 1989 and 1990) which could supply iron for heme biosynthesis. Gurgueira and Meneghini in 1996 reported that there was an ATP-dependent uptake system for iron-citrate and iron-ATP chelators from isolated rat liver nuclei and suggested that these may be the important ligands.

In cells, the LIP constitutes the cytosolic fraction of iron, which is accessible to permeable chelators. It contains the metabolically and catalytically reactive iron of the cells. The LIP ultimately causes peroxidative damage to vital cell structures due to its catalytic action in one-electron redox reactions. Unlike ferritin bound iron, the LIP is loosely bound to macromolecular complexes and they are sensed by the cytosolic IRPs. The LIP is maintained by a balanced movement of iron from extracellular and intracellular sources, which can be increased by endocytosis of Tf bound iron or non-Tf bound iron and degradation of ferritin. The decrease of LIP may occur following protein and heme synthesis as well as during exposure of cells to chelators (Epsztejn et al., 1997). The increased intracellular iron may bind to DNA and membranes, and make them a selective target for oxidative damage by forming $OH^{\bullet}$ in close proximity.

Iron bound to LMW ligands constitutes a potential source of catalytic iron upon UVA radiation. *In vitro*, physiological doses of UVA radiation could reduce Fe^{3+} bound to the LMW intracellular chelator citrate (Vile and Tyrrell, 1995). Various conditions of stress including UVA radiation (Pourzand et al., 1999), $O_2^{\bullet-}$ (Biemond et al., 1988), reducing agents (Baader et al., 1994) have been shown *in vitro* to induce iron release from ferritin. In rodent cell extracts, oxidative stress can release iron from ferritin (Cairo et al., 1995). LMW-Fe has been shown to be active in the cell damaging process caused by oxidative stress, promoting lysosome rupture and release of potent hydrolytic enzymes to the cytosol (Ollinger and Brunk, 1995). It has also been reported that UVA radiation leads to bacterial cell lethality, by creating a transit iron load, providing very favourable conditions for the production of highly deleterious free radical through a variety of mechanisms that lead to oxidative stress (Hoerter et al., 1996).

Recently, it has found that UVA radiation causes an immediate release of "free" iron in FEK4 cells as a result of UVA induced lysosomal damage, that leads to ferritin degradation in the cytosol by lysosomal proteases (Pourzand et al., 1999). UVA radiation of FEK4 cells also induces immediate heme release from microsomal hemoprotein (Kvam et al., 1999), which provides another potential source of harmful iron. This UVA-mediated iron release is likely to play a major role in UVA-mediated damage. The key role of iron in biological radical formation offers the potential for protective intervention by iron chelators such as DFO, and these have been studied both *in vivo* and *in vitro* (reviewed by Cabantchik, 1999) for treatment of imbalance in iron homeostasis, such as iron overload disease.

1.5.6 Determination of LMW-Fe or LIP

The LIP is the available cellular iron and has at least four potential functions: a) cellular iron transport b) expression of iron regulatory genes (TfR and ferritin) c) control of the activity of iron containing proteins d) catalysis of Fenton reactions. Attempts to quantify and assess the LMW-Fe pool, in the past, relied on methods that homogenise cells and tissue and the iron content is then determined using electron paramagnetic resonance (EPR) with iron chelators (Kozlov et al., 1992) or DFO-chelatable ^{59}Fe (Rothman et al., 1992). All the physicochemical methods used either require cell disruption or relatively large amounts of tissue because of the low sensitivity of the methods. As a consequence of tissue homogenization, the equilibrium between free and bound iron, as well as its oxidation state, may be altered. So the dynamic changes in this iron pool can not be measured. One method developed by Lytton et al. (1992) used nitrobenzdiazole-desferrioxamine (NBD-DFO), which is a fluorescent probe that can enter cells and extract iron thereby causing physical disruption. Binding of iron to this fluorescent

probe quenched its fluorescence, and subsequent removal restored fluorescence which, in turn, could be used to provide a quantitative determination of iron content. However, because of the poor cell tolerance and low quantum yield of the probe, it was difficult to assess the amount of iron bound to this probe (Epsztejn et al., 1997). It was shown that the fluorescence calcein assay (CA-assay), developed by Cabantchik and co-workers (Epsztejn et al., 1997), can measure intracellular iron.

Fluorescence calcein assay (CA-assay):

CA loading and intracellular LIP estimation

CA (see **Materials and Methods** for structure) is a fluorescent probe with a relative high fluorescence quantum yield. It has ethylenediaminetetracetic acid (EDTA)-like, two metal binding moieties and high affinity for Fe^{2+} and Fe^{3+} (10^{14} and 10^{24} M^{-1} respectively in aqueous salt solution), which are similar to those of EDTA (Epsztejn et al., 1997). The fluorescent probe CA binds readily, stoichiometrically (1:1), and reversibly with a fraction of Fe^{2+} associated with LIP, while forming fluorescence-quenched CA-bound iron complexes (CA-Fe). CA is an indicator for transition metal at neutral pH in solution. It is a hydrophilic-carboxylated compound, therefore impermeable to cells. It can serve as a metallo-sensitive probe for Fe^{2+} for the following reasons. i) Quenching of fluorescence ensues upon binding of iron and other metals, such as Cu^{2+}, Ni^{2+}, Co^{2+}, but not Ca^{2+} and Mg^{2+}, even at 1000-fold excess in physiological salt solutions because of their very low selectivity. However, the concentrations of Cu^{2+}, Ni^{2+}, Co^{2+}, are negligible in physiological solution. Binding of CA to Fe^{2+} is considerably faster than Fe^{3+}, reflecting the different chemical activity of the two forms of iron. ii) DFO which has a high affinity for Fe (10^{31} for Fe^{3+} and 10^{21} for Fe^{2+}) but low affinity for other metals can abrogate the CA-detectable LIP. iii) By

addition of Fe^{3+} chelators, the fluorescence produced by CA in cells is kept unchanged. Furthermore, although in the presence of ascorbate, Fe^{3+} can be reduced to Fe^{2+}, there is only slight increase in the fluorescence in cells (Breuer et al., 1995). Consequently, the quenched fluorescence of the CA-Fe complex in solution is fully restored by addition of excess chelators such as salicyladehyde isonicotinoyl hydrazone (SIH) or divalent metal Ionophore + DTPA (Diethylenetriamine pentaacetic acid, affinity for Fe > 10^{27}) (Breuer et al., 1995; Cabantchik et al., 1996) which can abstract iron from CA, so the CA fluorescence assay is based on the availability of fast permeating high affinity chelators (e. g. SIH which can chelate both Fe^{2+} and Fe^{3+} forms of iron and has a binding constant 10^{29} M^{-1} for Fe^{3+} and 10^{20} M^{-1} for Fe^{2+} (Epsztejn et al., 1997) and their capacity to abstract iron from CA, causing a dequenching of its fluorescence signal within the cells. These fluorescence changes evoked by SIH addition provides a basis for the CA-Fe and the dynamic monitoring of cytosolic iron in living cells using spectrofluorometry.

Inside the cells, LIP is operationally defined as free iron [Fe] plus [CA-Fe]. CA-Fe, CA and Fe are quick to reach equilibrium whose reaction is expressed as

$$[CA\text{-}Fe] <-> [CA] + [Fe] \quad (1)$$

[CA-Fe] can determined by CA-assay. The rest is to gain the dissociation constant (Kd) of [CA-Fe] by iron titration of CA-loaded cells (see **Materials and Methods**). In quantitative terms, the formation of CA-Fe in cells depends on the relative concentrations of free CA and free iron and the apparent Kd of CA-Fe, which is governed by equation (2).

$$Kd = \frac{[CA] \times [Fe]}{[CA - Fe]} \quad (2)$$

The [Fe] can be calculated by this equation. After the development of this assay, a number of different studies were carried to assess changes in the LIP after various treatments. Breuer et al (1996) showed that brief exposure to both Fe^{2+} salt, ferrous ammonium sulphate (FAS), and oxidative treatment (e. g. H_2O_2) caused increases in the LIP whereas DFO treatment decreases the LIP of the cells.

1.6 UVB

The short, more energetic solar UVB wavelengths (the most energetic in sunlight) readily cause erythema so it is also known as erythemal UV. UVB is mainly absorbed by the epidermis, but it also penetrates sufficiently into skin to cause damage in the dermis. The morphological and histological cellular changes that occur in skin include erythema, pigmentation and hyperkeratosis (thickening of the stratum corneum) (Pearse et al., 1987).

UVB is absorbed by most biological macromolecules (such as lipid, protein and nucleic acids). DNA is both the main absorbing chromophore and the target for critical biological effects in the UVB region. Epidemiological studies have shown that human skin cancer is linked to UVB exposure. UVB induces non-melanoma skin cancer (e.g. squamous cell carcinoma, SCC) in mice (reviewed by de Grujil et al., 2000). Only a few cases of experimental animal melanoma have been reported by UVB (reviewed by de Gruijl, 1999). Evidence exists that it is the direct absorption of UVB by DNA, which is potentially mutagenic and is linked to photocarcinogenesis *in vivo* in animal models (Ley et al., 1991). It is well established that UVB gives rise to mutations in proto-oncogenes and tumour suppressor genes that initiate the molecular cascade towards skin cancer (Brash et al., 1991; Ziegler et al., 1993; Berg et al., 1996). Furthermore, stimulation of DNA repair leads to a decrease in the incidence of UV-induced skin tumours in mice (Yarosh et al., 1992), further demonstrating the importance of the mechanism of repair to DNA damage in the biological effects of short UV wavelengths.

The most frequent bulk lesion of DNA photoproduct formed after UVB exposure is the pyrimidine dimer (Freeman et al., 1989). This is either a cyclobutane ring at

neighbouring bases which form a cyclobutane pyrimidine dimer (CPD), or binding at a position in one base to the adjacent base to form the 6-4 pyrimidine-pyrimidone photoproduct (6-4 PP). UVB also causes a limited number of strand breaks and induces base modifications such as 7,8-dihydro-8-oxo-2'deoxyguanosine (8-oxo-dG) formation (reviewed by de Gruijl, 2000), which is known to form a miscoding lesion which can cause G to T transversion after replication of the damaged DNA (Shibutani et al., 1990). UVB causes both local and systemic immunosuppression. UVB leads to decreased rejection of transplanted tumours in mice (Kripke et al., 1974). It has been demonstrated by using a sensitiser of contact hypersensitivity (CHS) that CHS is suppressed in murine models or humans after UVB radiation. This may be due to impaired antigen presenting ability of Langerhans cells or generation of suppressor T-lymphocytes. UVB radiation impaired Langerhans cells in the epidermis of mice (Greene et al., 1979) and humans (Cooper et al., 1992). DNA damage may also be an important initiating event in immunosuppression (reviewed by Tyrrell, 1994). Immounsuppression therapy (in renal transplant patients) increases skin cancer. UVB-induced immunosuppression may therefore contribute to sunlight-induced cancer.

UVB may also damage proteins. Protein absorption peaks in the 'non-solar' UVC range but extends through the UVB because aromatic amino acid residues (phenylalanine, tyrosine and tryptophan) absorb UV with a maximum around 280 nm. Although cell membranes are not primary targets of UVB, radiation of cultured human keratinocytes with biologically relevant doses of UVB has been shown to cause lipid peroxidation (Pounonen et al., 1991). In cultured human skin fibroblasts (FEK4), only lethal doses of UVB induced significant lipid peroxidation (Vile and Tyrrell, 1995).

1.7 UVA

1.7.1 General introduction

UVA radiation comprises lower energy photons and higher doses are needed to cause the same damage (such as erythema, sunburn and pigmentation and carcinogenesis) as that induced by UVB radiation. UVA is approximately a thousand times less as erythemagenic as that UVB per photon, this ratio of efficiency is also true in cultured cell systems. However, UVA reaches the Earth's surface at incident energy estimated to be 10-100 times greater than UVB and the UVA penetrates much deeper into the dermis than UVB (see **Fig. 1A**).

An action spectrum is a measure of the relative effectiveness of different wavelengths within the spectral region of study to produce a given response such as erythema and cytotoxicity. Action spectra, taken together with solar spectroradiometric measurements and the known transmission of human skin have led to the conclusion that the UVA component of solar UV is a major contributor (up to 80%) of the cytotoxic action of sunlight at the basal layer of the epidermis (Tyrrell and Pidoux, 1987).

Exposure of certain individuals to UVA radiation is actually increasing due, at least in part, to the longer exposure times permitted by the more widespread use of primarily UVB-absorbing sunscreens. Modern tanning technology also leads to UVA exposures. The absorption of UVA radiation leads to cellular oxidation (reviewed by Tyrrell, 1991) and there is considerable overlap between the types of cellular modification induced by UVA and those generated by oxidative pathways. Furthermore, it now appears that cellular defence against UVA damage involves antioxidant pathways.

1.7.2 UVA-induced oxidative stress

UVA is oxidative in nature. Most biological effects of UVA, either on cultured cells (Danpure and Tyrrell, 1976) or in skin are oxygen-dependent. *In vivo* tests showed that UVA-induced erythema and pigment darkening (both immediate and delayed) are dependent on oxygen (Tegner et al., 1983; Auletta et al., 1986; Rorsman and Tegner, 1988). GSH plays a major role in protection of cultured human skin cells from UVA radiation and this provide additional evidence that ROS generated by radiation are involved in UVA toxicity (Tyrrell and Pidoux, 1989). Studies in prokaryotic and eukaryotic cells both indicate that ROS may be generated *in vivo* by UVA radiation. The cytotoxicity action of UVA radiation on bacteria, fungi and yeast is known to be oxygen dependent (reviewed by Tyrrell, 1991). Further evidence that UV radiation generates ROS comes from studies utilising *Salmonella typhimurium* lacking the oxidative defence regulon (ΔoxyR). These strains are hypersensitive to UV radiation (Kramer and Ames, 1987).

The absorption of UVA by many cellular molecules can lead to the generation of ROS via interaction with endogenous chromophores such as porphyrins (reviewed by Tyrrell and Keyse, 1990). Photosensitised oxidation occurs as type I or type II reactions (Foote, 1991). The absorption of UV-photons by a sensitiser results in an electronically excited state. The excited sensitiser subsequently reacts directly with the target molecules, e.g. DNA (Type I reaction); or reacts with molecular oxygen (Type II reaction) to produce ROS, mainly singlet oxygen. The potential chromophores for UVA radiation including compounds such as quinones, steroids, flavins, porphyrins and heme-containing proteins such as cytochromes, peroxidases and catalase (reviewed by Tyrrell, 1991).

Evidences that UVA radiation generate ROS

Hydrogen peroxide (H_2O_2): Both spontaneous and enzymatic (via SOD) dismutation of $O_2^{\bullet-}$ are important sources of intracellular H_2O_2 generation. $O_2^{\bullet-} + H^+ \rightarrow HOO^{\bullet}$, $2HOO^{\bullet} \rightarrow H_2O_2 + O_2$. H_2O_2 can be generated by UVA radiation of tryptophan in an oxygenated solution (McCormick et al., 1976). H_2O_2 may also be produced by UVA radiation of cysteine (Cunningham et al., 1985). There is evidence suggesting that H_2O_2 can be generated in cultured human skin cells during UVA radiation (Peak et al., 1990a; Vile and Tyrrell, 1995) and that UVA-mediated lipid peroxidation and protein sulfhydryl loss in cultured human skin fibroblasts are related to the intracellular generation of H_2O_2 (Vile and Tyrrell, 1995), although H_2O_2 did not appear to be an important component in UVA-mediated cytotoxicity (Tyrrell and Pidoux, 1989; Peak et al., 1990).

H_2O_2 is a weak oxidising agent but in the presence of traces of transition metals, it is capable of inactivating proteins directly via oxidation of essential thiol (-SH) groups, or proteins containing iron-sulphur clusters, reduced heme moieties or copper prosthetic groups. Most of the damaging effects of H_2O_2 on biomolecules are thought to be the result of the formation of the $OH^{\bullet}$ in the Fenton reaction or the metal catalyzed Harber-Weiss reaction (Fenton, 1894; Haber and Weiss, 1934; see section **1.5.1**). Unlike $O_2^{\bullet-}$, H_2O_2 crosses membranes readily and can therefore migrate within the cell and extends the area of potential damage.

Superoxide anion ($O_2^{\bullet-}$) is formed when molecular oxygen acquires an additional electron. That is $O_2 + e^- \rightarrow O_2^{\bullet-}$. The most important sources of $O_2^{\bullet-}$ *in vivo* in aerobic cells are probably the electron transport chains of mitochondria and the endoplasmic

reticulum. However, phagocytic cells (e. g. macrophages, neutrophils) directly generate $O_2^{\bullet-}$ via the NADPH oxidase enzymatic system as a part of their defence against invading microorganisms (Babior, 1999). UVA radiation of NADPH and NADH *in vitro* generates H_2O_2 and $O_2^{\bullet-}$ (Czochralska et al., 1984; Cunningham et al, 1985), $O_2^{\bullet-}$ is then dismutated by SOD to give H_2O_2. $O_2^{\bullet-}$ is relatively unreactive towards most biomolecules, including lipids and nucleic acids (Fridovich, 1978). However, it may react with certain proteins and inactivate them, notably proteins in the presence of transition metals prosthetic groups such as haem moieties or iron-sulphur clusters (Gardner et al., 1995). While several oxygen species act as biological oxidants, $O_2^{\bullet-}$ may act as a reductant as well. For example it is able to reduce ferritin iron (Fe^{3+}) to its most reactive form Fe^{2+} (Biemond et al., 1988). As a consequence $O_2^{\bullet-}$ toxicity to cells will depend largely on the availability of iron in the system. However, it has been suggested that $O_2^{\bullet-}$ is not significantly involved in cellular effects mediated by UVA that include lipid peroxidation and protein oxidation (Vile and Tyrrell, 1995; Gaboriau et al., 1995).

Hydroxyl radical ($OH^{\bullet}$) is a product of the Fenton reaction that involves H_2O_2 and Fe^{2+}. However, it can also be formed in the absence of any transit metal. It has been shown *in vitro*: in the reaction between $O_2^{\bullet-}$ and $NO^{\bullet}$ or H_2O_2 and endogenous $NO^{\bullet}$ (Nappi and Vass, 1998). $OH^{\bullet}$ is likely to be generated in cells following upon UVA irradiation (Vile and Tyrrell, 1995). $OH^{\bullet}$ has also been detected in human skin biopsies irradiated with a UV source (mostly UVA) (Jurkiewicz and Buettner, 1996). $OH^{\bullet}$ generation, however, has not been linked to UVA cytotoxicity (Tyrrell and Pidoux, 1989), lipid peroxidation (Vile and Tyrrell, 1995; Morliere et al., 1997), protein activation (Giordani et al., 1997) or gene activation in cultured human skin fibroblasts (Basu-Modak and Tyrrell, 1993).

Singlet oxygen ($^1O_2$). $^1O_2$ is a derivative of molecular oxygen in which all valence electrons are spin paired. It elevates molecular oxygen to an excited "singlet" state. It may be generated via type II photodynamic process following absorption of with UVA radiation and/or visible light by cellular compounds (chromophores), or it may arise from non-photochemical sources such as the macrophage respiratory burst or membrane lipid peroxidation. $^1O_2$ is not a radical, yet it is a short-lived species and very active. $^1O_2$ may oxidise many organic molecules, including unsaturated membrane lipids, amino acids, thiols and nucleic acids (reviewed by Keyse and Tyrrell, 1998), at least *in vitro*. $^1O_2$ has been implicated in several deleterious biological effects of UVA on cultured cells, including cytoxicity (Tyrrell and Pidoux, 1989) and lipid peroxidation (Gaboriau et al., 1995) and in cellular signalling events leading to the induced expression of a variety of proteins (reviewed by Keyse and Tyrrell, 1998). Finally $^1O_2$ has been proposed as by-product of lipid peroxidation and is also able to induce lipid peroxidation process via its direct reaction with PUFAs to form LOOH and to as damage DNA (Cadenas, 1989). The involvement of $^1O_2$ in UVA cytotoxity to mammalian cells has been confirmed by using either specific scavengers (sodium azide or histidine) of $^1O_2$, or deuterium oxide (D_2O), which prolongs the lifetime of $^1O_2$ (Tyrrell and Pidoux, 1989).

Other ROS that may be produced intracellularly upon UVA radiation and have important effects include the lipid peroxidation chain intermediates i.e. $LO^{\bullet}$, $LOO^{\bullet}$ and organic LOOH. Lipid alkoxyl radicals have been detected in human skin biopsies irradiated with solar UV (Jurkiewicz and Buettner, 1996). Other radicals like $NO^{\bullet}$ or related species such as peroxynitrite ($ONOO^{\bullet}$) may also participate directly or indirectly in cellular oxidative stress following UVA radiation (Kuhn et al, 1998a). Based on such

studies, the UVA component of sunlight is now considered as a generator of intracellular oxidative stress (Tyrrell, 1991 and 1994; Pourzand et al., 1999a).

1.7.3 UVA induced DNA damage and skin cancer

Although DNA is a poor chromophore for the absorption of UVA radiation, the wavelengths produce ROS via photosensitisers and cause various types of DNA damage. UVA can induce 7,8-dihydro-8-oxo-2'deoxyguanosine (8-oxo-dG) and cyclobutane-type pyrimidine dimers, strand breaks and DNA-protein cross-links (covalent links between a protein and DNA) (reviewed by Tyrrell, 1994; Runger, 1999). Among them, 8-oxo-dG is the most studied type DNA lesion that occurs in the UVA range and has been shown in various mammalian cell types, notably human fibroblasts (Kvam and Tyrrell, 1997). Furthermore, this damage has been shown to depend on $^1O_2$ generation (Kvam and Tyrrell, 1997). Pyrimidine dimers, have been shown to occur in human skin *in vivo* following UVA radiation (Burren et al., 1998).

Like UVB radiation, UVA radiation proved to be a complete carcinogen in experiments in which skin carcinomas developed in (hairless) mice under chronic exposure (de Gruijl et al., 1993; Setlow et al., 1993). UVA radiation induced non-melanoma skin tumour in experimental animals was reviewed by de Grujil, (2000). UVA induced melanoma in fish (Setlow et al., 1993). UVA may be involved in human melanoma (de Grujil, 2000). But unlike UVB (exposure mainly induces a rapidly increasing number of squamous cell carcinomas (SCC) and keratoses as precursors), UVA radiation initially induces mainly benign papillomas (Kelfkens et al., 1992). UVB radiation appears to exert predominantly a "tumour initiating" effect, whereas "tumour promotion" is relatively more pronounced with UVA radiation. UVA radiation can be either

immunosuppressive or immunoprotective, depending on irradiation conditions. It was shown that UVA abrogated the immunosuppressive effects of UVB in mice, by a mechanism that may involve heme oxygenase (HO) (Reeve and Tyrrell, 1999). In mice UVA treatment causes local suppression of contact hypersensitivity (CHS), Langerhans cell depletion and T suppressor activation (Bestak and Halliday, 1996).

1.7.4 UVA activation of genes in skin cells

UVA radiation is capable of inducing gene expression in mammalian cells, including epidermal keratinocytes and dermal fibroblasts from human skin. The UVA activation of genes in skin cells has been implicated in the acute inflammatory response of erythema and immune suppression and the chronic responses of photoageing and skin cancer. Among these genes are HO-1, matrix metalloproteinases (MMPs), an intercellular adhesion molecule (ICAM-1), a dual specific phosphatase (CL-100), the FAS-ligand molecule and various cytokines (reviewed by Tyrrell, 1999). The mechanism of UVA induction of genes differs from UVB induction and involves the generation of ROS. Among the ROS, $^1O_2$ appears to be the primary effector of UVA-mediated gene activation. Many transcription factors are also induced by UVA radiation, such as c-Fos, c-Jun and nuclear factor kappa B (NF-kB), and these have been induced in keratinocytes as well as fibroblasts (reviewed Tyrrell, 1997).

Keratinocytes: UVA-I (340-400 nm) induced genes include pro-inflammatory cytokines such as interlenkin (IL)-6 and IL1-α in KB cells (an epithelial carcinoma derived cell lines) when depleted of cellular glutathione prior to radiation (Morita et al., 1997). TNF-α was induced by UVA-I in this cell line but this was independent of the endogenous glutathione levels. The anti-inflammatory cytokine, IL-10, is also induced

in normal human skin keratinocytes as well as in KB cells (Grewe et al., 1995). In HaCaT, another human keratinocyte cell line, a dose dependent decrease in IL-1α mRNA was observed 24 h after UVA radiation (Park et al., 1997). Mitogenic factors such as vascular endothelial growth factor (VEGF) are induced in HaCaT cells and A431 cells (another human keratinocyte cell line derived from a vulvar epithelioma, Mildner et al., 1999) but not primary keratinocytes. Granulocyte macrophage-colony stimulating factor (GM-CSF), a growth factor for epithelial cells, was induced by UVA in HaCaT cells (Park et al., 1997). ICAM-1 was induced by UVA radiation in keratinocyte (Krutmann and Grewe, 1995). There is indirect evidence (based on arachidonate release) that UVA radiation can activate phospholipase A2 (PLA2) in human keratinocytes (Hanson and deLeo, 1990).

Fibroblasts: HO-1 is strongly induced by UVA radiation in human skin fibroblasts FEK4 (Keyse and Tyrrell, 1989). HO-1 is clearly a redox-regulated gene (see section **1.7.6**). Interstitial collagenase or MMP-1 is a neutral metalloproteinase that degrades extracellular matrix proteins including type I, type III and type IV collagen. UVA radiation increases the production of collagenase by cultured skin fibroblasts (reviewed by Tyrrell, 1997). UVA radiation induced type II collagen (a matrix protein that is a major component of anchoring fibrils) but does not alter the mRNA levels of fibronectin (another dermal matrix protein) in cultured skin fibroblasts (Chen et al., 1997). The protein phosphatase, CL100, is up-regulated by UVA irradiation of fibroblasts (Keyse and Emslie, 1992).

1.7. 5 UVA induced lipid peroxidation and membrane damage

Although all classes of macromolecules are susceptible to radical attack, poly unsaturated fatty acids (PUFAs) are extremely susceptible to oxidation owing to their conjugated double bond structures. Higher levels of PUFAs in biomembranes contribute to preserve membrane fluidity at low temperatures and thereby ensure functioning of integral membrane proteins. At the same time a higher degree of lipid unsaturation could exacerbate membrane susceptibility to lipid peroxidation.

Lipid peroxidation of the biological membranes is highly detrimental to cell membrane structure and function (reviewed by Bucala, 1996). This process has been linked to effects such as i) increased ion permeability ii) loss of fluidity iii) cross-linking of aminolipids and polypetides, and iv) inactivation of membrane enzymes and receptors (reviewed by Girotti, 1990). Lipid peroxidation is an autocatalytic, uncontrolled process started by the abstraction of a hydrogen atom (H) from PUFA' double carbon-carbon bond to form lipid radical ($L^{\bullet}$) – 'Initiation'

$$LH + \text{oxidant} \rightarrow L^{\bullet}$$

Then $L^{\bullet}$ is combined with oxygen to give a peroxyl radical ($LOO^{\bullet}$). $LOO^{\bullet}$ abstracts a hydrogen atom from neighbouring PUFAs, thus producing a lipid hydroperoxides (LOOH) on the original PUFAs and a new lipid radical $L^{\bullet}$. The break down of LOOH to form new $LO^{\bullet}$ or $LOO^{\bullet}$, thus allowing the chain of lipid peroxidation to continue – 'Propagation'

$L^{\bullet} + O_2 \rightarrow LOO^{\bullet}$, $LH + LOO^{\bullet} \rightarrow LOOH + L^{\bullet}$

$LOOH \rightarrow LO^{\bullet} + OH^{\bullet}$

LOOH breakdown is important for two reasons: it generates radicals to propagate lipid peroxidations, and it also generates non-radical fragmentation products, such as aldehydes, e. g. Malondialdehyde or hydroxynonenal, many of which are biologically active. Ultimately, the extent of $LOO^{\bullet}$ and $L^{\bullet}$ cycling is governed by various competing 'Termination' reactions.

$L^{\bullet} + L^{\bullet} \rightarrow$ non-radical species

$L^{\bullet} + LOO^{\bullet} \rightarrow$ non-radical species

$LOO^{\bullet} + LOO^{\bullet} \rightarrow$ non-radical species

Iron can catalyse the formation of $OH^{\bullet}$ and the decomposition of LOOH to produce $LO^{\bullet}$ which are capable of abstracting hydrogen atoms from PUFAs and LOOH, producing $LO^{\bullet}$ and $LOO^{\bullet}$ which can continue to propagate lipid peroxidation.

UVA irradiation has been shown to induce lipid peroxidation in a number of studies (reviewed by Tyrrell, 1994). UVA radiation has been shown to cause a linear increase in liposomal lipid peroxidation in the absence of photosensitisers (Bose et al., 1989 and 1990). There are a number of studies showing that lipid peroxidation and membrane damage occur in cultured human cell lines such as fibroblasts and keratinocytes after UVA radiation (Morliere et al., 1991; Punnonen et al., 1991; Moysan et al., 1993:

Gaboriau et al., 1993; Vile and Tyrrell, 1995; Applegate et al., 1995; Clement-Lacroix et al., 1996). UVA induced lipid peroxidation was detected by thiobarbituric acid-reactive species (TBARs) and was decreased by vitamin E treatment in most of the studies. Membrane damage was measured by the lactate dehydrogenase (LDH) leakage assay. The UVA induced lipid peroxidation process and LDH leakage in human skin fibroblasts can be prevented by vitamin E or DFO (Gaboriau et al., 1993; Vile and Tyrrell, 1995). UVA radiation induced lipid peroxidation was found to be dependent on the "chemical" composition of membrane, enrichment of human keratinocytes with PUFAs increased the lipid peroxidation (Quiec et al., 1995).

UVA radiation induced membrane damage has been shown to be directly correlated with cell death in normal human skin fibroblasts from patients with the 'photosensitivity dermatitis/actinic reticuloid syndrome' (Applegate et al., 1994). It has also been shown that cell membranes are peroxidised by UVA radiation and become rigid and lose their integrity and selective permeability (Gaboriau et al., 1993). UVA radiation decreases both receptor-mediated and non-specific uptake of exogenous molecules (e.g. LDL) and sucrose in a dose dependent manner (Djavaheri-Mergny et al., 1993). UVA induces membrane damage in yeast and changes in permeability correlate well with lethality and are strongly oxygen dependent (Ito and Ito, 1983). UVA irradiation of skin fibroblasts of both human and mouse or human skin keratinocytes leads to the release of arachidonic acid (AA) metabolites and cyclooxygenase from the membrane (Hanson and de Leo, 1989 and 1990). This may be involved in the biosynthesis of eicosanoids. The released AA may contribute to UVA induced inflammation.

In culture systems, the two main skin cell types, keratinocytes and fibroblasts, react differently when challenged with oxidative stress. The epidermal keratinocytes, which are the major targets for carcinogenic events, are more resistant to UVA-mediated membrane damage, compared with dermal fibroblasts (Tyrrell and Pidoux, 1988; Applegate et al., 1995; Moysan et al., 1996; Leccia et al., 1998). UVA radiation caused apoptosis of fibroblasts but not keratinocytes of human skin reconstructed *in vitro* (Bernerd et al., 1998). Primary human epidermal keratinocytes are radiation resistant when compared with human fibroblasts (Kasid et al., 1987). This resistance was retained in the immortalised as well as the transformed cell lines. The mechanism behind this surprising finding has yet to be clarified. Cultured keratinocytes have a higher level of antioxidant defence pathways than fibroblasts (see section **1.4**). So it was proposed that the different sensitivity to UVA radiation may link to different antioxidant capacities. Other endogenous chromophores and membrane PUFA composition or even passage, media, buffer composition (calcium), and confluence also contribute.

Epidermal tissue of humans has a higher antioxidant level than the dermis (Shindo et al., 1994 and 1997). The skin cells derived from sun-exposed areas always have higher ferritin levels and it is proposed that they sustain less membrane damage than non-exposed skin cells (Applegate et al., 1996).

1.7.6 UVA and FEK4 fibroblasts

It has been found in our laboratory that primary human skin keratinocytes possess high basal levels of HO (provided by HO-2), and this has been proposed as a form of cellular defence against oxidative stress. The HO-1 mRNA levels are strongly inducible in primary dermal fibroblasts but barely inducible in human primary epidermal keratinocytes following oxidative stress (UVA radiation and H_2O_2) (Keyse and Tyrrell, 1990). Interestingly, constitutive HO-2 mRNA, HO-2 activity and ferritin levels are higher in primary keratinocytes when compared with matching fibroblasts. This higher ferritin level would enhance the cellular iron sequestering capacity and this may increase the resistance to oxidative stress (Balla et al., 1992; Vile et al., 1994). Both fibroblasts and keratinocytes derived from the same biopsy are sensitised to UV radiation by GSH depletion, however, the keratinocytes are sensitised to a much lesser extent, an observation which agrees quantitatively with the higher residual levels of cellular glutathione remaining after maximum depletion by BSO (approximately 25% for keratinocytes vs. 5% for the fibroblasts). GSH levels in the keratinocytes are approximately three times higher than in the fibroblasts (Tyrrell and Pidoux, 1988). UVA radiation damages membranes of the keratinocytes to a much lesser extent than those of the fibroblasts (Applegate et al., 1995). In cultured skin FEK4 fibroblasts, UVA radiation has shown short term effect (earlier events, immediately following UVA radiation up to 2 h) and long term effect (14 h to 48 h following UVA radiation).

Table 1.2 Summary of the effects of UVA radiation on cultured FEK4 cells

Short term effect	Long term efect
GSH depletion	HO-1 activity increase
Ferritin degradation, free iron increase	Microsomal heme decrease
Microsomal heme release	Ferritin level increase
Lysosome damage	Adaptive response
Lipid peroxidation in plasma membrane	

Short term effects (0 h to 2 h after UVA irradiation): immediately after UVA radiation, lipid peroxidation increases in a dose-dependent manner (Vile et al., 1994 and 1995). GSH is increasingly depleted as a function of UVA fluence (Lautier et al., 1992). 'Free' iron is released in the cells immediately following UVA radiation (Pourzand et al., 1999a). UVA also induces lysosomal damage as measured by leakage of the fluorescence lysoSensor dye in a dose dependent manner as detected by epifluorescence microscopy and by measuring the level of lysosomal chymotrypsin activity (Pourzand et al., 1999a). It also releases heme within microsomal membranes (Kvam et al., 1999) and the release of heme from hemeproteins appears to determine the degree of induction of HO-1 transcription in human fibroblasts after oxidative stress.

Long term effects (14 to 48 h after UVA radiation): UVA (250 kJ/m^2) radiation of FEK4 cells led to an increased HO-1 activity between 14 and 48 h post radiation (Vile

and Tyrrell, 1993 and 1994) and decreased microsomal heme content (Kvam et al., 1999). Heme recovered to 90% of control level 22 h post-irradiation. UVA irradiation also increased ferritin levels and this may provide protection of cells challenged with a second dose of UVA radiation (see next section).

Adaptive response in FEK4 cells

The ability of a cell, tissue, or organism to develop a better resistance to damage following exposure to the same or related stress is known as an adaptive response. In FEK4 cells, the increased ferritin level (22-46 h after UVA radiation), which was dependent on HO-1 protected FEK4 cells from subsequent UVA-induced oxidative damage to the cellular membrane (Vile et al., 1994). FEK4 cells that had been pre-irradiated showed a 2-fold increase in ferritin, leaked less LDH (which reflects cell membrane integrity) and showed less lipid peroxidation (as measured by thiobarbituric acid-reactive species, TBARs) when compared with sham-pre-irradiated cells when they were challenged with a second dose of UVA radiation. Treating cells with HO-1 antisense oligonucleotide inhibited UVA radiation dependent induction of ferritin and HO-1 and abolished the protective effect of UVA pre-radiation. DFO, an iron chelator, blocked the increase in ferritin (but not HO-1) and also abolished the protection (Vile et al., 1994).

The objectives of the project

The main objective of this project was to examine changes in labile iron following single or repeated exposures of human skin keratinocytes and fibroblasts to UVA radiation and to correlate the changes with critical biological end points such as lysosomal and plasma membrane damage. The overall aim was to gain a clearer understanding of the factors controlling the susceptibility of skin cells to solar ultraviolet radiation. Furthermore an attempt was made to identify the key reactive oxygen species that may play a role in UVA-mediated iron release. Finally the role of ferritin as a potential source of iron release was also examined in FEK4 cells.

2. Materials and methods

2.1 Chemicals

All the reagents were from Sigma Chemical Co. (Poole, UK) unless otherwise specified. All the cell culture materials were obtained from Life Sciences Technologies (Paisley, UK), except the foetal calf serum (FCS) which was obtained from PAA (Austria). Calcein (CA) and its acetoxymethyl ester (CA-AM) and LysoSensor DND-153 were obtained from Molecular Probes (Leiden, Netherlands). Salicyladehyde isonicotinoyl hydrazone (SIH) was kindly provided by P. Ponka (Lady Davis Institute, Canada). Desferrioxiamine mesylate (DFO) was from Ciba-Geigy (Basel, Switzerland). See **Fig. 2A** for their structures. MilliQ water used to prepare phosphate buffered saline (PBS) and other stock solutions were issued from a Millipore purification system (MilliQ cartridge: Millipore, Bedford, MA) in order to minimize the presence of trace elements such as transition metals. Deuterium oxide (D_2O) solution was prepared by dissolving one PBS tablet in 100 ml of 100% D_2O. Protease inhibitors (phenylemthylsulfonyl fluoride: PMSF, Leupeptin and Chymostatin) were from Boehringer, Mannheim, Germany).

2.2 Cell culture

All the cell lines outlined below were cultured routinely and incubated in a humidified atmosphere at 37°C with 5% CO_2.

FEK4 (human primary skin fibroblasts derived from infant foreskin):

The medium was 15% FCS (heat-inactivated at 56°C for 45 min before use)-EMEM (Earle's modified minimum essential medium) with 0.25% sodium bicarbonate, 2 mM L-glutamine, 50 IU/ml of each of penicillin/ streptomycin (P/S). Cells were passaged by

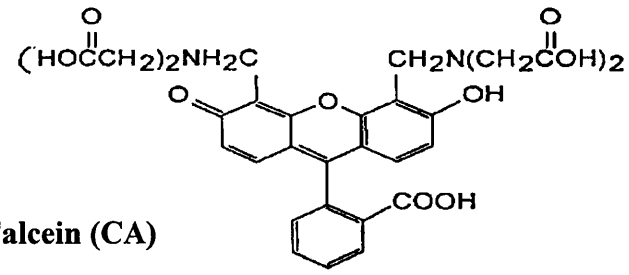

a. Calcein (CA)

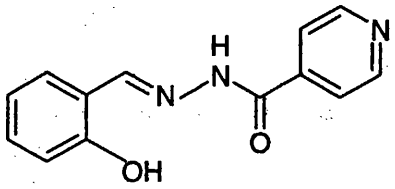

b. Salicylaldehyde isonicotinoyl hydrazone (SIH)

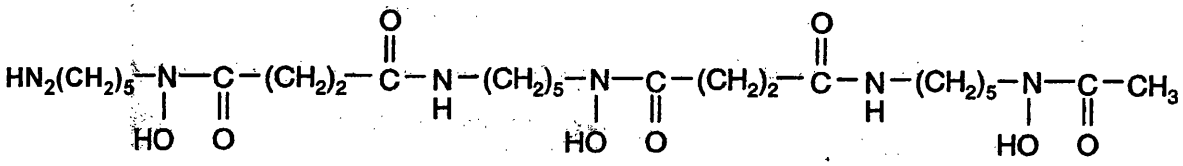

c. Desferrioxamine (DFO)

Fig. 2A Chemical structures of CA (a), SIH (b) and DFO (c)

trypsinisation once a week and were used for experiments between passages 11 and 16 as follows: 3.5×10^5 FEK4 cells were seeded and grown in 10-cm plastic plates to reach 80-85% confluency for three days, and to 95% confluency for 4 days. In some cases, cells were further cultured for one more day (5 days in culture) to reach 100% confluency. In order to study the effects of confluency on the results obtained, some cells were kept for 2 additional days after reaching 100% confluency (i.e. 7 days in culture).

1BR3 (human primary skin fibroblasts derived from adult arm)

The medium was 15% FCS-EMEM, the same as used for FEK4 cells. For experiments, 3.0×10^5 cells were seeded and grown in 10-cm plastic plates to reach 80% confluency for 4 days, and to 90% confluency for 5 days. The cells were passaged by trypsinisation once a week and were used for experiments between passages 10 and 16.

HaCaT (spontaneously immortalised human skin keratinocyte cell line derived from an adult back). This cell line maintains fully epidermal differentiation capacity, but remains non-tumorigenic. See Boukamp et al., 1988). The medium was 5% FCS-DMEM (high-glucose Dulbecco's modified eagles medium) containing 50 IU/ml P/S. For experiments, $1.8\text{-}2 \times 10^5$ cells were seeded and grown in 10-cm plastic plates for 3 days to reach 80% confluency, and to 90-95% confluency for 4 days. In some cases, cells were cultured for an additional day (5 days in culture) to reach 100% confluency.

HFK-SV61 (human foetal skin keratinocyte cell line transformed with a recombinant plasmid pSV_{61}, which contained an origin defective SV_{40} genome). This immortalised human cell line may lead to the acquisition of a malignant phenotype. See Parkinson

and Newbold, 1980). The medium was 10% FCS-EMEM containing (0.2 μg/ml) hydrocortisone. For experiments, 3×10^5 cells were seeded in 10-cm plastic plates and grown to 75%-80% confluency for 4 days, and to 90% confluency for 5 days.

2.3 Treatments

2.3.1 Chemical treatments

Hemin treatment

Stock solution: 20 mM in dimethyl sulfoxide (DMSO)

Cells were treated with 10, 20 or 50 μM (final concentration in conditioned medium in which cells had been grown) for 18 h at 37°C prior to treatments (e. g. UVA-irradiation).

Iron citrate treatment

Stock solution: 10 mM in PBS

Iron citrate was freshly made by mixing 100 mM of iron chloride with 100 mM tri-sodium citrate (in H_2O), then diluted to 10 mM in PBS and filtered. Cells were then treated with 50 μM or 100 μM iron citrate (final concentration in conditioned medium) for 18 h at 37°C prior to experiments.

DFO treatment

Stock solution: 150 mM in H_2O

DFO treatments were usually performed with 10, 50, or 100 μM (final concentration in conditioned medium) for 18 h at 37°C. In some experiments 1 mM DFO pre-treatment was undertaken (final concentration in conditioned medium) for 2 h at 37°C. For experiments involving DFO treatment following UVA radiation, DFO was added at the

final concentration of 100 μM in conditioned medium for 20 h at 37°C. The treatment was usually followed by a second challenge dose of UVA radiation.

H_2O_2 treatment

Stock solution: 25 mM H_2O_2 in PBS

Prior to the experiment, monolayer cells were rinsed twice thoroughly with pre-warmed serum free EMEM medium (SFM), in order to remove any trace of catalase from the medium. The cells were then incubated with H_2O_2 in SFM at the final concentrations of 20, 50, 100, 250, 500 and 1000 μM for 30 min at 37°C.

ATZ (3-amino-1,2,4-triazole) treatment

Stock solution: 2 M in water

Monolayer cells were washed as described above (as for H_2O_2 treatment). Cells were incubated with 50 mM ATZ in SFM at 37°C for 90 min, shaded from direct light. For H_2O_2 + ATZ treatment: H_2O_2 was added during the last 30 min treatment at the desired concentrations.

Deuterium oxide (D_2O) treatment

Stock solution: made with 100% D_2O instead of H_2O

Cells were washed with D_2O and irradiated in PBS and Ca^{2+}/Mg^{2+} based D_2O solution. That means using D_2O instead of water as a solvent during the procedure.

α-tocopherol succinate treatment

Stock solution: 20 mM in methanol

Cells were incubated with 10, 20 and 40 μM α-tocopherol succinate, respectively, in conditioned medium for 18 h at 37°C.

Butylated hydroxytoluene (BHT) treatment

Stock solution: 100 mM in ethanol

Cells were incubated with 100 and 200 μM BHT, respectively, in conditioned medium for 2 h 37°C.

Protease inhibitor treatment

Stock solutions: Chymostatin, 50 mg/ml in DMSO; Leupeptin, 20 mg/ml in H_2O

FEK4 cells were treated with 50 μg/ml Chymostatin and 20 μg/ml Leupeptin for 18 h in conditioned medium. These protease inhibitors were present during the experiment except the step in which cells were detached with cell dissociation solution (Sigma).

The final concentration of DMSO, ethanol or methanol in the cultured medium did not exceed 0.2%.

2.3.2 UVA irradiation:

Irradiation of cells in plates

Prior to irradiation, the medium was removed from the plates, and cells were washed thoroughly with PBS. Cells were then covered with PBS (4 ml for 6-cm, 10 ml for 10-cm plates) containing 5 ppm Ca^{2+} and Mg^{2+}. This was followed by irradiation of cells at doses of 100, 250 and 500 kJ/m^2. The incident dose was between 300-350 W/m^2. The UVA doses were measured using an IL1700 radiometer (International Light, Newbury, MA). The lamp emits primarily UVA radiation (significant emission in the range of

350-400 nm, see **Fig. 2B**). Irradiation was carried out in an air-conditioned room at 18°C in order to maintain the temperature of the cells to approximately 25°C throughout the irradiation procedure. In challenge dose experiments, following the first irradiation (i.e. pre-irradiation), the irradiation solution was aspirated and replaced by the saved medium (the retained medium in which cell had been grown). After the appropriate incubation time (e. g. 24 or 48 h) at 37°C, the cells were detached by trypsinization then the cell suspension was irradiated with a second dose of UV as outlined below.

Irradiation of cells in suspension

In many cases, cells were irradiated in suspension. For this purpose, the medium was first removed from the plates, and then the cells were rinsed with PBS. Next, cells were detached with 0.125% trypsin made in PBS, and then transferred to 14 ml Falcon tubes. After addition of 3% bovine serum albumin (BSA) the cell suspension was centrifuged at 1000 rpm for 1.5 min in a Jouan B 3.11 centrifuge at room temperature (RT). The supernatant was then aspirated, and PBS containing 3% BSA was added. At this point, cells were counted, and centrifuged at 1000 rpm for 1.5 min in a Jouan B 3.11 centrifuge. The supernatant was then aspirated and the pellet re-suspended in PBS containing 5 ppm Mg^{2+} and Ca^{2+} (density: 5×10^5 cells/ml). The irradiation of cells in suspension was performed in quartz cuvettes (Scientific Laboratory Supplies, UK) under constant swirling on a mixing platform (IKA Laboratechnik, Germany). Sham-irradiated samples were treated in the same manner except that they were not exposed to UVA irradiation.

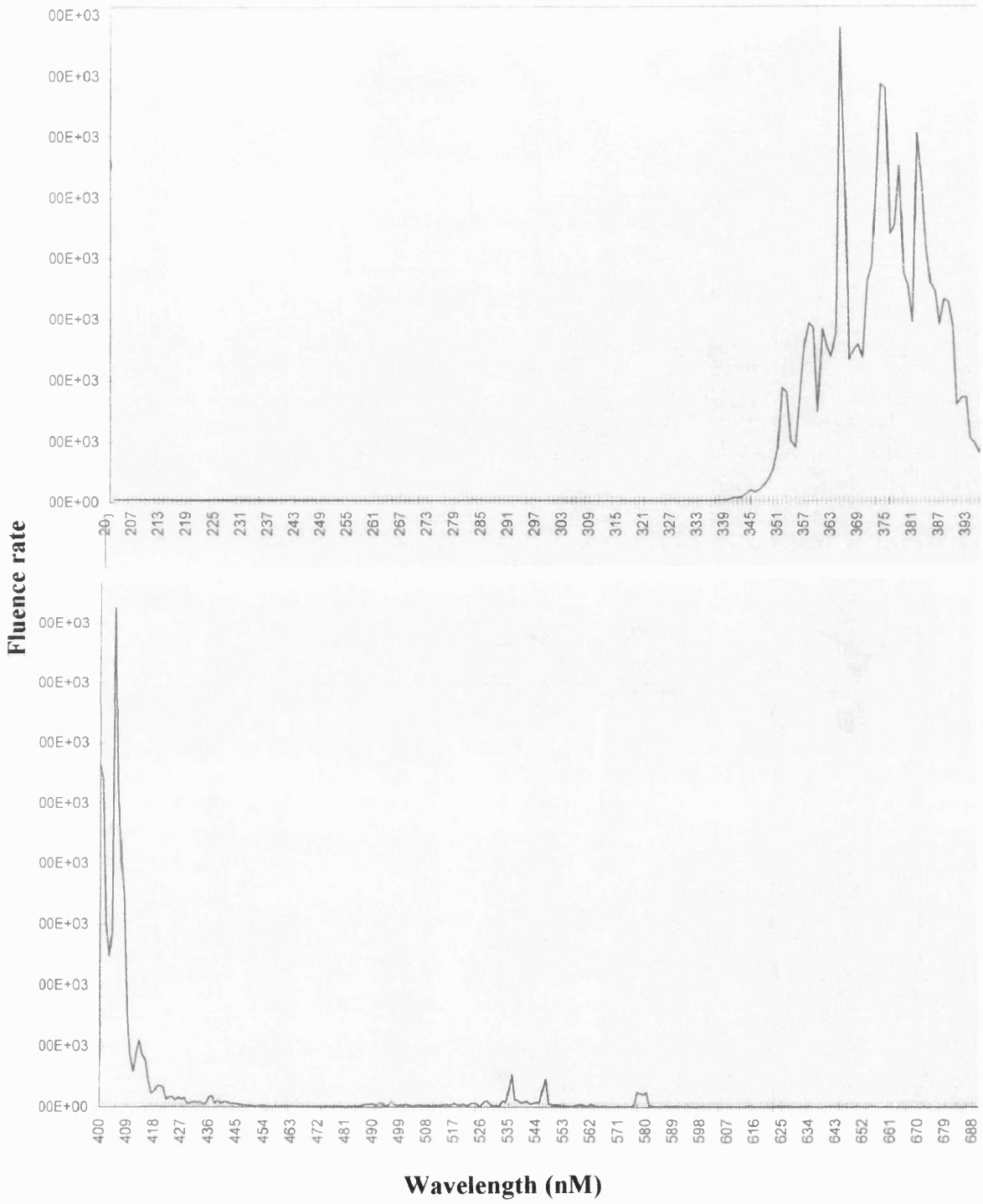

Fig. 2B The spectrum of the UVA lamp

2.4 Fluorescence calcein assay (CA-assay) and LIP measurement

2.4.1 CA-assay

CA has been used as a vital dye and has a high affinity for iron. It can be loaded easily to cells *via* its esterified acetomethoxy precursor (CA-AM) to produce intracellular CA fluorescence. A portion of the CA binds iron to form a CA bound iron complex (CA-Fe) which then has iron-quenched fluorescence. Based on this iron chelation property of CA, the group of Cabantchik (Epsztejn et al., 1997) set up a methodology to measure the CA-Fe and free iron. This method consists of measuring the magnitude of CA fluorescence dequenching by addition of a lipophilic, high affinity chelator such as SIH and allows non-invasive measurements of iron in intact living cells. By taking into account the Kd of CA-Fe, the free iron concentration can be obtained (see section **1.5.6**). The method is not cytotoxic to cells. In our original CA-assay, the procedure was long, with several centrifugation steps. Thus, it had a high and variable cell loss; poor cell recovery and decreased cell viability. The base line of CA was also variable and erratic. CA leakage from cells was high (up to 30%). Under these conditions, FEK4 fibroblasts gave a very small response or no response to SIH at all. Therefore, the CA-assay was modified as follows (unpublished results, this laboratory):

The schematic presentation of the steps for measuring CA-Fe by CA-assay

Step I

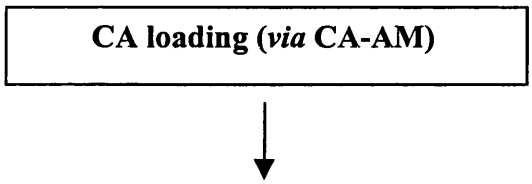

Step II

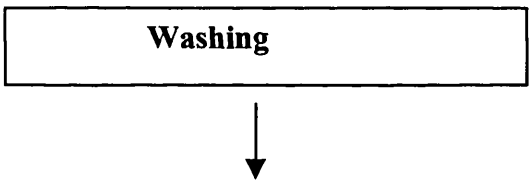

Step III

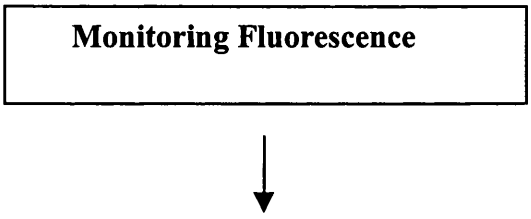

Step IV

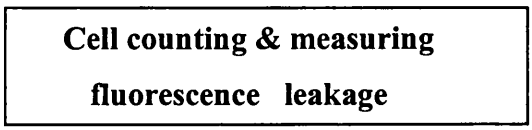

Step I: CA loading

In order to get intracellular CA, cells were loaded with CA-AM.

Immediately after treatment, cells were harvested by trypsinization (unless the cells had already been irradiated in suspension) and transferred to 14 ml Falcon tubes. BSA was then added to the cell suspension at a final concentration of 3% in PBS to keep the osmotic integrity of the cells. The cell suspension was then centrifuged at 1000 rpm for 1.5 min in a Jouan B 3.11 centrifuge. The supernatant was aspirated and the cells were loaded with 0.05 μM CA-AM in 1 ml of **loading buffer** (20 mM Hepes in bicarbonate free EMEM, pH 7.3) for 15 min at 37°C.

Step II: washing

This step allows the elimination of the excess CA-AM from the cell suspension. After loading, BSA (3% in PBS) was added to the cells followed by centrifugation at 1000 rpm for 1.5 min in a Jouan B 3.11 centrifuge. The supernatant was then aspirated and the cells were re-suspended in 4 ml of PBS containing 3% BSA centrifuged at 1000 rpm for 1.5 min in a Jouan B 3.11 centrifuge. The supernatant was then aspirated.

Step III: fluorescence monitoring

This step allows the measurement of basal fluorescence intensity of free CA, CA-Fe and total CA. After washing, the cell pellet was re-suspended in 1 ml of **fixing buffer** (10 mM Hepes in EMEM, pH7.3 with 150 mM NaCL and 2 mM diethylenetriamine pentaacetic acid, DTPA which is a non-permeable iron chelator, affinity > 10^{27}). At this point cells were transferred to a quartz spectrofluorometer cuvette. Steady state fluorescence was then measured in the thermostated (37°C) cuvette with a magnetic

stirrer in a Kontron (SMF-25, Zurich) spectrofluorometer (parameters set up excitation at 480 nm, emission at 517 nm, 10 nm slit). **Fig. 2.1** shows a schematic presentation of the CA-fluorescence measurement in the spectrofluorometer. As you can see, the initial level of fluorescence (F) attained represents the amount of free CA present in the cells. Upon additional of SIH (final concentration 40 μM) the level of fluorescence increases (i.e. dequenching). The increase in fluorescence (ΔF) resulting from addition of SIH (which has a greater affinity for iron than CA) provides an *in situ* measurement for the CA-Fe. The total fluorescence of CA (F_t) contains F plus ΔF. The ΔF can also be expressed as the percentage of F_t. That is $\Delta F / F_t$. Also see **Fig 2.2** for FEK4 cells.

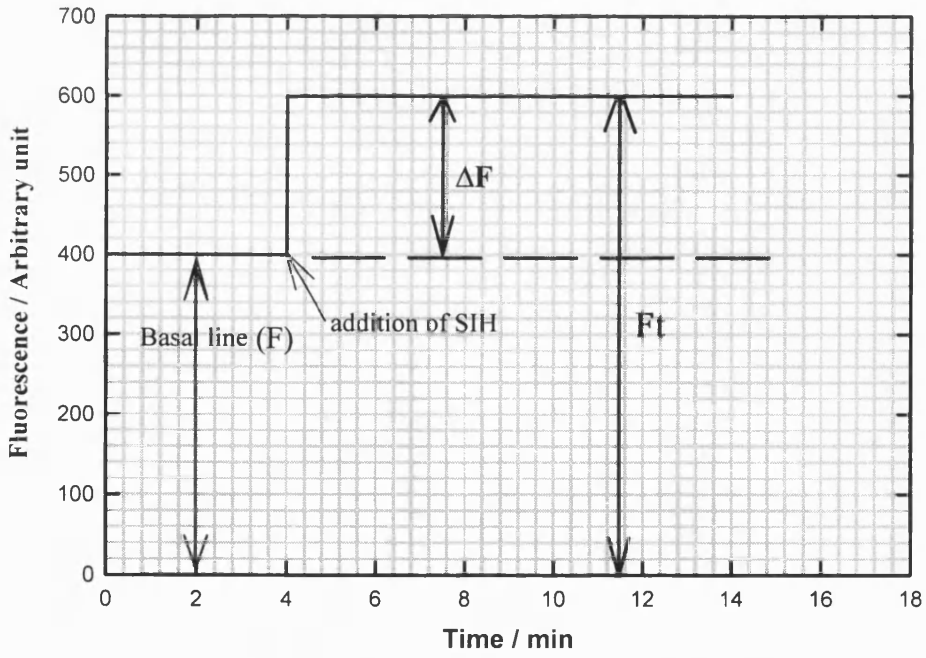

Fig. 2.1 Schematic diagram of the change in fluorescence after adding SIH

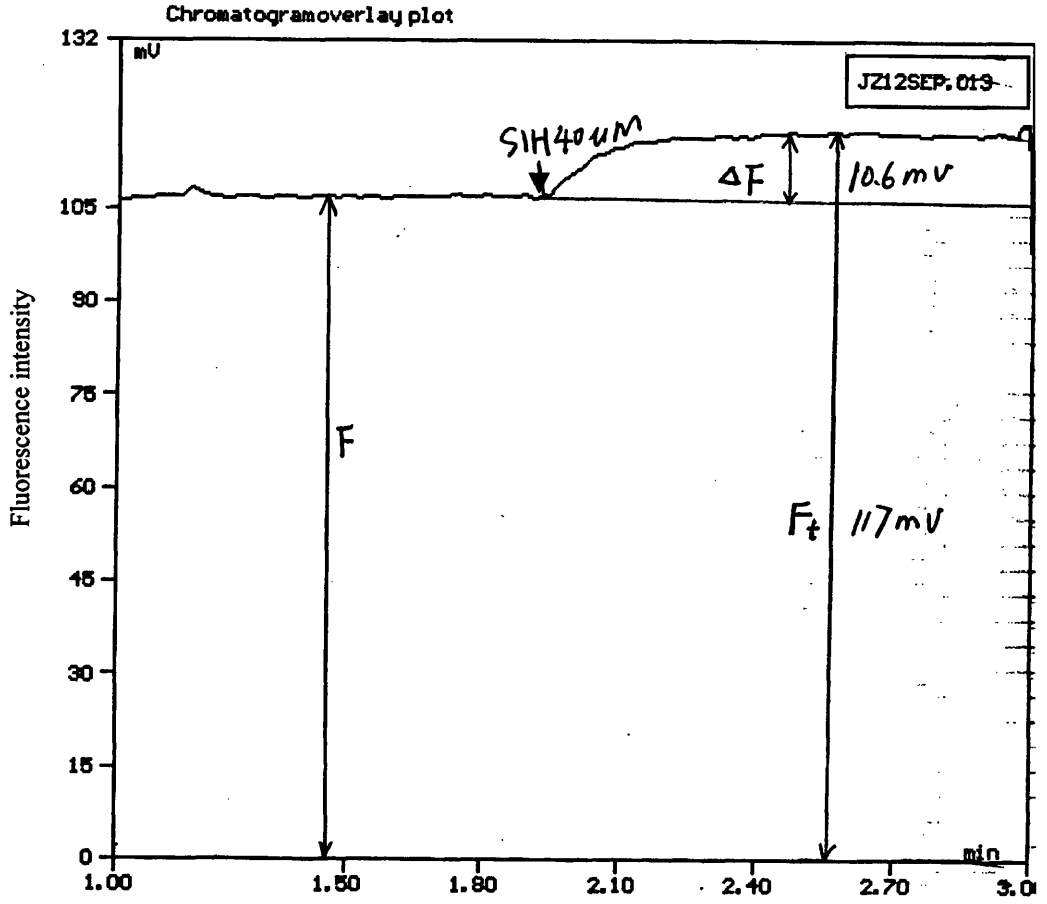

Fig. 2.2 CA-Fe estimation

CA-loaded cells (see CA-assay) were re-suspended in fixing buffer supplemented with DTPA to chelate extracellular Fe. After fluorescence (F, free CA) signal stabilisation, permeable iron chelator SIH (40 μM final concentration) was added, causing an increase in fluorescence signal (ΔF), which represent CA-Fe and can be expressed as fractional changes of the total fluorescence (free CA + CA-Fe). That is $F_f = \Delta F/F_t = 10.6/117 = 0.0906$

Step IV: cell counting and the estimation of the fluorescence leakage

This step allows the normalisation of both intracellular and extracellular fluorescence. Cells were counted under the microscope and then the suspension was transferred to a 14 ml Falcon tube and centrifuged at 1000 rpm for 2 min in a Jouan 3.11 centrifuge. The supernatant was then transferred to the cuvette and fluorescence was recorded in a spectrofluorometer, as mentioned above, and calculated by reference to the fluorescence of total CA, as the percentage of CA leakage. The CA leakage was normally below 10% of the total CA, demonstrating an improvement with methodology. So the total fluorescence measured (including a small part of extracellular CA fluorescence) in the cuvette can still represent the major fluorescence inside of the cell. Treatment that causes significant injury to cells may result in an unstable basal CA fluorescence during measurement and high leakage of CA because of damaged cell membranes. In our experiments, the basal and total CA fluorescence were stable during measurements except when cells were treated with higher concentrations of H_2O_2 (e. g. 500 μM or 1 mM). Such experiments increased the leakage of CA to more than 40% of the total fluorescence.

Significance of the fluorescence curves in the CA-assay

In order to ascertain that the response to SIH is entirely due to the chelation of intracellular CA-Fe, CA-Fe dequenching by SIH was performed in a fixing buffer supplemented with DTPA, which is an impermeable chelator, so it can be determined that the response to SIH is entirely due to the chelation of iron of intracellular CA-Fe. In the experiments, this chelator did not cause a gradual dequenching of CA that would be indicative of membrane leakage. The basal and total (after adding SIH for 10-20 min)

CA fluorescence are stable so the mobilisation of iron from macromolecular sources such as ferritin is unlikely. Therefore the method differentiates well between the small pool of cellular chelatable iron and the bulk of iron, which is bound to enzymes and proteins.

In CA-loaded cells, CA is relatively well retained inside the cells (Parish et al., 1999), has no detectable effect on a range of cellular function, e. g. In K562 cells: CA pre-loading or post-loading did not change transferrin iron uptake, indicating the cell integrity is not disturbed by CA-loading (Breuer et al., 1995a). The CA competes weakly with intracellular ligands for Fe^{2+} entering the cytoplasm (Breuer et al., 1995; Epsztejn et al., 1997), so there is a minimum disturbance to LIP itself (Breuer et al., 1995).

Cells can be easily loaded with CA via its non-fluorescent esterified acetomethoxy precursor CA-AM. For example, loading of cells with 0.5 μM CA-AM for 5 min can lead to an intracellular concentration of the de-esterified CA up to 10 μM, while cells retain full viability (Cabantchik et al., 1996). The concentration of free CA inside of the cells was found to be directly proportional to the incubation time and CA-AM concentration.

2.4.2 Calibrations: In order to obtain the relationship between the changes in fluorescence elicited by SIH and LIP in cells, all fluorescence intensities were to be converted to an intracellular CA concentration and CA-loaded cells were titrated with FAS.

The schematic presentation of the steps for calibration of LIP:

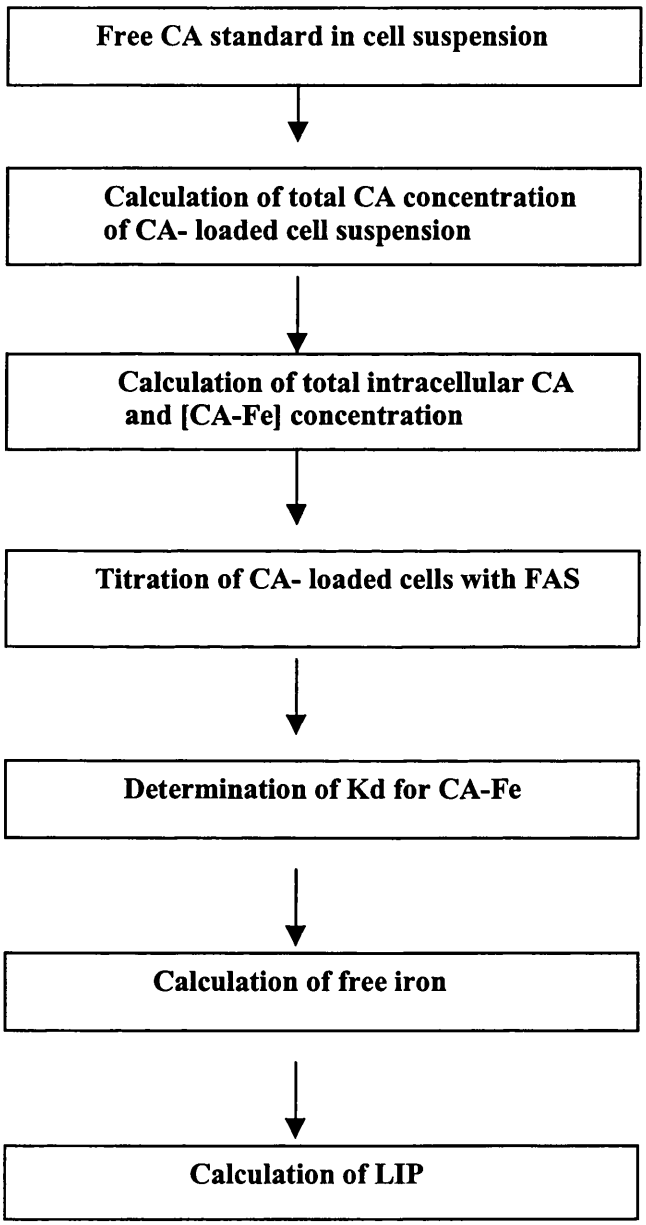

Free CA standard curve in cell suspension

In order to convert the arbitrary fluorescence intensity value to free CA concentration, incremental amount of non-permeable free CA were added to the non-treated cell suspension to monitor the subsequent change in fluorescence.

Procedure: A stock of 10 μM free CA (commercial powder) was prepared in water and diluted to either 0.1 μM (used to check the fluorescence) or 1 μM (used for a free CA standard). In this procedure, an original auto-fluorescence of cell suspension (in Hepes-EMEM) was observed. SIH (at a final concentration of 40 μM) was then added to chelate iron or other metals that could be bound to free CA. Next, a 1 nM or 2 nM free CA solution was cumulatively added into the cell suspension in order to obtain a steady increase in the fluorescence signal (see **Fig. 2.3a**). The fluorescence intensity (y) can then be plotted against free CA concentration (x) from the curve as exemplified in **Fig 2.3a**. The resulting plot is illustrated in **Fig. 2.3b** which shows that the fluorescence intensity is proportional to the concentration of free CA. By using linear regression, the relationship between fluorescence (Y) and the free CA concentration (x) can be obtained and expressed as $Y = A + Bx$, where A is cell auto-fluorescence and B is the proportional constant (slope). **Table 2a** shows the free CA standard curves for all the cell lines.

Table 2a Free CA standard of the cell lines:

Cell line	Fluorescence (Y) = A + Bx
FEK4	10.2 + 7.3x
HaCaT	11.4 + 7.3x
HFK-SV61	10.7 + 8.3x
1BR3	20.6 + 6.5x

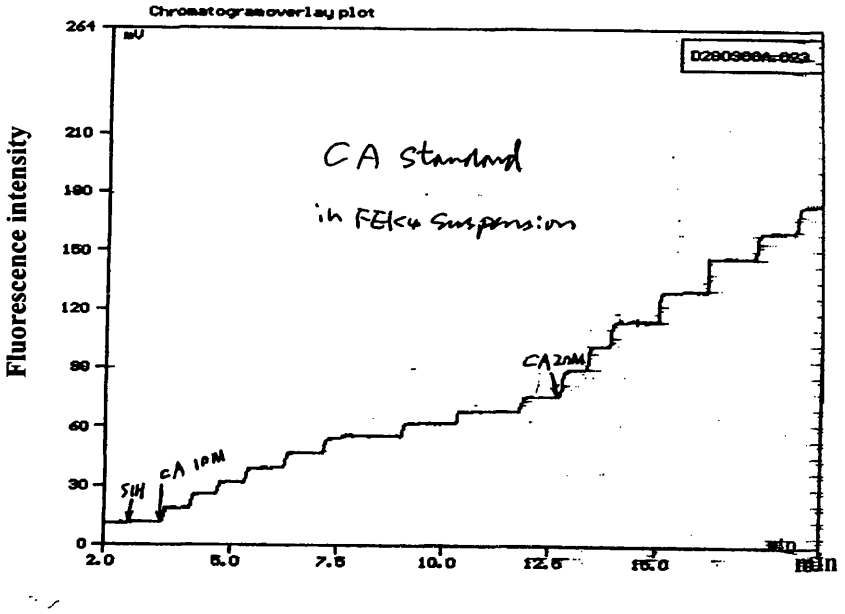

Fig. 2.3a Free CA titration of FEK4 cells
FEK4 cells were re-suspended in Hepes buffer supplemented with SIH (40 μm final concentration). 1 or 2 μM of free CA solution was added cumulatively to produce steady increase in fluorescence.

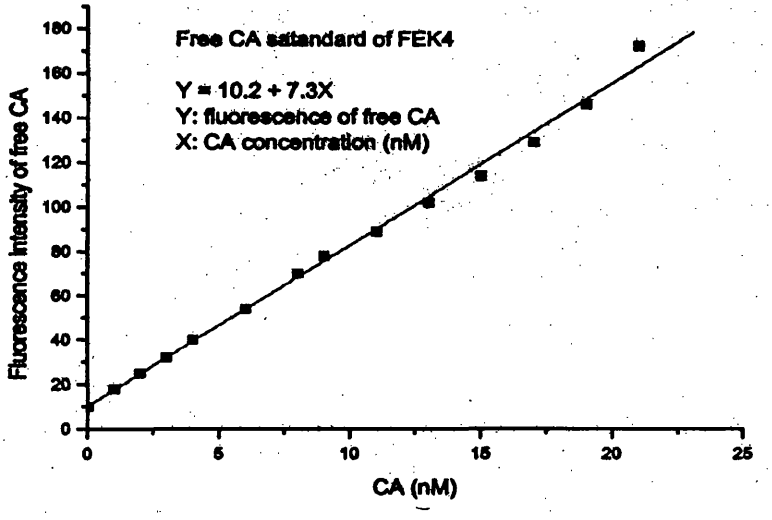

Fig. 2.3b Calibration curve for CA standard
The fluorescence intensity (Y) is converted to free CA concentration (X) using the linear regression. Y = A + Bx, e.g. FEK4 cells, Y = 10.2 + 7.3x

Total CA concentration of CA-loaded cells in suspension: $[CA]_{sus}$

Once the relationship between the fluorescence intensity and the concentration of free CA was obtained by the CA standard curve, the total CA concentration of CA-loaded cell suspension can be calculated by the total fluorescence intensity (F_t) measured by CA-assay. The conversion formula is very simple, since it only requires the rearrangement of $Y = A + Bx$ to $x = (Y - A)/B$. For example, the F_t for FEK4 is 117 mv, therefore, the free CA concentration can be calculated as $x = (Y - 10.2)/7.3$. Therefore the concentration of total CA in FEK4 cell suspension $[CA]_{sus}$ will be $(117-10.2)/7.3 = 14.63$ nM.

Total intracellular concentration of CA in CA- loaded cells: $[CA]_t$

After obtaining the total CA concentration in cell suspension, it is necessary (for calibration purposes) to determine the total intracellular CA concentration: $[CA]_t$. The $[CA]_t$ of CA-loaded cells can be worked out using the material conservation relationship. The total amount of CA in the cell suspension, $[CA]_{sus} \times V_{sus}$, must be equal to the total amount of CA inside the cells, $[CA]_t \times (Vc \times Nc)$. Here $[CA]_{sus}$ is the total CA in suspension, V_{sus} is the total volume of the suspension, Vc is the volume of unit cell and Nc is the total number of cells in the suspension. That is:

$$\mathbf{[CA]_{sus} \times V_{sus} = [CA]_t \times (Vc \times Nc)}$$

So the intracellular CA concentration can be expressed as:

$$\mathbf{[CA]_t = [CA]_{sus} \times V_{sus} / (Vc \times Nc)}$$

The unit cell volume, Vc, can be measured (see below) and Nc is obtained by counting cells under microscope. When $[CA]_{sus}$ is known, the $[CA]_t$ can be easily obtained from the above formula e. g. FEK4 cells, 1 ml of cell suspension is used.

Nc is 1.62×10^6 and Vc is 5.7 pl, and $[CA]_{sus}$ is 14.63 nM, so

$[CA]_t = [CA]_{sus} \times V_{sus} / (Vc \times Nc) = 14.63\ nM \times 1ml / (1.62 \times 10^6 \times 5.7\ pl)$

$= 14.63 \times 10^{-3}\ \mu M \times 1ml / (1.62 \times 10^6 \times 5.7 \times 10^{-9} ml) = 1.58\ \mu M.$

Cell volume measurement

The unit cell volume was measured by spinning down a certain amount of cell suspension (e. g. 4 ml $\times 10^6$ FEK4) at 1000 rpm for 1.5 min in a Jouan 3.11 centrifuge. The pellet was then re-suspended in 200 µl PBS and transferred into an eppendrof tube, then transferred into the capillary tubes with Cristasel to seal them and centrifuged at 1000 for 1 min in a Haematocrit centrifuge GIBA-GEIGY TH12. The volume of supernatant and packed cells was measured using a Haematocrit reader or a ruler. The cell volume (Vc) was calculated by using the percentage of cell packed volume divided by the number of cells, e.g. for FEK4:

$Vc = 11.4\% \times 200\ \mu l / 4 \times 10^6 = 11.4\% \times 200 \times 10^6\ pl / 4 \times 10^6 = 5.7\ pl$ (picoliter).

The cell volumes of all the cell lines used in this study were measured using this methodology as follows:

1) FEK4: $5.7 \pm 0.73\ pl$

2) HaCaT: $3.2 \pm 0.32\ pl$

3) HFK-SV61: $3.3 \pm 0.32\ pl$

4) 1BR3: $6.5 \pm 0.97\ pl$

5) Confluent FEK4: $4.0 \pm 0.3\ pl$

6) Confluent HaCaT: $2.6 \pm 0.2\ pl$

(n = 5-8)

The intracellular concentration of CA-Fe in CA- loaded cells

The concentration of the CA-Fe, which is corresponding to the change in fluorescence (ΔF) from each CA-assay fluorescence curve, elicited by adding SIH, can be expressed as the fraction of total concentration of CA as follows:

$$\mathbf{F_f = \Delta F/F_t = [CA\text{-}Fe]/[CA]_t}$$

[CA-Fe] can then be worked out when F_f and $[CA]_t$ are known from the above concentrations. The concentration of CA-Fe is equal to $Ff \times [CA]_t$.

e. g. for FEK4, $F_f = 0.09$ and $[CA]_t = 1.58$ μM, So [CA-Fe] = $0.09 \times 1.58 = 0.14$ μM.

Titration of CA- loaded cells with FAS

In order to investigate the relationship between fluorescence intensity of CA and intracellular iron concentration, the CA-loaded cells need to be titrated with a certain amount of ferrous ammonium sulphate (FAS). Since FAS is a source of Fe^{2+}, a divalent metal ionophore A23187 was used to internalise the compound. Ionophore A23187 allows the equilibrium the metal between cells and medium. Incremental amounts of doses of FAS were added, and the change in the fluorescence intensity corresponding to each step increase was recorded.

Procedure

A stock of FAS was prepared by dissolving the compound in argon treated MilliQ water and the solution maintained under argon to prevent oxidation of the ferrous iron. Non-irradiated FEK4 cells were loaded with CA *via* CA-AM as described above and re-suspended in 20 mM Hepes-EMEM, 150 mM NaCL without DTPA, pH 7.3 and transferred to the cuvette in the spectrofluorometer. Next, the cells were treated with 10 μM divalent metal ionophore A23187 (from a 5 mM stock solution in DMSO), which increased the permeability of divalent metal ions to the cell membranes, and also caused

around 5% increase in the original fluorescence due to the metal gradient. A stable basal line of the fluorescence signal was obtained, which corresponds to the concentration of free CA in the cell suspension. Next, a 0.5 or 1μM FAS (final concentration in cell suspension) was added cumulatively to the cell suspension, and the discrete decreases in fluorescence (CA-Fe) were monitored and recorded until a plateau was reached, where the fluorescence did not change upon further addition of FAS.

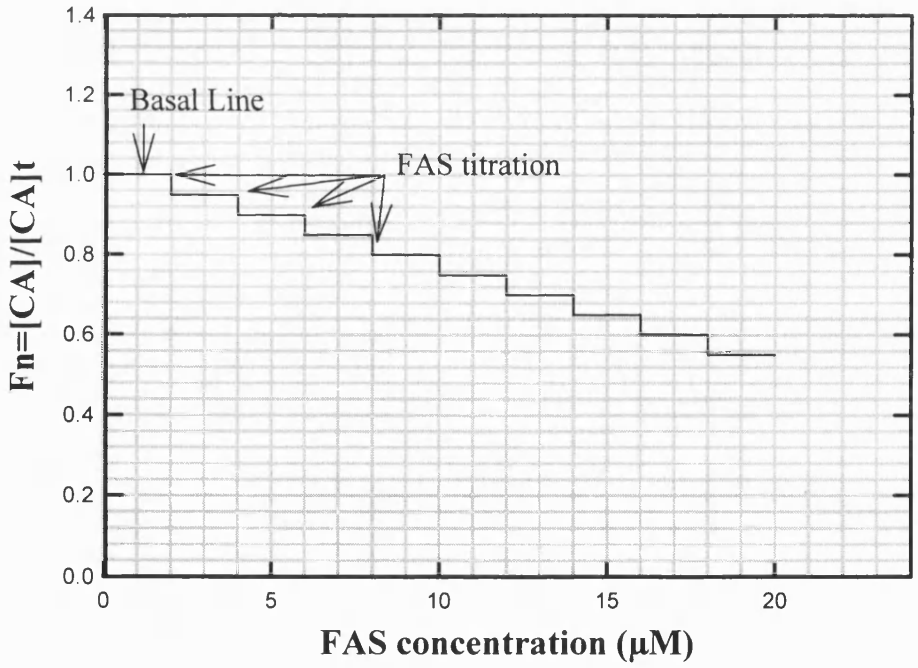

Fig. 2.4a A schematic diagram for a FAS titration curve in the cell suspension

Fig. 2.4a shows schematically a curve for titration of the cells with ferrous solution. The concentration of the free CA, was normalised as Fn = $[CA]/[CA]_t$. It is worthy of the notion that this titration relies on the assumption that in the presence of ionophore A23187, ion channels are fully open and that ferrous ions can freely move in/out the cell membrane. See **Fig. 2.9a** for FEK4 cells.

Determination of the dissociation constant (Kd) of CA-Fe

As mentioned earlier, LIP in cells is operationally defined as

$$\mathbf{LIP = [Fe] + [CA\text{-}Fe]}$$

Indeed, upon addition of CA-AM to cells, [CA] and [Fe] rapidly reach equilibrium, i.e.

$$\mathbf{CA\text{-}Fe} \overset{\mathbf{Kd}}{\rightleftharpoons} \mathbf{CA} + \mathbf{Fe} \qquad (1)$$

at time 0	0	$[CA]_t$	0
at equilibrium	[CA-Fe]	[CA]	[Fe]

The concentrations of intracellular [CA] and [CA-Fe] can be obtained by the method described in previous sections. However, in order to calculate the level of free iron in the cells (i.e. [Fe] unbound to CA, the Kd of CA-Fe needs to be calculated. In

$$Kd = \frac{[CA] \times [Fe]}{[CA\text{-}Fe]} \qquad (2)$$

quantitative terms, the formation of CA-Fe in cells will depend on the relative concentrations of free C a nd free Fe and the apparent Kd of CA-Fe. At equilibrium, the Kd of CA-Fe can be calculated as follows:

$$[CA]_t = [CA] + [CA\text{-}Fe] \qquad (3)$$

$$[Fe]_{add} = [Fe] + [CA\text{-}Fe] \qquad (4)$$

Where [CA], [Fe], and [CA-Fe] are concentrations of CA, Fe and CA-Fe in solution at equilibrium, and $[Fe]_{add}$ is the concentration of Fe added to reach new equilibrium into cell suspension after starting the titration. The concentrations of CA and CA-Fe can be expressed as a function of concentration of CA by simple transformation from (3) and (4). They are

$$[CA\text{-}Fe] = [CA]_t - [CA] \tag{5}$$

$$[Fe] = [Fe]_{add} - [CA\text{-}Fe] = [Fe]_{add} - [CA]_t + [CA] \tag{6}$$

The substitution of equations (5) and (6) into equation (2) will yield the equation (7) as follows:

$$Kd = \frac{[CA]\{[Fe]_{add} - [CA]_t + [CA]\}}{[CA]_t - [CA]} \tag{7}$$

So have

$$Kd\,[CA]_t - Kd\,[CA] = [CA]\,\{[Fe]_{add} - [CA]_t\} + [CA]^2 \tag{8}$$

$$[CA]^2 + [CA]\,\{[Fe]_{add} - [CA]_t\} + Kd\,[CA] - Kd\,[CA]_t = 0 \tag{9}$$

$$[CA]^2 + \{[Fe]_{add} - [CA]_t + Kd\}[CA] - Kd\,[CA]_t = 0 \tag{10}$$

Equation (10) can be easily solved and its solution can then be expressed as

$$[CA] = \frac{-\{[Fe]_{add} - [CA]_t + Kd\} \pm \sqrt{\{[Fe]_{add} - [CA]_t + Kd\}^2 + 4Kd[CA]_t}}{2} \tag{11}$$

The dimensionless parameter, Fn, can be defined in the case as

$$Fn = \frac{[CA]}{[CA]_t} \tag{12}$$

Dividing $[CA]_t$ in the two sides of equation (11) and therefore have

$$Fn = 1 - \frac{\{[Fe]_{add} + Kd + [CA]_t\} \pm \sqrt{\{[Fe]_{add} + [CA]_t + Kd\}^2 - 4[Fe]_{add}[CA]_t}}{2[CA]_t} \quad (13)$$

If set Y = Fn; P1 = $[CA]_t$, the total CA concentration; P2 = Kd, the CA-metal dissociation constant; X = $[Fe]_{add}$, the concentration of free metal Fe in solution. The above equation then becomes

$$Y = 1 - \{P1 + P2 + X - [(P1 + P2 + X)^2 - 4*P1*X]^{1/2}/2P1\} \quad (14)$$

This equation is a general form for titration of Fe in solution and is identical to the one cited in the literature (i.e. Epsztejn et al., 1997). In our experiments, Kd of CA-Fe was obtained by non-linear fitting of the curve using the Origin program (version 6).

Significance of the Kd value in CA-assay

It can be seen that when the concentrations of CA and CA-Fe are obtained by the methods above, and the Kd is determined, the free iron concentration in the cells can be worked out. Both Kd and the concentration of the CA are unknown; Kd is the property of the system studied, therefore, by addition of a known amount of Fe (i.e. FAS) into the system and monitor the fluorescence intensity changes (F) of the CA versus the metal concentration, which is termed as titration, the Kd of CA-Fe could be obtained.

Analysis of the titration curves for determination of cell dependent Kd values

First the titration curve is estimated when Kd is given with a 5 μM intracellular CA solution. **Fig. 2.5** and **Fig. 2.6** show a range of Kd from 1000 to 2 μM and 1 to 0.01 μM, respectively. Those curves will shift up or down when different initial CA concentrations are used but their shapes will remain the same under a chosen Kd. This is difficult for comparison, so that normalised concentrations of free CA which are

defined as $[CA]/[CA]_t$, are used. **Fig. 2.5** and **Fig. 2.6** are then therefore re-plotted as **Fig. 2.7** and **2.8**. It can be seen from **Fig 2.7** and **Fig. 2.8** that the Kd is greater than 20 or smaller than 0.1, the titration method is not sensitive enough for the determination of the Kd. This is because the change in the concentration of free CA is either too small or too big to be identified. That also means that the best values of Kd analysed by titration method are those between 0.1 and 20. Kd can be estimated using above predicted curves form the original shape of titration curve. Values of Kd analysed by titration method are those between 0.1 and 20. See **Fig. 2.9a** and **2.9b** for FEK4 cells.

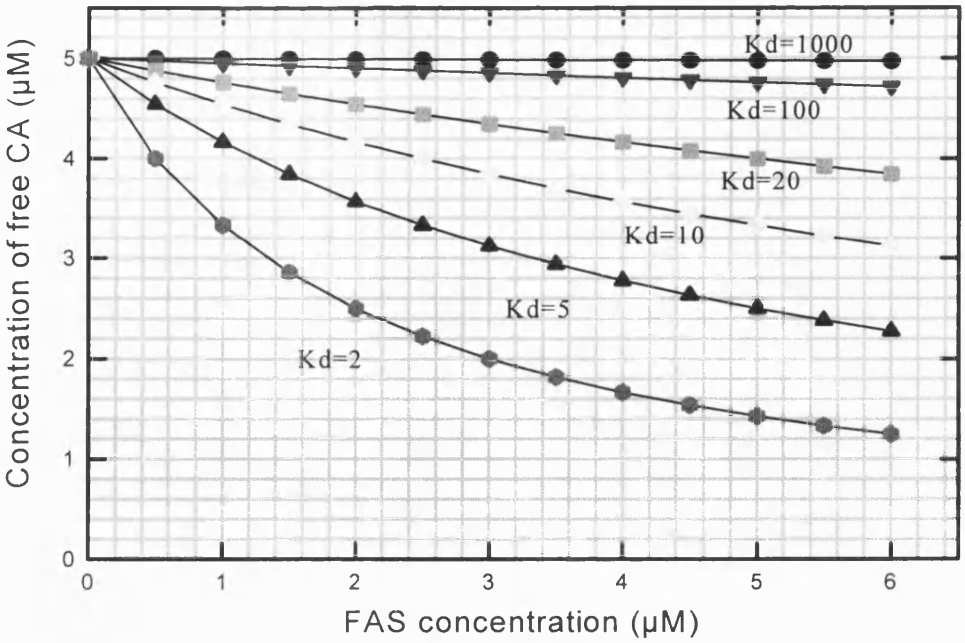

Fig. 2.5 Titration curves of Fe^{2+} calculated by equation (2)
in a 5 μM CA solution under different Kd ranged from 1000 to 2 μM

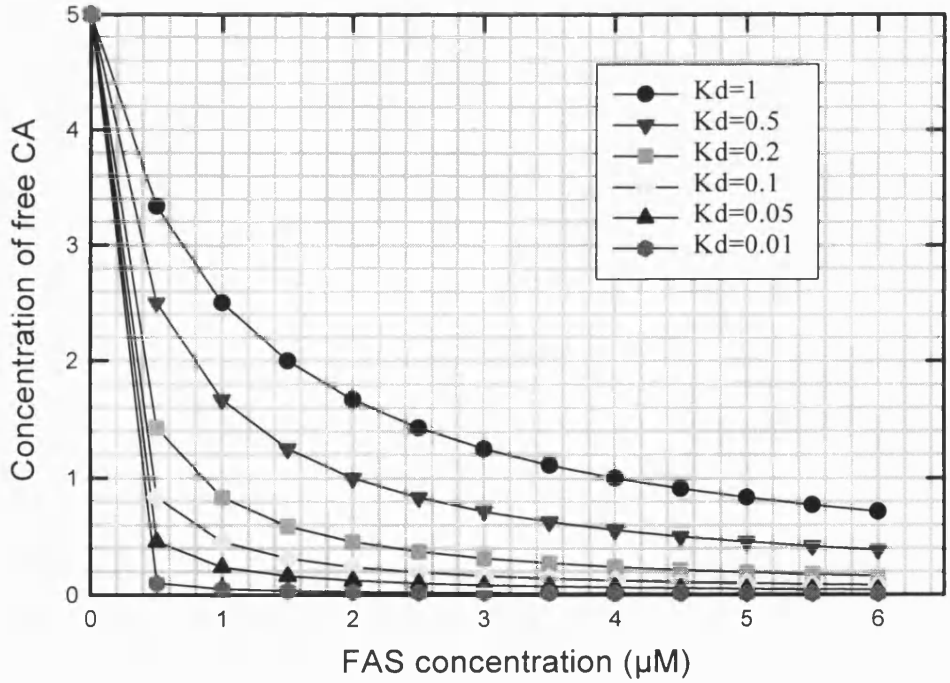

Fig. 2.6 Titration curves of Fe^{2+} calculated by equation (2)
in a 5 μM CA solution under different Kd ranged from 1 to 0.01 μM

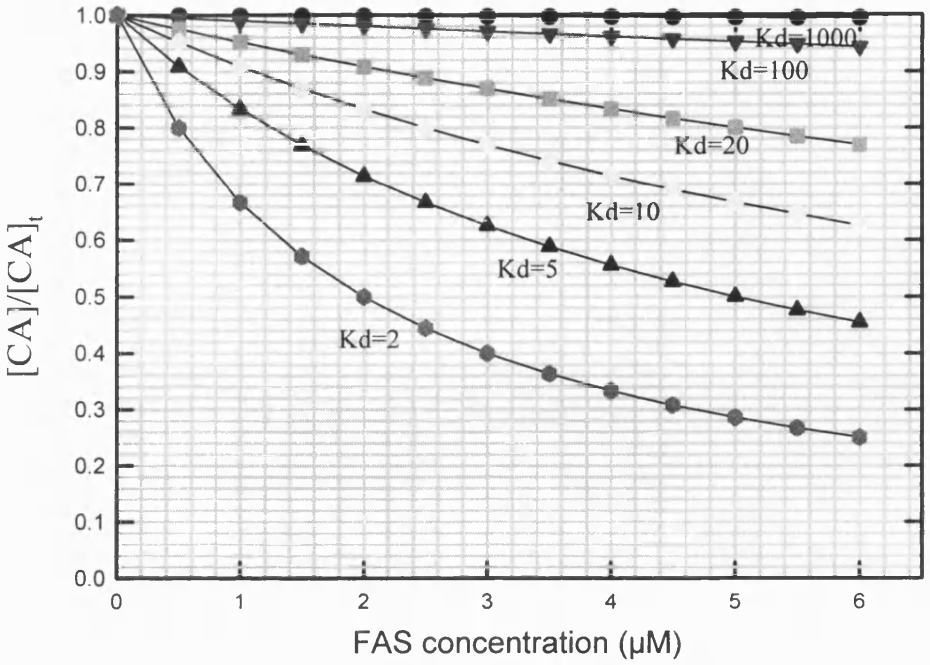

Fig. 2.7 Titration of Fe^{2+} in a 5 μM CA solution.

This one is the same as Fig. 2.5 but $[CA]/[CA]_t$ instead of [CA]

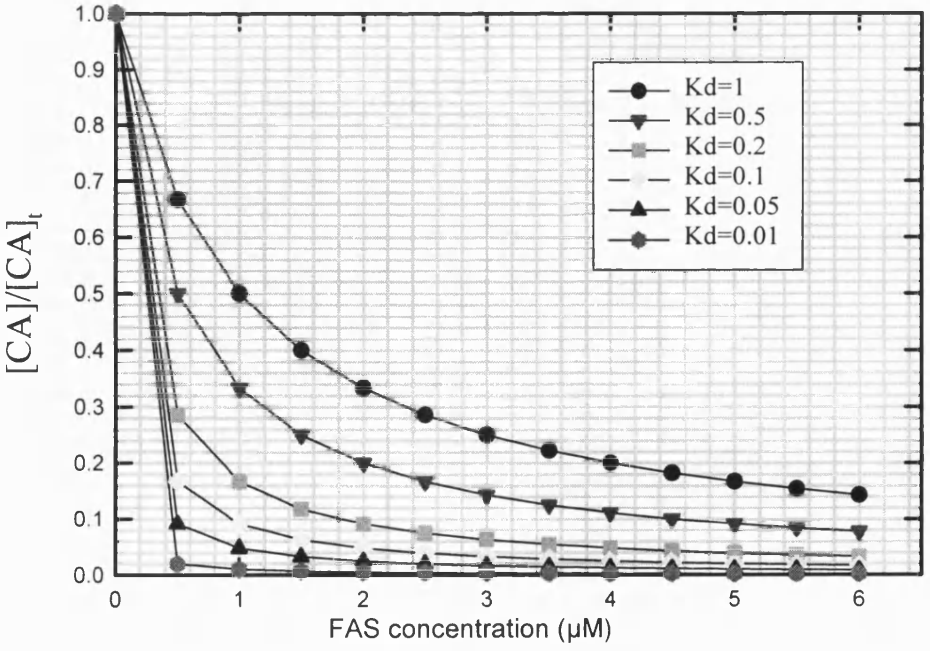

Fig. 2.8 Titration of Fe^{2+} in a 5 μM CA solution.

This one is the same as Fig. 2.6 but $[CA]/[CA]_t$ instead of [CA]

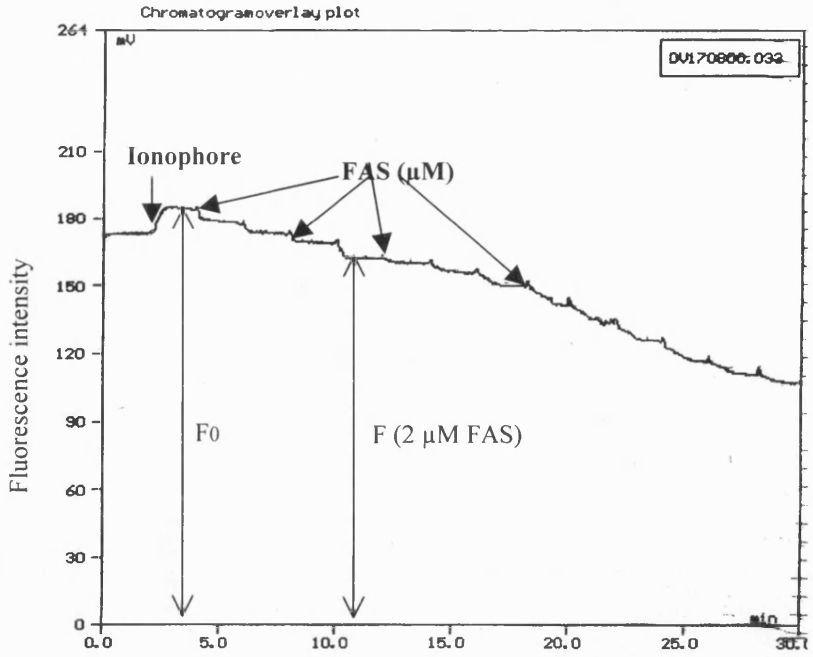

Fig. 2.9a Titration of CA-loaded FEK4 cells with FAS

Ionophore (final concentration 10 μM) was added to CA-loaded cells to allow permeabilization of cells to divalent metal FAS. Each 2-3 min, 0.5-1 μM FAS was added (from a 0.5 or 1 mM stock) to cell suspension and the fluorescence quenching by metal concentration was recorded. For each metal concentration, the fluorescence intensity of free CA was then expressed as the fractional of the original fluorescence, e.g. 2 μM FAS, Fn = F/F0

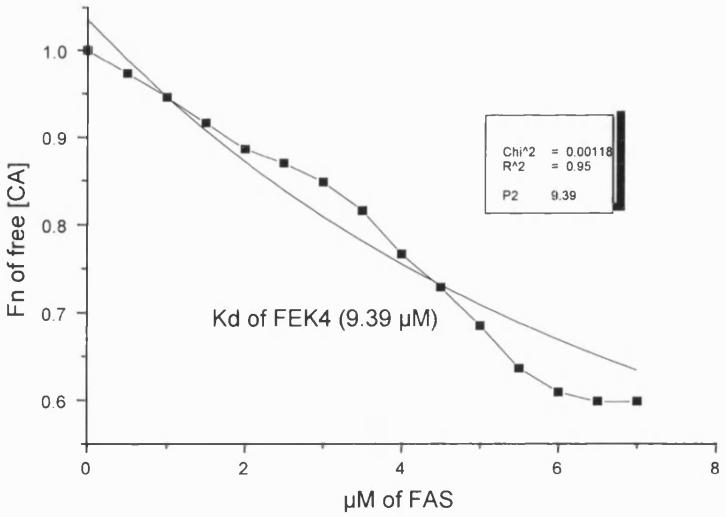

Fig. 2.9b Estimation of Kd of CA-Fe of FEK4 cells

From the titration of **Fig. 2.9a**, the free CA fluorescence intensity was first normalised to the initial fluorescence value (Fn), and then plotted against the metal concentration. The curve through the experimental points represents the non-linear least-squares best fit yielding Kd = 9.49 μM, as described under **materials and methods**.

The Kd value for the cell lines

FEK4: 12.7 (median, n = 20)

1) HaCaT: 9.8 (median, n = 12)
2) HFK-SV61: 4.5 ± 0.6 (n = 6)
3) 1BR3: 19.6 ± 1.23 (n = 5)

Free iron [Fe] of the cells

Kd = [CA] x [Fe]/ [CA-Fe], so

[Fe] = Kd [CA-Fe]/{[CA]t – [CA-Fe]}

i.e. for FEK4, [Fe] = 12.7 x 0.14/(1.58-0.14) = 1.23 μM

LIP of the cells

LIP = [CA-Fe] + [Fe], for FEK4 cells:

LIP = 0.14 + 1.23 = 1.37 μM

2.5 Ferritin ELISA

The objective of the study was to quantitatively determine the level of ferritin after specified treatments using a polyclonal (anti-ferritin) enzyme-linked immunosorbent assay (ELISA) kit known as the Enzyme-Test ® Ferritin kit (Roche, UK). Principles of the method: Cytosolic extracts are prepared and added to a streptavidin tube along with biotinylated (monoclonal, mouse anti-ferritin antibodies) and monoclonal, mouse anti-ferritin antibodies labelled with peroxidase (the incubation solution). [one-step sandwich]. The antibodies bind to streptavidin, thus anchoring the ferritin/antibody complexes to the tube. Excess antibodies are then removed by a washing step. Next, the substrate-chromogen solution, ABTS ® (di-ammonium 2, 2'-azino bis 3-ethylbenzothiazoline-6-sulphonate), is added. ABTS® is a peroxidase substract and is cleaved by the peroxidase to produce a characteristic green coloured product, which is measured spetrophotometrically. This is intended to provide a quantitative determination of ferritin present in the sample's cytosolic extract.

Preparation of cytoplasmic extracts for ferritin analysis

Immediately after the treatments, cells were collected from plates by trypsinization (or directly collected when cells were in suspension) and re-suspended in ice-cold PBS and centrifuged at 1500 rpm for 5 min at 4°C in a Jouan CR412 centrifuge. The supernatant was then removed and cells were suspended in 1 ml of fresh ice-cold PBS. Next, cells were counted and centrifuged as above. The supernatant was then aspirated and the cells were re-suspended in ice-cold (1X) Munroe lysis buffer containing 10 mM Hepes pH 7.5, 3 mM $MgCL_2$, 40 mM KCl, 5% glycerol and chymostatin (50 µg/ml), leupeptin (20 µg/ml), and 0.3% NP-40 (Merck, UK) and lysed on ice for 10 min (30 µl of 1X Munroe

lysis buffer/1x10^6 cells). Lysates were then centrifuged at 2500 rpm for 7 min at 4°C in a Jouan CR412 centrifuge. Next, the cell extract (supernatant) was removed and placed in a 1.5 ml tube for flash freezing in a mixture of dry ice and 95% methanol. Extracts were then stored at –70°C till use.

Protein measurement

Quantification of cytosolic proteins: The extracts were thawed and protein concentration was determined by Bradford assay with the BioRad reagent kit, UK (Bradford, 1976). A series of concentrations of BSA (100 mg/ml stock, Roche, UK) were made from 0 to 20 µg/ml for standard calibration curve and absorbance measurements obtained using a 96-well microplate reader (Dynatech MR5000) at 595 nm. Measurements were performed in duplicate on 2-10 µl aliquots of the extracts and the mean values were obtained from duplicate experiments.

Procedure for ferritin :

Cells extracts were prepared for the measurement of ferritin content. All reagents were brought to room temperature before use. Ferritin standards and cell extracts were added to separate streptavidin-coated tubes. Incubation buffer (containing the anti-ferritin antibodies) was added to each tube and incubated at room temperature for 30 min. The tube contents were then aspirated, and rinsed with the washing solution followed by aspiration. The chromogen-substrate solution was then added to each tube. The tubes were incubated for 15 min at RT and the absorbance was determined immediately at 420 nm using the spectrophotometer (UVIKON 922). The concentration of ferritin protein in each extract was determined against the ferritin standards. This value was

then normalised using the total cytosolic protein content obtained from the Bradford assay and expressed as ng of ferritin per mg of protein (ng ferritin/mg).

2.6 Epifluorescence microscopy studies

The LysoSensor Green DND-153 dye was used to monitor the integrity of lysosomal membrane in both the fibroblasts and keratinocytes following UVA radiation treatment using epifluorescence microscopy. The LysoSensor dyes are pH indicators which partition into acidic organelles (lysosomes and Golgi apparatus). These acidotropic probes accumulate in acidic organelles as a result of protonation. This protonation also relieves the fluorescence quenching of the dye by its weak base side chain, resulting in an increase in fluorescence intensity. They freely permeate to cell membranes and typically concentrate in spherical organelles.

LysoSensor treatment (loading)

Cells grown on coverslips (inside 10-cm plates) for 3 days (80% confluency) were irradiated and then incubated for 2 h with fresh medium containing 1 μM LysoSensor probe. Then the medium (with the excess dye that was not taken up by the cells) was aspirated. Next, the coverslips (on which the stained cells were growing) were removed and placed on microscope slides suspended in approximately 20 μl of fixing medium (EMEM without phenol red supplemented with 5% FCS and glutamine). Coverslips were then fixed to the slides using nail vanish, and were viewed under the epifluorescence microscopy (Nikon, Japan; Excitation at 443 nm and emission at 505 nm). Photographs were taken (using a 35 mm Nikon camera) at 400 × magnifications at a range of exposure times from 10 to 45 seconds.

2.7 Cathepsin B (Cath B) ELISA

The objective of the study was to quantitatively determine the level of either total Cath B present in cells or in cytosol devoid of intact membrane (cytosolic S-100 fraction, see Dignam et al., 1988). Cath B test (supplied by KRKA, d.d. Jozef Stefan Institute, Ljubljana, Slovenia) is a sandwich immunoassay for the quantitative measurement of human Cath B (HCB) in tissue, cytosols and body fluids. Microtiter strip wells are supplied as a solid phase coated with rabbit polyclonal antibodies specific for HCB.

During the first incubation period antigens present in samples, controls or calibrators are bound to the antibodies at the solid phase. Unbound material is removed by a washing step. In the second incubation sheep anti-HCB antibodies, conjugated with horseradish peroxidase (HRP) are added into each well resulting in the formation of a sandwich complex:

Immobilised rabbit anti-HCB IgG*cathepsinB*sheep anti-HCB IgG-HRP

The unbound conjugate is removed by the second washing step. Enzyme-linked complex is then detected by incubation with TMB substrate solution (i.e. 3,3,5,5, -tetramethylbenzidine and H_2O_2). The developed blue colour is changed into yellow by stopping the reaction with 2 M sulphuric acid. The intensity of the colour developed is read at 450 nm using microtiter plate reader (Dynatech MR5000) and is proportional to the concentration of Cath B in the specimen, within the working range of the test. The Cath B concentration of the specimen and control was then determined from the calibration curve obtained by plotting the Cath B concentration of the calibrators versus the absorbance at 450 nm. Cath B concentration is expressed as nmol/l.

Preparation of S-100 cytoplasmic extracts

Immediately after treatment (i.e. UVA irradiation), cell suspension was transferred to 14 ml Falcon tube and centrifuged. Cell pellets were re-suspended in 5 ml of ice-cold PBS and spun at 1500 rpm for 5 min at 4°C in a Jouan CR412 centrifuge. Supernatants were aspirated and cell pellets were re-suspended in five packed cell pellet volumes of Dignam (1983) buffer A (10 mM Hepes, pH 7.9, 1.5 mM $MgCL_2$, 10 mM KCL) and incubated on ice for 10 min. Cells were collected by centrifugation as before and resuspended in 4 packed cell pellet volumes. Cell suspension were transferred to glass homogeniser tubes and lysed by 10 to 12 strokes to obtain 90% cell lysis (depends on cell lines). Alternatively, the homogenisation step was replaced with mild detergent lysis (i.e. 0.3% NP-40). Cells were transferred to 14-ml Falcon tubes and centrifuged at 1850 rpm for 10 min at 4°C in a Jouan CR412 centrifuge. Supernatant were then carefully transferred into eppendorf tubes (avoid mixing with the unwanted nuclei) and mixed with 0.11 volumes of Dignam buffer B (300 mM Hepes, pH 7.9, 30 mM $MgCL_2$, 1.4 M KCL). This was followed by centrifugation at 35,000 rpm for 1 h in a Beckman L8-M Ultracentrifuge (rotor type ILI 70,000). Supernatant were then transferred to fresh eppendorf tubes (i.e. to avoid the contamination with the pellet) and flash-frozen and kept at –70°C till use.

Total protein was measured according to the Bradford assay. The concentration of the extracts for the Cath B was adjusted to 0.06 and 0.12 or even 0.2 mg/ml protein (depends on the cell lines) with Cath B standards.

Prepartion of total cell extracts

FEK4 cells grown on 10-cm plates to 80-85% confluency were washed with PBS, then scraped in cold PBS (3 ml/plate) and collected in 14-ml Falcon tubes. Cells were spun at 1500 rpm for 7 mins in a Jouan CR412 centrifuge at 4^0C. Supernatant was aspirated and cells were re-suspended in 1 ml PBS and counted. Cells were then spun as above. The supernatant was aspirated, cells were lysed in **solubilisation buffer** (50 mM Tris-HCL, pH7.5, 150 mM NaCL, 10% Glycerol, 5 mM EDTA, freshly supplied with 1% NP-40 and 1 mM PMSF) at 30-50 µl/1x10^6. The lysate was transfer to an eppendorf tube and spun at 13,000 rpm for 2 min in Heraeus Bio-fuge13 at 4^0C. Supernatants were transferred to clean tubes for the Bradford assay.

Procedure for Cath B

Calibrators (standard, 100 µl), diluted cytosol S-100 or total cell extracts were pipetted into selected wells which coated with rabbit anti HCB IgG; 100 µl of dilution buffer was used as for the substrate blank (0 nmol/l calibrator). After 2 h incubation at 37°C (under dark condition), the content of the wells was aspirated and the wells were washed 3 times with 400 µl of *washing solution.* Then the remaining fluid was removed by tapping the microtiter strips on absorbing paper. Next, 100 µl of sheep anti HCB IgG conjugate with HRP solution was dispensed into the wells and incubated 2 h at 37^0C (under dark condition). The solution was then aspirated and the wells were washed 3 times with 400 µl of *washing solution* as before. Next, 200 µl of *TBM Reagent plus Substrate* (3,3,5,5, -tetramethylbenzidine and H_2O_2) was added into the wells and the microtiter was incubated 15 min at RT in the dark. The enzymatic reaction was stopped by adding 50 µl of *stopping solution* (2 M sulphuric acid) to all the wells after which, the absorbance was measured at 450 nm with a plate reader (Dynatech MR5000).

2.8 Cath B immunohistochemistry

Antibody coupled to Fluorescein Isothiocyanate (FITC) was used to visualise the lysosomal enzyme, Cath B.

Cells were grown on coverslips for the LysoSensor experiments. After treatments, cells were re-incubated in conditioned medium for 1 h. Medium was aspirated, cell coverslips were rinsed with cold PBS 3-4 times and fixed with methanol for 5-6 min at RT, and kept at -20^0C till use. Cells were rehydrated by soaking the coverslips for 10 to 15 min in PBS at RT (checked under microscope), and drained gently with absorbing paper. Next, cells were blocked (to decrease non-specific binding) for 10 min at RT with 40 µl of Buffer X (BSA, 0.4 g; 100% Triton 20 µl; PBS, 20 ml) for each coverslip. Next, cells were drained of excess liquid and incubated with the polyclonal rabbit anti-human Cath B IgG (supplied by KRKA, d.d. Jozef Stefan Institute, Ljubljana, Slovenia) in 1:25 dilution Buffer X for 1 h at RT. Thereafter, the coverslips were washed gently with PBS at RT (coverslips were soaked in the buffer for 3 min). After washing, cells were incubated with the goat anti-rabbit IgG antibody coupled to FITC (dilution: 1:80) for 1 h at RT under dark conditions. Coverslips were then drained as before and mounted on slides with 20 µl of 4-Diazabicyclo[2.2.2]octane (DABCO). Excess liquid was drained with absorbing paper and sealed with nail vanish and dried for 10 min on the bench. Slides were analysed by epifluorescence microscopy as described before for lysoSensor experiments. It is critical to avoid letting the cells dry and cells should be covered with parafilm during incubation.

2.9 LDH assay

Lactate dehydrogenase (LDH) reflects cell membrane integrity, which catalyses pyruvic acid reduced to lactic acid in the presence of NADH. The reaction scheme used is as follows:

$$\textbf{Pyruvic Acid + NADH} \xrightarrow{\textbf{LDH}} \textbf{Lactic Acid + NAD}$$

The objective of the LDH assay was to measure the integrity of cell membranes by monitoring the leakage of LDH into the extra cellular media following different treatments. For this purpose, the LDH activity was spectrophotometrically determined by measuring the rate NADH disappearance at 340 nm during the LDH-catalysed conversion of pyruvic acid to lactic acid. The maximum wavelength of absorption of pyruvic acid is at 340 nm and this wavelength was used in our measurements. The LDH activity was expressed as arbitrary units (Vile et al., 1994).

LDH measurements

1) LDH of supernatant: immediately after UVA irradiation (the first or the second dose), irradiation buffer was aspirated and cells in 6-cm plates were incubated in 2 ml Minimum essential medium (MEM) containing glutamine and P/S for 2 h, after which aliquots of medium were removed and spun at 13,000 rpm for 2 min in a Heraeus Bio-fuge13 to remove any cells present.

2) Total LDH: after UVA irradiation, cells were incubated with MEM for 2 h at 37°C. Then 0.025% NP-40 detergent was added during the last 30 min incubation period (Vile et al., 1994) in order to lyse the cells and measure the total LDH. The percentage of LDH leakage was expressed as LDH of supernatant/total LDH.

2.10 Survival assay

Cell survival was judged by the ability of a cell to divide and form colonies, which is a good indication of cytotoxity.

Procedure: Cells were grown to 80-90% confluency then irradiated as described before. Immediately after the irradiation, cells were detached by trypsinization, and counted. After a serial of dilution of the cells, 400, 1600 and 6400 cells were seeded for each condition in 10-cm plates in triplicate. Cells were incubated in a sealed box containing 5% CO_2 at 37^0C with no further medium changes for 14-21 days. The medium was removed and cell clones were stained with 2 ml of 1% crystal violet in methanol for 2-3 min and then washed with tap water. Clones were counted. Clone-efficiency was calculated as number of clones formed /per total number of cells seeded in control plates.

2.11 Neutral red assay

This assay measures the function of the ATP-dependent H_3O^+ pump which maintains the lysosomal pH gradient responsible for the uptake of the lysosomotopic neutral red. It is therefore related to both the energy state of the cells and lysosomal membrane integrity.

Procedure: Neutral red stock solution was prepared by thoroughly dissolving 0.02 g neutral red powder in 5 ml Milli Q water. After dissolution, 500 µl of the solution was transferred to 39.5 ml of 15% FCS-EMEM to get the final concentration of 0.005%. This solution was kept in the dark overnight at RT. The following day the solution was filtered through a 0.2 µM filter and spun at 3000 rpm for 10 min in a Jouan CR412 centrifuge. Cells were irradiated in plates as described before. After irradiation, cells were incubated for 30 min at 37°C in conditioned medium. Then the medium was aspirated, cells were rinsed once with PBS and 2 ml of 0.005% neutral red medium was added to a 3-cm plate and re-incubated at 37°C for 1.5 h. Then the neutral red medium was aspirated, cells were washed 3 times in PBS. Then cells were lysed with 1 ml of a solution containing 50% ethanol, 1% acetic acid in water. The plates were swirled for a few min. Then 100 µl solution from each plate was transferred into a 96-well plate and the absorbance was measured at 560 nm in a plate reader (Dynatech MR5000).

2.12 Explanations of the experimental design and symbols

I. Dose-response and Kinetic experiments

- In both dose-response and kinetic experiments, cells were cultured to 80% confluency and then irradiated at the indicated dose (250 or 500 kJ/m^2). In dose-response experiments, the CA-assay was performed immediately following UVA irradiation of the cells (0 h, in bold):

General formula for dose-response experiments:

$$X^{0h}$$

Where "X" is the dose of UVA used in kJ/m^2 and "**0h**" is the time (h) at which the CA-assay is performed following UVA irradiation of cells.

- To study the effect of DFO on UVA-induced iron release, cells were treated with DFO (100 μM, final concentration) in conditioned media 20 h prior to UVA radiation treatment.

General formula for DFO treatment in single-dose experiments:

$$DFO + X^{0h}$$

Where "X" is the dose of UVA used in kJ/m^2 and "0h" is the time (h) at which the CA-assay is performed following UVA irradiation of cells.

- In Kinetic experiments, following irradiation, the irradiation buffer was replaced with conditioned-media and the cells were incubated for the indicated time (h in bold) at 37°C prior to CA-assay:

  General formula for kinetic experiments:

  X^{ah}

  Where "X" is the dose of UVA in kJ/m^2 and "**ah**" is the time (h) at which the CA-assay is performed following UVA irradiation of cells.

Ia Dose-response

$\mathbf{0^{0h}}$**:** Cells were sham-irradiated i.e. Cells were kept under dark in irradiation buffer for the time of irradiation.

250^{0h}: Cells were irradiated with UVA dose of 250 kJ/m^2.

500^{0h}: Cells were irradiated with UVA dose of 500 kJ/m^2.

Ib Effect of DFO on UVA-induced iron release

DFO + 0^{0h}: Cells were pre-treated with 100 μM DFO for 20 h in conditioned media. The next day cells were sham-irradiated i.e. Cells were kept under dark in irradiation buffer for the time of irradiation.

DFO + 250^{0h}: Cells were pre-treated with 100 μM DFO for 20 h in conditioned media. The next day cells were irradiated with UVA dose of 250 kJ/m^2.

DFO + 500^{0h}: Cells were pre-treated with 100 μM DFO for 20 h in conditioned media. The next day cells were irradiated with UVA dose of 500 kJ/m^2.

Ic Kinetics

$0^{2,6h}$: Non-irradiated control for the following 2 samples.

250^{2h}: Cells were irradiated with a UVA dose of 250 kJ/m^2 and then incubated for 2 h in conditioned media prior to CA-assay.

250^{6h}: Cells were irradiated with a UVA dose of 250 kJ/m^2 and then incubated for 6 h in conditioned media prior to CA-assay.

0^{24h}: Non-irradiated control for the next sample:

250^{24h}: Cells were irradiated with a UVA dose of 250 kJ/m^2 and then incubated for 24h in conditioned media prior to CA-assay.

0^{48h}: Non-irradiated control for the next sample.

250^{48h}: Cells were irradiated with a UVA dose of 250 kJ/m^2 and then incubated for 48h in conditioned media prior to CA-assay.

II. Challenge dose experiments

In challenge dose experiments, cells were cultured to 80% confluency, and then irradiated at the indicated dose (day 0, in bold). After the first irradiation, the irradiation buffer was replaced with conditioned media and cells were incubated for one (day 1, in bold) or two (day 2, in bold) additional days. The second challenge dose with UVA was performed either in 24 h (day 1) or 48 h (day 2) after the first irradiation performed on day 0. The CA-assay was performed immediately following the second irradiation (either in day 1 or day 2).

General formula for challenge-dose experiments:

$$X^{d0} / Y^{d1\text{-}2}$$

Where "X" is the dose of UVA used in kJ/m^2 for the first irradiation and "Y" is the dose of UVA used in kJ/m^2 for the second irradiation. "**d0**" is the day at which the first irradiation was carried out. "**d1**" or "**d2**" are the days at which the second irradiation was performed. "/" is the 20-48 h incubation period between the first and second irradiation treatments.

To study the effect of DFO on UVA-induced iron release, cells were treated with DFO (100 μM, final concentration) in conditioned media 20 h prior to the second irradiation in challenge dose experiments

General formula for DFO treatments in challenge-dose experiments:

$$X^{d0} + DFO / Y^{d1\text{-}2}$$

$0^{d0} / 0^{d1}$

Cells were sham-irradiated during both the first and second irradiations in "day 0" and "day 1". After the first sham-irradiation, the irradiation buffer was replaced with conditioned media and cells were incubated for an additional day at 37°C.

$0^{d0} + DFO / 0^{d1}$

Cells were sham-irradiated during the first and second irradiations in "day 0" and "day 1". After the first sham-irradiation the irradiation buffer was replaced with conditioned media supplemented with DFO and cells were incubated for an additional day at 37°C.

0^{d0} / 250^{d1}

Cells were sham-irradiated during the first irradiation. After a day of incubation in conditioned media, cells were irradiated with a UVA dose of 250 kJ/m^2 in " day 1".

0^{d0} + DFO / 250^{d1}

Cells were sham-irradiated during the first irradiation (i.e. in day 0). After a day of incubation in conditioned media supplemented with DFO, cells were irradiated with a UVA dose of 250 kJ/m^2 in "day 1".

250^{d0} / 0^{d1}

Cells were irradiated with a UVA dose of 250 kJ/m^2 in "day 0" and then incubated in conditioned media for an additional day. Cells were then sham-irradiated in "day 1".

250^{d0} + DFO / 0^{d1}

Cells were irradiated at 250 kJ/m^2 in "day 0". The irradiation buffer was then replaced with conditioned media supplemented with DFO and cells were incubated at 37°C for an additional day. Cells were then sham-irradiated at 250 kJ/m^2 in "day 1".

250^{d0}/ 250^{d1}

Cells were irradiated with a UVA dose of 250 kJ/m^2 in "day 0". After a day of incubation in conditioned media, cells were re-irradiated with a UVA dose of 250 kJ/m^2 in "day 1".

250^{d0} + DFO/ 250^{d1}

Cells were irradiated in "day 0" at 250 kJ/m^2 and then incubated in conditioned media supplemented with DFO for an additional day. Cells were then re-irradiated with a UVA dose of 250 kJ/m^2 in "day 1".

$0^{d0}/\ 0^{d2}$

Cells were sham-irradiated during the first and second irradiations in "day 0" and "day 2". After the first sham-irradiation, the irradiation buffer was replaced with conditioned media and cells were incubated for two additional days at 37°C.

$250^{d0}\ /\ 0^{d2}$

Cells were irradiated with a UVA dose of 250 kJ/m^2 in "day 0" and then incubated in conditioned media for two additional days. Cells were then sham-irradiated in "day 2".

$0^{d0}/\ 250^{d2}$

Cells were sham-irradiated during the first irradiation. After two days incubation in conditioned media, cells were irradiated with a UVA dose of 250 kJ/m^2 in "day 2".

$250^{d0}/\ 250^{d2}$

Cells were irradiated with a UVA dose of 250 kJ/m^2 in "day 0". After two days incubation in conditioned media, cells were re-irradiated with a UVA dose of 250 kJ/m^2 in "day 2".

2.13 Statistical analysis

Paired or unpaired Student's two-tailed *t*-test was used as appropriate to test differences between groups of data. Note that the rejection p value is 0.05. The statistical analyses were performed using the Origin program (version 6).

3. Results

3.1 Characterisation of LIP release in cultured human skin cells following single or repeated exposures to UVA radiations

It has been shown in our laboratory that UVA radiation induces chelatable iron release in a human primary skin fibroblast cell line, FEK4 (Pourzand et al., 1999a). The objective of the present study was to characterise this phenomenon further in a series of human skin fibroblasts and keratinocytes following single or repeated exposures to UVA radiation. Using the Calcein (CA)-assay, first the dissociation constant (Kd) of calcein-bound iron (CA-Fe) was determined in CA-loaded cells, the results were then expressed as "LIP" which is operationally defined as the sum of free CA-unbound iron [Fe] and [CA-Fe] (see **Materials and Methods** and Epsztejn et al., 1997). In order to estimate the extent of LIP release following irradiation treatment, both fibroblasts and keratinocytes were exposed to a range of doses of UVA irradiation at natural exposure levels (i.e. 150, 250 and 500 kJ/m^2, see **Dose-response**). Furthermore, the kinetics of UVA-induced increase in LIP were monitored up to 48 h (LIP levels of 1BR3 and HFK-SV61 were monitored only up to 24 h) post-irradiation time with UVA doses of 250 kJ/m^2 (see **Kinetics**). To investigate whether UVA-induced LIP release also occurs following a second irradiation, the UVA-irradiated cells (i.e. 250 kJ/m^2) were challenged with a second dose of UVA (i.e. 250 kJ/m^2), 24 or 48 h after the first radiation. The results of these investigations are summarised below for both fibroblasts and keratinocytes:

3.1.1 Fibroblasts

The fibroblasts used in this study were FEK4 (human foreskin fibroblast cell line) and 1BR3 (human skin fibroblast cell line). **Table 3.1** summarises the basal level concentration of LIP ([CA-Fe] + [Fe]), in both FEK4 and 1BR3, as determined by the Kd values with CA-assay for each cell line (see **Materials and Methods**). These results demonstrated that the basal level of LIP in 1BR3 fibroblasts is 1.7 fold higher than that of FEK4 fibroblasts.

Table 3.1 Determination of basal LIP in FEK4 and 1BR3 cells

Cell line	[Fe] μM	[CA-Fe] μM	LIP=[Fe]+[CA-Fe] μM
FEK4 0^{0h}	1.07 ± 0.41	0.14 ± 0.05	1.21 ± 0.45
1BR3 0^{0h}	1.79 ± 0.38	0.21 ± 0.07	1.99 ± 0.41

Note: Kd of CA-Fe for FEK4 and 1BR3 were 12.7 and 19.1 μM, respectively (n=6-20). The concentrations of Fe, CA-Fe and LIP are expressed as the mean ± SD (n = 3-6).

3.1.1a Dose response

The LIP levels were measured using the CA-assay immediately after irradiation of fibroblasts with UVA doses of 150, 250 and 500 kJ/m^2. The results (**Table 3.2**) revealed that the levels of LIP in both 1BR3 and FEK4 cells are increased in a dose-dependent manner up to 2.8 fold of the control values. For FEK4 cells, the threshold of UVA-dose necessary for induction of iron release was determined, which was found to be around 150 kJ/m^2. These results illustrated that although LIP release occurs in both cell lines, the UVA-induced LIP concentration in 1BR3 remains 1.7 fold higher than in FEK4 cells.

Table 3.2 Modulation of the LIP levels following a range of doses of UVA irradiation in FEK4 and 1BR3 cells

FEK4 Samples	UVA dose (kJ/m^2)	Time (h) post-UVA	LIP (μM)	Fold increase compared to control
0^{0h}	0	0	1.21 ± 0.45	1
150^{0h}	150	0	2.23 ± 0.51*	1.61 ± 0.28
250^{0h}	250	0	2.46 ± 0.67*	2.14 ± 0.51
500^{0h}	500	0	3.08 ± 0.71* +	2.79 ± 0.51
1BR3 Samples	**UVA dose (kJ/m^2)**	**Time (h) post-UVA**	**LIP (μM)**	**Fold increase compared to control**
0^{0h}	0	0	1.99 ± 0.41	1
250^{0h}	250	0	4.06 ± 0.44*	2.11 ± 0.52
500^{0h}	500	0	5.02 ± 0.45* +	2.60 ± 0.57

Note: Kd of CA-Fe for FEK4 and 1BR3 were 12.7 and 19.1 μM, respectively (n=6-20).
Measurements were performed at indicated times (h) after UVA irradiation.
The concentrations of LIP are expressed as the mean ± SD (n = 3-6).
* : Significantly different from the sham-irradiated control (0^{0h}), $p < 0.05$.
+ : Significantly different from 250 kJ/m^2-irradiated sample (250^{0h}), $p < 0.05$.

3.1.1b Kinetics

The kinetics of iron mobilisation in FEK4 cells was followed using the CA-assay up to 48 h post-irradiation time with a UVA dose of 250 kJ/m^2. The results (**Table 3.3**) showed that the immediate increase in LIP is sustained up to 2 h after irradiation with a UVA dose of 250 kJ/m^2 and returns to around the control value at 6 h post-irradiation. The CA-assay performed 24 or 48 h after UVA irradiation of both FEK4 and 1BR3 cells revealed no further change in LIP concentration.

Table 3.3 Modulation of the LIP levels following UVA 250 kJ/m^2 irradiation in FEK4 and 1BR3 cells

FEK4 Samples	UVA dose (kJ/m^2)	Time (h) post-UVA	LIP (μM)	Fold increase compared to control
0^{0h}	0	–	1.21 ± 0.45	1
250^{0h}	250	2	2.46 ± 0.67*	2.14 ± 0.51
$0^{2,6h}$	0	–	1.04 ± 0.12	1
250^{2h}	250	2	1.71 ± 0.33*	1.68 ± 0.29
250^{6h}	250	6	1.01 ± 0.28	0.95±0.23
0^{24h}	0	–	1.13 ± 0.22	1
250^{24h}	250	24	1.07 ± 0.28	0.95 ± 0.12
0^{48h}	0	–	1.27 ± 0.30	1
250^{48h}	250	48	1.08 ± 0.27	0.89 ± 0.04
1BR3 Samples	**UVA dose (kJ/m^2)**	**Time (h) post-UVA**	**LIP (μM)**	**Fold increase compared to control**
0^{0h}	0	0	1.99 ± 0.41	1
250^{0h}	250	0	4.06 ± 0.44*	2.11 ± 0.52
0^{24h}	0	–	1.92 ± 0.35	1
250^{24h}	250	24	1.64 ± 0.45	0.85 ± 0.13

Note: Kd of CA-Fe for FEK4 and 1BR3 were 12.7 and 19.1μM, respectively (n=6-20).
Measurements were performed at indicated times (h) after UVA irradiation.
The concentrations of LIP are expressed as the mean ± SD (n = 3-6).
* : Significantly different from the sham-irradiated controls, $p < 0.05$.

3.1.1c Effect of confluency on UVA-induced LIP release in FEK4 cells

It is known that confluent human skin fibroblasts are more resistant to both UVA-mediated membrane damage (Gaboriau et al., 1993) and cytotoxicity (unpublished data, this laboratory). Furthermore, Pourzand et al. (1999a) have reported that confluent FEK4 fibroblasts have significantly less chelatable iron than exponentially growing cells by IRP/IRE binding. The extent of UVA-induced iron release in confluent fibroblasts was therefore investigated. For this purpose, FEK4 cells were grown to confluency and incubated for 2 to 4 additional days in the incubator. The levels of LIP were then measured by CA-assay immediately after UVA irradiation of confluent cells (UVA doses of 250 and 500 kJ/m^2). The results (**Table 3.4**) showed that although the basal level of LIP in confluent fibroblasts was similar to that of exponentially growing cells (i.e. 80% confluent fibroblasts), the level of UVA-induced LIP was much lower in confluent cells. For example with a UVA dose of 250 kJ/m^2, the level of LIP increased up to 2.46 μM in growing cells and only up to 1.80 μM in confluent cells. Nevertheless the immediate release of LIP in confluent cells following UVA radiation appeared to be dose-dependent and significantly different from the sham-irradiated controls.

Table 3.4 Effect of UVA on the LIP levels in confluent FEK4 fibroblasts

FEK4	UVA dose (kJ/m^2)	Time (h) post-UVA	LIP (μM)	Fold increase compared to control
0^{0h}	0	-	1.22 ± 0.11	1
250^{0h}	250	0	1.80 ± 0.28*	1.48 ± 0.23
500^{0h}	500	0	2.40 ± 0.25*	1.97 ± 0.12

Note: Kd of CA-Fe for confluent FEK4 was 12.7 μM (n = 20).
Measurements were performed at indicated times (h) after UVA irradiation.
The concentrations of LIP are expressed as the mean ± SD (n = 3-4).
* : Significantly different from the sham-irradiated control (0^{0h}), $p < 0.05$.

3.1.1d The second challenge dose

The phenomenon of UVA-induced iron release was investigated following repeated exposures of fibroblasts to UVA radiation. This was achieved by designing experiments to monitor the release of LIP with a second challenge dose of UVA 24 or 48 h after the first irradiation.

The results (**Table 3.5**) showed that a second challenge dose of UVA 24 or 48 h after the first treatment, still promotes LIP release within fibroblasts. Indeed in both FEK4 and 1BR3 fibroblasts, the pre-irradiated samples (250^{d0} / 250^{d1} or 250^{d0} / 250^{d2}) yielded the same increase in LIP as the corresponding non-pre-irradiated samples (0^{d0} / 250^{d1} or 0^{d0} / 250^{d2}). Furthermore in FEK4 cells, the irradiation of pre-irradiated samples 24 or 48 h after the first dose (250^{d0} / 250^{d1} and 250^{d0} / 250^{d2}, respectively) triggered a similar amount of LIP release. Also, in agreement with dose-response experiments, the sham-irradiation of pre-irradiated cells 24 or 48 h after the first UVA irradiation (250^{d0} / 0^{d1} or 250^{d0} / 0^{d2}) did not modulate the level of LIP as compared to the corresponding sham-irradiated control (0^{d0} / 0^{d1} or 0^{d0} / 0^{d2}). This is presumably due to the fact that the UVA-induced increase in LIP returns to around the control value by 6 h post-irradiation time and does not further change for the next 24 or 48 h following irradiation treatment.

Taken together, these results suggest that UVA-induced iron release within fibroblasts is a general response to UVA since it occurs to the same extent following single or repeated exposure to radiation treatment.

Table 3.5 Modulation of the LIP levels following a second dose of UVA irradiation in FEK4 and 1BR3 cells

FEK4 Samples	UVA dose (kJ/m^2) Day 0	UVA dose (kJ/m^2) Day 1	UVA dose (kJ/m^2) Day 2	LIP (μM)	Fold increase compared to control
$0^{d0}/0^{d1}$	0	0	-	1.13 ± 0.22	1
$250^{d0}/0^{d1}$	250	0	-	1.07 ± 0.28	0.95 ± 0.12
$0^{d0}/250^{d1}$	0	250	-	2.42 ± 0.58*	2.16 ± 0.40
$250^{d0}/250^{d1}$	250	250	-	1.85 ± 0.56*	1.65 ± 0.31
$0^{d0}/0^{d2}$	0	-	0	1.27 ± 0.30	1
$250^{d0}/0^{d2}$	250	-	0	1.08 ± 0.27	0.89 ± 0.04
$0^{d0}/250^{d2}$	0	-	250	2.21 ± 0.52*	1.78 ± 0.45
$250^{d0}/250^{d2}$	250	-	250	1.90 ± 0.30*	1.53 ± 0.27
1BR3 Samples	**UVA dose (kJ/m^2) Day 0**	**UVA dose (kJ/m^2) Day 1**	**UVA dose (kJ/m^2) Day 2**	**LIP (μM)**	**Fold increase compared to control**
$0^{d0}/0^{d1}$	0	0	-	1.92 ± 0.35	1
$250^{d0}/0^{d1}$	250	0	-	1.64 ± 0.45	0.85 ± 0.13
$0^{d0}/250^{d1}$	0	250	-	3.70 ± 1.01*	1.95 ± 0.52
$250^{d0}/250^{d1}$	250	250	-	3.54 ± 0.74*	1.84 ± 0.14

Note: Kd of CA-Fe for FEK4 and 1BR3 were 12.7 and 19.1μM, respectively (n=6-20).
Measurements were performed 0 h after the second UVA irradiation.
The concentrations of LIP are expressed as the mean ± SD (n = 3-6).
*: Significantly different from the sham-irradiated controls ($0^{d0}/0^{d1(2)}$), $p < 0.05$.

3.1.1e Effect of DFO on the LIP levels following single or repeated exposure of fibroblasts to UVA radiation

Pourzand et al. (1999) have previously demonstrated that treatment of FEK4 cells with DFO, 18-20 h prior to UVA radiation could abolish both the basal and UVA-induced levels of chelatable iron. To study the effect of DFO on suppression of UVA-induced LIP release, the CA-assay was performed with both FEK4 and IBR3 cells that were either treated with the iron-chelator 20 h prior to the first irradiation or 20 h prior to the second irradiation. The results (**Table 3.7**) showed that in agreement with findings from Pourzand et al. (1999), DFO treatment prior to the first UVA radiation abolished both the basal and induced level of LIP in both FEK4 and 1BR3 cells. Furthermore the addition of DFO following the first irradiation also completely abolished the level of LIP release in both pre-irradiated and non-pre-irradiated samples following a second challenge dose of UVA radiation (**Table 3.8**).

These results emphasize the importance of iron-chelator treatment on the suppression of the harmful effects of UVA-induced iron release (see section **4**).

Table 3.7 Effect of DFO on the LIP levels following UVA irradiation in FEK4 and 1BR3

FEK4 Samples	DFO treatment (μM)	UVA dose (kJ/m^2)	Time (h) post-UVA	LIP (μM)	Fold increase compared to control
0^{0h}	-	0	–	1.21±0.45	1
DFO + 0^{0h}	100	0	–	0	-
250^{0h}	-	250	0	2.46±0.67*	2.14±0.51
DFO + 250^{0h}	100	250	0	0	-
500^{0h}	-	500	0	3.08±0.71* $^{+}$	2.79±0.51
DFO + 500^{0h}	100	500	0	0	-

1BR3 Samples	DFO treatment (μM)	UVA dose (kJ/m^2)	Time (h) post-UVA	LIP (μM)	Fold increase compared to control
0^{0h}	-	0	–	1.99±0.41	1
DFO + 0^{0h}	100	0	–	0	-
250^{0h}	-	250	0	4.06±0.44*	2.11±0.52
DFO + 250^{0h}	100	250	0	0	-
500^{0h}	-	500	0	5.02±0.45* $^{+}$	2.60±0.57
DFO + 500^{0h}	100	500	0	0	-

Note: Kd of CA-Fe for FEK4 and 1BR3 were 12.7 and 19.1μM, respectively (n=6-20).
DFO treatments were performed for 20 h prior to UVA radiation treatment.
Measurements were performed at indicated times (h) after UVA irradiation.
The concentrations of LIP are expressed as the mean ± SD (n = 3-6).
* : Significantly different from the sham-irradiated control (0^{0h}), $p < 0.05$.

Table 3.8 Effect of DFO on the LIP levels following a second dose of UVA irradiation in UVA FEK4 and 1BR3 cells

FEK4 Samples	UVA dose (kJ/m^2) Day 0	DFO (μM) Day 0	UVA dose (kJ/m^2) Day1	LIP (μM)	Fold increase compared to control
$0^{d0}/0^{d1}$	0	-	0	1.13±0.22	1
0^{d0} + DFO / 0^{d1}	0	100	0	0	-
$250^{d0}/0^{d1}$	250	-	0	1.07±0.28	0.95±0.12
250^{d0} + DFO / 0^{d1}	250	100	0	0	-
$0^{d0}/250^{d1}$	0	-	250	2.42±0.58*	2.16±0.40
0^{d0} + DFO / 250^{d1}	0	100	250	0	-
$250^{d0}/250^{d1}$	250	-	250	1.85±0.56*	1.65±0.31
250^{d0}+DFO/ 250^{d1}	250	100	250	0	-
1BR3 Samples	**UVA dose (kJ/m^2) Day 0**	**DFO (μM) Day 0**	**UVA dose (kJ/m^2) Day1**	**LIP (μM)**	**Fold increase compared to control**
$0^{d0}/0^{d1}$	0	-	0	1.92±0.35	1
0^{d0} + DFO / 0^{d1}	0	100	0	0	-
$250^{d0}/0^{d1}$	250	-	0	1.64±0.45	0.85±0.13
250^{d0} + DFO/ 0^{d1}	250	100	0	0	-
$0^{d0}/250^{d1}$	0	-	250	3.70±1.01*	1.95±0.52
0^{d0} + DFO/250^{d1}	0	100	250	0	-
$250^{d0}/250^{d1}$	250	-	250	3.54±0.74*	1.84±0.14
250^{d0}+DFO/250^{d1}	250	100	250	0	-

Note: Kd of CA-Fe for FEK4 and 1BR3 were 12.7 and 19.1 μM, respectively (n=6-20). DFO treatments were performed for 20 h prior to UVA radiation in fibroblasts. Measurements were performed 0 h after the second UVA irradiation. The concentrations of LIP are expressed as the mean ± SD (n = 3-6).

* : Significantly different from the sham-irradiated control ($0^{d0}/0^{d1}$), $p < 0.05$.

3.1.2 Keratinocytes

The upper layer of skin (epidermis) is frequently exposed to UV radiation and therefore is thought to be a major target for the carcinogenic events in the skin. It is generally observed that skin keratinocytes are more resistant to UVA-mediated membrane damage (Morliere et al., 1997; Applegate et al., 1995) and cytotoxicity (Pidoux and Tyrrell, 1988). Since UVA-induced iron release might be an important factor for skin damage, it was hypothesized that higher resistance of human keratinocytes to UVA may be related to the lower level of UVA-mediated LIP release in these cells. The keratinocyte cell lines used in this study were HaCaT (transformed human adult skin keratinocytes) and HFK-SV61 (transformed human foetal skin keratinocytes). Although these cell lines are transformed, they maintain full epidermal differentiation capacity and are therefore suitable for use as models to study the effect of UVA on human skin keratinocytes. The basal LIP levels in these cell lines were measured using the CA-assay. **Table 3.9** summarises the basal LIP levels of LIP ([CA-Fe] + [Fe]) in both HaCaT and HFK-SV61, as determined by the Kd values for each cell line (see **Materials and Methods**). These results demonstrated that although the basal LIP levels in these two cell lines are similar, the basal LIP level in keratinocytes is 2-4 fold lower than in fibroblasts.

Table 3.9 Determination of basal LIP in HaCaT and HFK-SV61 cells

Cell line	[Fe] μM	[CA-Fe] μM	LIP=[Fe]+[CA-Fe] μM
HaCaT 0^{0h}	0.34±0.05	0.16±0.04	0.50±0.06
HFK-SV61 0^{0h}	0.32±0.09	0.20±0.07	0.52±0.17

Note: Kd of CA-Fe for HaCaT and HFK-SV61 were 9.8 and 4.5 μM, respectively (n=5-12). The concentrations of Fe, CA-Fe and LIP are expressed as the mean ± SD (n=3-6).

3.1.2a Dose response

The LIP levels were measured using the CA-assay immediately after irradiation of keratinocytes with UVA doses of 250 and 500 kJ/m^2. The results (**Table 3.10**) revealed that the phenomenon of UVA-induced immediate release of LIP occurs also in a dose-dependent manner in keratinocytes. However, the UVA-induced LIP concentration in these cells still remained 2-4 fold lower than for fibroblasts.

Table 3.10 Modulation of the LIP levels following irradiation of HaCaT and HFK-SV61 cells with a range doses of UVA

HaCaT	UVA dose (kJ/m^2)	Time (h) post-UVA	LIP (μM)	Fold increase compared to control
0^{0h}	0	0	0.50 ± 0.06	1
250^{0h}	250	0	0.97 ± 0.10*	1.93 ± 0.23
500^{0h}	500	0	2.01 ± 0.44* +	3.99 ± 0.64
HFK-SV61	**UVA dose (kJ/m^2)**	**Time (h) post-UVA**	**LIP (μM)**	**Fold increase compared to control**
0^{0h}	0	0	0.52 ± 0.17	1
250^{0h}	250	0	0.92 ± 0.30*	1.78 ± 0.16
500^{0h}	500	0	1.42 ± 0.39* +	2.81 ± 0.57

Note: Kd of CA-Fe for HaCaT and HFK-SV61 were 9.8 and 4.5 μM, respectively (n = 5-12). Measurements were performed at indicated times (h) after UVA irradiation. The concentrations of LIP are expressed as the mean ± SD (n = 3-6).
* : Significantly different from the sham-irradiated control, $p < 0.05$.
+: Significantly different from 250 kJ/m^2-irradiated sample (250^{0h}), $p < 0.05$.

3.1.2b. Kinetics

The kinetics of iron mobilisation in HaCaT cells were followed using the CA-assay up to 48 h post-irradiation with a UVA dose of 250 kJ/m^2. The results (**Table 3.11**) showed that 2 h after UVA radiation, the LIP level was significantly higher than that of the non-irradiated control, however, at 6 h post-irradiation time, the LIP level returned to the

control value. The CA-assay performed 24 h or 48 h after UVA irradiation of both HaCaT and HFK-SV61 cells revealed no further change in LIP concentration. These results illustrated that the kinetics of LIP release in UVA-irradiated keratinocytes was similar to fibroblasts.

Table 3.11 Modulation of the LIP levels following irradiation of HaCaT and HFK-SV61 cells with UVA 250 kJ/m^2

HaCaT	UVA dose (kJ/m^2)	Time (h) post-UVA	LIP (μM)	Fold increase compared to control
0^{0h}	0	–	0.50 ± 0.06	1
250^{0h}	250	0	0.97 ± 0.10*	1.93 ± 0.23
$0^{2,6h}$	0	–	0.54 ± 0.20	1
250^{2h}	250	2	0.84 ± 0.35*	1.60 ± 0.33
250^{6h}	250	6	0.53 ± 0.12	1.07 ± 0.37
0^{24h}	0	–	0.65 ± 0.16	1
250^{24h}	250	24	0.57 ± 0.13	0.88 ± 0.18
0^{48h}	0	–	0.53 ± 0.17	1
250^{48h}	250	48	0.51 ± 0.20	0.95 ± 0.15
HFK-SV61	**UVA dose (kJ/m^2)**	**Time (h) post-UVA**	**LIP (μM)**	**Fold increase compared to control**
0^{0h}	0	0	0.52 ± 0.17	1
250^{0h}	250	0	0.92 ± 0.30*	1.78 ± 0.16
0^{24h}	0	–	0.52 ± 0.09	1
250^{24h}	250	24	0.52 ± 0.12	1.04 ± 0.40

Note: Kd of CA-Fe for HaCaT and HFK-SV61 were 9.8 and 4.5 μM, respectively (n = 5-12). Measurements were performed at indicated times (h) after UVA irradiation. The concentrations of LIP are expressed as the mean ± SD (n = 3-6).
*: Significantly different from the relevant sham-irradiated controls, $p < 0.05$.

3.1.2c The second challenge dose

The levels of LIP in keratinocytes were also monitored following a second challenge dose with UVA 24 or 48 h after the first treatment. The results (see **Table 3.12**) confirmed that the UVA-induced immediate increase in LIP in pre-irradiated keratinocytes (250^{d0} / 250^{d1} or 250^{d0} / 250^{d2}) occurred to the same extent as in the corresponding non-pre-irradiated samples (0^{d0} / 250^{d1} or 0^{d0} / 250^{d2}). Furthermore in HaCaT cells, the irradiation of the pre-irradiated samples 24 or 48 h after the first dose (250^{d0} / 250^{d1} and 250^{d0} / 250^{d2} respectively) triggered a similar amount of LIP release. Also, in agreement with dose-response experiments, the sham-irradiation of pre-irradiated cells 24 or 48 h after the first UVA dose (250^{d0} / 0^{d1} or 250^{d0} / 0^{d2}) did not modulate the level of LIP as compared to the sham-irradiated controls (0^{d0} / 0^{d1} or 0^{d0} / 0^{d2}), since the UVA-induced increase in LIP returns to around the control value by 6 h post-irradiation time and does not change further for the next 24 or 48 h. This was similar to the observations previously made in fibroblasts.

Taken together, these results indicate that iron release within skin fibroblasts and keratinocytes is an immediate response to UVA-induced oxidative stress and could occur following single or repeated exposure to radiation treatments.

Table 3.12 Modulation of the LIP levels following irradiation of HaCaT and HFK-SV61 with a second dose of UVA

HaCaT Samples	UVA dose (kJ/m^2) Day 0	UVA dose (kJ/m^2) Day 1	UVA dose (kJ/m^2) Day 2	LIP (μM)	Fold increase compared to control
$0^{d0}/0^{d1}$	0	0	-	0.65±0.16	1
$250^{d0}/0^{d1}$	250	0	-	0.57±0.13	0.88±0.18
$0^{d0}/250^{d1}$	0	250	-	1.36±0.16*	2.15±0.45
$250^{d0}/250^{d1}$	250	250	-	1.18±0.23*	1.84±0.29
$0^{d0}/0^{d2}$	0	-	0	0.53±0.17	1
$250^{d0}/0^{d2}$	250	-	0	0.51±0.20	0.95±0.15
$0^{d0}/250^{d2}$	0	-	250	1.07±0.49*	1.97±0.39
$250^{d0}/250^{d2}$	250	-	250	0.97±0.38*	1.80±0.17
HFK-SV61 Samples	**UVA dose (kJ/m^2) Day 0**	**UVA dose (kJ/m^2) Day 1**	**UVA dose (kJ/m^2) Day 2**	**LIP (μM)**	**Fold increase compared to control**
$0^{d0}/0^{d1}$	0	0	-	0.52±0.09	1
$250^{d0}/0^{d1}$	250	0	-	0.52±0.12	1.04±0.40
$0^{d0}/250^{d1}$	0	250	-	0.92±0.17*	1.77±0.28
$250^{d0}/250^{d1}$	250	250	-	0.80±0.19*	1.52±0.23

Note: Kd of CA-Fe for HaCaT and HFK-SV61 were 9.8 and 4.5 μM, respectively (n = 5-12). Measurements were performed 0 h after the second UVA irradiation. The concentrations of LIP are expressed as the mean ± SD (n = 3-7).

*: Significantly different from the sham-irradiated controls ($0^{d0}/0^{d1(2)}$), $p < 0.05$.

3.1.2d Effect of DFO on the LIP levels following single or repeated exposure of keratinocytes to UVA radiation

The effect of DFO treatment was tested in keratinocytes either prior to a single exposure to UVA or following the first dose of UVA in challenge dose experiments. The results (**Table 3.13**) showed that DFO treatment prior to UVA radiation abolished both the basal and induced level of LIP in both HaCaT and HFK-SV61 cells. In the second challenge dose experiments, the addition of DFO following the first irradiation also completely abolished the level of LIP release in both pre-irradiated and non-irradiated samples (**Table 3.14**). This was similar to the observations previously made in fibroblasts.

Overall these results indicate that iron-chelator treatment could suppress the UVA-induced iron release in both fibroblasts and keratinocytes.

Table 3.13 Effect of DFO on the LIP levels following UVA

UVA irradiation of HaCaT and HFK-SV61 cells

HaCaT Samples	DFO treatment (μM)	UVA dose (kJ/m^2)	Time (h) post-UVA	LIP (μM)	Fold increase compared to control
0^{0h}	-	0	–	0.50± 0.06	1
DFO + 0^{0h}	100	0	–	0	-
250^{0h}	-	250	0	0.97±0.10*	1.93±0.23
DFO + 250^{0h}	100	250	0	0	-
500^{0h}	-	500	0	2.01±0.44* $^{+}$	3.99±0.64
DFO + 500^{0h}	100	500	0	0	-

HFK-SV61 Samples	DFO treatment (μM)	UVA dose (kJ/m^2)	Time (h) post-UVA	LIP (μM)	Fold increase compared to control
0^{0h}	-	0	–	0.52±0.17	1
DFO + 0^{0h}	100	0	–	0	-
250^{0h}	-	250	0	0.92±0.30*	1.78±0.16
DFO + 250^{0h}	100	250	0	0	-
500^{0h}	-	500	0	1.42±0.39* $^{+}$	2.81±0.57
DFO + 500^{0h}	100	500	0	0	-

Note: Kd of CA-Fe for HaCaT and HFK-SV61 were 9.8 and 4.5 μM, respectively (n = 9-12). DFO treatments were performed for 20 h prior to UVA radiation treatment. Measurements were performed at indicated times (h) after UVA irradiation.
The concentrations of LIP are expressed as the mean ± SD (n = 3-6).
*: Significantly different from the sham-irradiated control (0^{0h}), $p < 0.05$.

Table 3.14 Effect of DFO on the LIP levels following irradiation of HaCaT and HFK-SV61 cells with a second dose of UVA

HaCaT Samples	UVA dose (kJ/m^2) Day 0	DFO (μM) Day 0	UVA dose (kJ/m^2) Day 1	LIP (μM)	Fold increase compared to control
$0^{d0}/\ 0^{d1}$	0	-	0	0.65±0.16	1
0^{d0} + DFO/ 0^{d1}	0	100	0	0	-
$250^{d0}/\ 0^{d1}$	250	-	0	0.57±0.13	0.88±0.18
250^{d0}+ DFO/ 0^{d1}	250	100	0	0	-
$0^{d0}/\ 250^{d1}$	0	-	250	1.36±0.16*	2.15±0.45
0^{d0} + DFO/250^{d1}	0	100	250	0	-
$250^{d0}/\ 250^{d1}$	250	-	250	1.18±0.23*	1.84±0.29
250^{d0}+DFO/250^{d1}	250	100	250	0	-
HFK-SV61 Samples	**UVA dose (kJ/m^2) Day 0**	**DFO (μM) Day 0**	**UVA dose (kJ/m^2) Day1**	**LIP (μM)**	**Fold increase compared to control**
$0^{d0}/\ 0^{d1}$	0	-	0	0.52±0.09	1
0^{d0} + DFO/ 0^{d1}	0	100	0	0	-
$250^{d0}/\ 0^{d1}$	250	-	0	0.52±0.12	1.04±0.40
250^{d0} + DFO / 0^{d1}	250	100	0	0	-
$0^{d0}/\ 250^{d1}$	0	-	250	0.92±0.17*	1.77±0.28
0^{d0} + DFO / 250^{d1}	0	100	250	0	-
$250^{d0}/\ 250^{d1}$	250	-	250	0.80±0.19*	1.52±0.23
250^{d0}+DFO/250^{d1}	250	100	250	0	-

Note: Kd of CA-Fe for HaCaT and HFK-SV61 were 9.8 and 4.5 μM, respectively (n = 5-12). DFO treatments were performed for 20 h prior to UVA radiation.
Measurements were performed 0 h after the second UVA irradiation.
The concentrations of LIP are expressed as the mean ± SD (n = 3-6).
*: Significantly different from the sham-irradiated control ($0^{d0}/\ 0^{d1}$), $p < 0.05$.

3.1.3 Range of other cell-types

Additional experiments from this laboratory (Watkin, R., Holley, P., Yiakouvaki, A., Brown, J. E and Hejmadi, V.) show that in addition to fibroblasts and keratinocytes, the increase in LIP also occurred following UVA irradiation of cell lines A532 (human skin derived transformed endothelial cell line), Jurkat (human T cell lymphoma cell line), Hela (HtTA1, human cervical cancer cell line), murine R6 (transformed rat embryo fibroblast) and C57 IF_{γ} -/- cells (primary skin fibroblasts derived from "Interferon gamma" knock out mouse). These results (not shown here) strongly suggest that the phenomenon of iron release is a general response of cells to UVA-induced oxidative stress.

3.2 The role of ROS on the UVA-mediated LIP release in FEK4 cells

It is known that UVA radiation generates ROS in cells via interaction with intracellular chromophores (reviewed by Tyrrell, 1991). $^1O_2$ and H_2O_2 are thought to be the most important ROS generated intracellularly by UVA, promoting biological damage in exposed tissues via iron catalysed oxidative reactions (Vile and Tyrrell, 1995). Since UVA triggers both iron release and ROS formation, an attempt was made to investigate the relationship between the level of ROS generated by UVA and the extent of UVA-induced increase in LIP. For this purpose the intracellular levels of ROS induced by UVA irradiation were modulated by various treatments. The FEK4 cell line was used as the model and the level of LIP was measured using the CA-assay as described in **Materials and Methods**. The results are summarized below.

3.2.1 H_2O_2

H_2O_2 itself is an oxidising agent. Exposure of cells to this agent has been shown to promote biological damage due to its reactivity towards lipids, proteins and DNA (Shigenaga et al, 1994; Brunk et al, 1995). The toxicity of H_2O_2 within the cells is exacerbated by the presence of Fe^{2+}, which reacts with the compound by Fenton chemistry to yield the highly reactive $OH^{\bullet}$ (see section **1.5.1**). Since UVA, the oxidising component of sunlight, promotes the release of LIP within the skin cells, an attempt was made to investigate whether H_2O_2 as an oxidising agent could also be a mediator of iron release within cells.

3.2.1a Exogenous H_2O_2

To mimic the deleterious effects of UVA radiation, in the first approach FEK4 cells were directly challenged with increasing concentrations of H_2O_2. The results (**Table 3.2a**) showed that H_2O_2 induces a dose-dependent increase in LIP in FEK4 cells up to 100 μM final concentrations. Treatment of cells with higher concentrations of H_2O_2 i.e. 500 μM or 1 mM (data not shown) caused significant leakage of CA from CA-loaded cells, and therefore made the outcome of LIP data questionable. The CA leakage from CA-loaded cells is presumably due to cell membrane damage as a result of the cytotoxic concentrations of H_2O_2 applied.

The data indicate that in addition to UVA, H_2O_2, a well-characterised oxidising agent can trigger LIP release within human skin fibroblasts.

Table 3.2a Modulation of the LIP levels following treatment of FEK4 cells with a range of doses of H_2O_2

FEK4 Samples	LIP (μM)	Fold increase compared to control
Control	1.21± 0.31	1
20 μM H_2O_2	1.43± 0.33	1.16± 0.21
50 μM H_2O_2	2.11± 0.33 *	1.87± 0.38
100 μM H_2O_2	2.83± 0.83 * +	2.43± 0.75
250 μM H_2O_2	2.81± 0.12 (n = 2)	-
500 μM H_2O_2	3.41± 0.59 *	2.70± 0.59

Note: Kd of CA-Fe for FEK4 was 12.7 μM (n = 20).
Measurements were performed 0 h after H_2O_2 treatment. The concentrations of LIP are expressed as the mean ± SD (n = 4-11) except when indicated.
*: Significantly different from the control, $p < 0.05$.
+: Significantly different from 50 μM H_2O_2 sample, $p < 0.05$.

3.2.1b Endogenous H_2O_2

The level of endogenous H_2O_2 can be increased in cells by inhibition of catalase activity with potent inhibitors such as 3-amino-1,2,4-triazole (ATZ). It has been shown that treatment of FEK4 cells with 50 mM ATZ for 90 min can inhibit the activity of catalase up to 95% of its control value (Reelfs, unpublished data, this laboratory). In order to find out whether increasing the level of endogenous H_2O_2 could exacerbate the level of exogenous H_2O_2- or UVA-induced LIP release, FEK4 cells were pre-treated with ATZ (under the conditions outlined above) and then the level of LIP was monitored immediately after treatment of cells with either increasing concentrations of exogenous H_2O_2 or with a UVA dose of 250 kJ/m^2. The results (**Table 3.2b**) showed that ATZ pre-treatment itself has no significant impact on LIP level. However pre-treatment of cells with ATZ slightly increases the effect of exogenous H_2O_2 on LIP release within

fibroblasts. In the case of UVA, treatment of cells with ATZ prior to radiation treatment has no effect on the level of LIP release within the cells (**Table 3.2c**). Taken together these results strongly suggest that endogenous H_2O_2 formation following oxidising treatments have a minor effect on modulation of oxidant-induced LIP release in FEK4 cells.

Table 3.2b Modulation of the LIP levels by exogenous H_2O_2 with ATZ treatment of FEK4 cells

FEK4 Samples	LIP (μM)	Fold increase compared to control
Control	1.17 ± 0.23	1
50 mM ATZ	1.31 ± 0.29	1.14 ± 0.25
20 μM H_2O_2	1.32 (n = 2)	-
ATZ + 20 μM H_2O_2	1.40 (n = 2)	-
50 μM H_2O_2	2.11 ± 0.42*	1.81 ± 0.18
ATZ + 50 μM H_2O_2	2.31 ± 0.34 *	2.02 ± 0.44
100 μM H_2O_2	2.71 ± 0.94*	2.30 ± 0.47
ATZ + 100 μM H_2O_2	3.09 ± 0.96*	2.62 ± 0.58

Note: Kd of CA-Fe for FEK4 was 12.7 μM (n = 20).
Measurements were performed 0 h after ATZ/H_2O_2 treatments.
The concentrations of LIP are expressed as the mean ± SD (n = 4-6) except when indicated.
*: Significantly different from the control, $p < 0.05$.

Table 3.2c Effect of ATZ treatment on the LIP levels following UVA irradiation of FEK4 cells

FEK4 Samples	LIP (μM)	Fold increase compared to control
Control	1.36± 0.22	1
UVA 250 kJ/m^2	2.92± 0.70*	2.17± 0.46
50 mM ATZ + Control	1.47± 0.36	1
ATZ + UVA 250 kJ/m^2	2.57± 0.49*	1.81± 0.46

Note: Kd of CA-Fe for FEK4 was 12.7 μM (n = 20).
Measurements were performed 0 h following UVA irradiation.
The concentrations of LIP are expressed as the mean ± SD (n = 4-6) except when indicated.
*: Significantly different from the controls, $p < 0.05$.

3.2.2 Singlet oxygen ($^1O_2$)

Singlet oxygen can be produced in cells upon UVA radiation, via the interaction of light with cellular chromophores, such as porphyrins (see **section 1.7**). Our purpose was to investigate whether $^1O_2$ could be involved in UVA-mediated LIP release. The half-life of $^1O_2$ can be enhanced in cells by the presence of deuterium oxide (D_2O). By taking advantage of this system, the FEK4 cells were irradiated in irradiation buffer where H_2O was replaced with D_2O. The results (**Table 3.2d**) showed that enhancing the lifetime of $^1O_2$ upon UVA treatment (250 kJ/m^2) does not significantly change the level of UVA-induced LIP release in cells. This finding is consistent with the notion that $^1O_2$ is not a mediator in the release of LIP by UVA.

Table 3.2d Effect of D_2O treatment on the LIP levels following UVA irradiation of FEK4 cells

FEK4 Samples	LIP (μM)	Fold increase compared to control
Control	1.41± 0.24	1
UVA 250 kJ/m^2	2.98± 0.80*	2.15± 0.52
D_2O + Control	1.31± 0.38	1
D_2O + UVA 250 kJ/m^2	2.51± 0.56 *	2.03± 0.76

Note: Kd of CA-Fe for FEK4 was 12.7 μM (n = 20).
Measurements were performed 0 h after D_2O/UVA treatment.
The concentrations of LIP are expressed as the mean ± SD (n = 5).
*: Significantly different from the controls, $P < 0.05$.

3.2.3 Modulation by antioxidant, α-tocopherol succinate

Our approach to study the involvement of lipid peroxidation in UVA-mediated LIP release was to use the lipophilic chain-breaking antioxidant α-tocopherol succinate (α-Toco). This antioxidant has been shown to protect primary skin fibroblasts against UVA- induced peroxidative damage presumably as a result of stopping the propagation of the lipid peroxidation chain reaction (Gaboriau et al., 1993; Skoog et al., 1997).

For this purpose, FEK4 cells were treated with α-Toco for 18 h at concentrations up to 40 μM and the threshold of toxicity was monitored prior to UVA-irradiation and the CA-assay. α-Toco at concentration of 40 μM showed some toxicity to the cells, so 10 μM was chosen for the pre-treatment prior to UVA (250 kJ/m^2) treatment. The results (**Table 3.2e**) showed that α-Toco treatment does not affect the level of UVA-induced

LIP release, suggesting that LIP increase by UVA is not triggered by lipid peroxidation within cells (see section **4**).

Table 3.2e Effect of α-tocopherol succinate treatment on the LIP levels following UVA irradiation of FEK4 cells

FEK4 Samples	**LIP (μM)**	**Fold increase compared to control**
Control	1.33± 0.50	1
UVA 250 kJ/m^2	3.14± 0.56*	2.65± 1.23
α-Toco + Control	1.30± 0.37	1
α-Toco + UVA 250 kJ/m^2	3.70± 1.17 *	2.84± 0.41

Note: Kd of CA-Fe for FEK4 was 12.7 μM (n = 20).
Measurements were performed 0 h after UVA treatment.
The concentrations of LIP are expressed as the mean ± SD (n = 4).
*: Significantly different from the controls, $p < 0.05$.

3.3 The role of ferritin on UVA-mediated LIP release in skin cells

It is known that the iron storage protein ferritin has a half-life of 24 h within the cytosol after which it is taken up by lysosomes and degraded by specific lysosomal proteases. The lysosomal degradation of ferritin molecules promotes the release of free iron from the protein shells to the lysosomal organelles. It has been shown that this iron can be transported across the lysosomal membrane either to stimulate the production of new ferritin molecules in human fibroblasts (Radisky and Kaplan, 1998) or to be utilized for haemoglobin synthesis in developing human erythroid precursors (Vaisman et al, 1997).

The proteolytic degradation of ferritin (as measured by immunoprecipitation of ^{35}S-methionine labelled cytosolic protein extracts with a human polyclonal ferritin antibody) may also occur in the cytosol as a result of UVA-induced destabilisation of the lysosomal membrane and the subsequent leakage of proteolytic enzymes from these organelles (Pourzand et al., 1999). Since the UVA-mediated proteolytic degradation of ferritin molecules within the cytosol coincides with the phenomenon of UVA-induced immediate iron release, Pourzand et al. (1999) suggested that the release of iron from ferritin following its degradation might play a key role in UVA-mediated LIP release. However when the fibroblasts were pre-treated with specific lysosomal protease inhibitors (Chymostatin and Leupeptin), they could only partially recover the level of UVA-induced iron release (as monitored by the IRP/IRE bandshift assay), indicating that other sources of iron in addition to ferritin are responsible for the observed phenomenon.

The objective of the work described in this section was to investigate to what extent ferritin iron participates in the UVA-induced increase in LIP. For this purpose the basal

level of ferritin was first modulated with various treatments and then the ferritin concentration was correlated with the level of UVA-induced LIP release in both HaCaT keratinocytes and FEK4 fibroblasts by the CA-assay. The results are summarised below.

3.3.1 Comparison of the basal level of ferritin in fibroblasts and keratinocytes

The results in sections **3.1.1** and **3.1.2** showed that the basal levels of LIP in HaCaT and HFK-SV61 keratinocyte cells were 2-4 fold lower than in FEK4 fibroblasts. In this section, the basal level concentration of ferritin was compared between keratinocytes and fibroblasts using a ferritin ELISA kit (Roche, UK). The results (**Table 3.21**) showed that the ferritin content of HaCaT and HFK-SV61 cells is approximately 5-fold lower than that of FEK4 cells.

Table 3.21 Determination of the basal level of ferritin in FEK4, HaCaT and HFK-SV61 cells

Cell line	Ferritin content (ng/mg protein)
FEK4	93.70±9.4
HaCaT	19.7±6.2
HFK-SV61	17.6 (n=2)

Note: Ferritin levels were measured using an ELISA kit as described in **Materials and Methods**. The concentrations of ferritin are expressed as the mean ± SD (n = 3), except when indicated.

3.3.2 Modulation of ferritin levels in FEK4 and HaCaT cells

Several studies have shown that iron can be successfully supplied to cells either in the form of ferric heme (Hemin) or ferric iron (iron-citrate). These studies have also shown that an increase in iron supply within the cells causes an increase in ferritin synthesis as a result of inactivation of iron regulatory proteins (i.e. IRP1 and IRP2) leading to induction of ferritin mRNA translation (Eisenstein et al., 1991). It is also known that iron deprivation in cells by iron chelator treatment could significantly decrease the level of ferritin synthesis via activation of IRPs and the subsequent inhibition of ferritin mRNA translation (Cario et al., 2000).

To increase the intracellular level of ferritin, HaCaT and FEK4 cells were loaded with increasing concentrations of Hemin or iron-citrate for 18 h and then the level of ferritin accumulation was monitored using an ELISA kit. The results (**Table 3.22**) demonstrated that Hemin loading of cells at the maximum non-toxic concentration increases the level of ferritin up to 4-fold of the control values in FEK4 fibroblasts and up to 2-fold of control values in HaCaT keratinocytes. Iron citrate treatment at its maximum non-toxic concentration was less effective than Hemin, since the intracellular content of ferritin increased only up to 2.5-fold of the control values in FEK4 cells and up to 1.7 fold in HaCaT cells.

Since Vile and Tyrrell (1993) have previously shown that the level of ferritin can be enhanced in FEK4 cells 24 or 48 h following the UVA irradiation of cells (i.e. 1.8 fold of the control values), such experiments were performed and included as additional controls in the present study. The results (**Table 3.22**) confirmed the findings by Vile and Tyrrell, i.e. the level of ferritin doubled that of the control values within 24 or 48 h

after UVA irradiation of FEK4 cells. In HaCaT cells, the same treatment increased the cellular content of ferritin only up to 1.6-fold of the control values.

In order to decrease the level of ferritin in cells, the cells were treated with the highly potent iron chelator Desferrioxiamine (DFO) that is known to scavenge not only the intracellular LIP (Pourzand et al., 1999a) but also ferritin iron as demonstrated by White and Jacob (1978). The overnight treatment of FEK4 cells with 100 μM DFO decreased the level of ferritin up to 5-fold of the control values (**Table 3.22**).

Table 3.22 Modulation of ferritin levels in HaCaT and FEK4 cells following various treatments

Treatment	(ng ferritin /mg protein) FEK4	(ng ferritin/mg protein) HaCaT
Control	93.70±9.4	19.7±6.2
DMSO control	137.3±16.1	29.6±9.9
5 μM Hemin	217.5±22.3	37.2±12.9
20 μM Hemin	399.8±53.6 * +	44.3±8.3 *
50 μM iron citrate	214.5 (n =2)	31.1±6.1
100 μM iron citrate	253.6± 30.0 *	33.1±7.0
100 μM DFO	17.81±6.7 *	
$250^{d0}/0^{d1}$	189.1±52.1 *	32.3±4.3
$250^{d0}/0^{d2}$	173.1±24.4 *	30.3±3.9

Ferritin levels were measured using an ELISA. Hemin, iron-citrate and DFO treatments were carried out for 18 h in conditioned media. The concentrations of ferritin are expressed as the mean ± SD (n = 3) except when indicated.
*: Significantly different from control, $p < 0.05$.
+: Significantly different from 100 μM iron-citrate sample, $p < 0.05$.

3.3.3 Effect of iron loading on UVA-mediated LIP release in FEK4 cells

Table 3.3.3 shows the level of LIP in FEK4 cells following UVA radiation of cells that have been pre-treated for 18 h with either 20 μM Hemin or 100 μM iron-citrate. Hemin or iron-citrate treatments *per se* do not modulate the level of LIP in FEK4 cells. However UVA irradiation of Hemin pre-treated cells causes an immediate increase in LIP (i.e. 3.4-fold of the control values) that is significantly higher than the UVA-irradiated sample alone (i.e. 2.5-fold of the control values). Interestingly, UVA-irradiation of iron-citrate pre-treated FEK4 cells does not increase significantly the level of LIP when compared to the UVA-irradiated sample alone. These results suggest that since ferritin iron is only partially involved in the UVA-induced iron release, a significant increase in UVA-mediated LIP can only be detected in Hemin pre-treated cells, where the level of increase in ferritin molecules is substantially higher (around 4-fold) than that in control cells. In contrast, in iron-citrate pre-treated cells, where the enhancement of ferritin level is only around 2.5-fold control values, the CA-assay fails to detect a significant increase in LIP as compared to UVA-irradiated cells alone. The latter explanation seems also to be true for the samples involved in the UVA challenge dose experiments. Indeed, the level of ferritin increase only up to 2-fold control value 24 h following the first irradiation (i.e. 250^{d0} / 0^{d1}) and consequently the CA-assay performed immediately following the second challenge dose (i.e. 250^{d0} / 250^{d1}), fails to show a significant difference in LIP levels as compared to the corresponding non-pre-irradiated control (i.e. 0^{d0} / 250^{d1}).

Table 3.3.3 Effect of iron loading on UVA-induced LIP release in FEK4 cells.

FEK4 Samples	[LIP] μM	Fold increase compared to control
Control	1.33± 0.35	1
UVA 250 kJ/m^2	3.05± 0.94*	2.01± 0.305
Iron-citrate + Control	1.54±0.53	1
Iron-citrate + UVA 250 kJ/m^2	3.38±0.93*	2.24±0.32
DMSO + Control	1.20±0.29	1
DMSO + UVA 250 kJ/m^2	2.53±0.24*	2.20±0.44
Hemin + Control	1.04±0.16	1
Hemin + UVA 250 kJ/m^2	3.43±0.64* +	3.31±0.53
0^{d0} / 0^{d1}	1.13±0.22	1
0^{d0} / 250^{d1}	2.42±0.58*	2.16±0.40
250^{d0} / 0^{d1}	1.07±0.28	0.95±0.12
250^{d0} / 250^{d1}	1.85±0.56*	1.65±0.31

Note: Kd of CA-Fe for FEK4 was 12.7 (n = 20).
Measurements were performed 0 h after UVA treatment.
The concentrations of LIP are expressed as the mean ± SD (n = 6-11).
*: Significantly different from the controls, $p < 0.05$.
+: Significantly different from the control (DMSO + UVA 250 kJ/m^2), $p < 0.05$.

3.3.4 Effect of protease inhibitors on UVA-mediated LIP release in FEK4 cells

As noted above, Pourzand et al. (1999) have previously demonstrated that preventing UVA-mediated immediate ferritin degradation by pre-treatment of FEK4 cells with specific lysosomal protease inhibitors (Leupeptin and Chymostatin) could only partially recover the UVA-induced iron release (as determined by the IRP/IRE bandshift assay), indicating that ferritin iron is involved in the UVA-induced increase in LIP. In this

section an attempt was made to measure the level of UVA-induced iron release by the CA-assay in FEK4 cells that have been treated with protease inhibitors Chymostatin (50 μg/ml) and Leupeptin (20 μg/ml) for 18 h prior to UVA irradiation. The results **(Table 3.3.4)** showed that although the level of UVA-induced LIP release was lower in FEK4 cells treated with protease inhibitors as compared to UVA-irradiated sample alone, a statistically significant difference could not be established between those two conditions. These results suggest that, as previously suggested, ferritin iron is only partially involved in the pool of labile iron that was measured following UVA irradiation and that the IRP/IRE bandshift assay is a more sensitive assay for detecting subtle differences in intracellular chelatable iron pool than the CA-assay.

Table 3.3.4 Effect of protease inhibitor (PI) on UVA-induced LIP release in FEK4 cells

Sample	LIP (μM)	Fold increase compared to control
DMSO Control	1.29±0.42	1
DMSO + UVA 250 kJ/m^2	2.40±0.38*	1.98±0.53
PI + Control	1.20±0.36	1
PI + UVA 250 kJ/m^2	1.97±0.47*	1.71±0.46

Note: Kd of CA-Fe for FEK4 was 12.7 (n = 20).
Cells were pre-treated for 18 h with protease inhibitors (PI) Chymostatin (50 μg /ml) and Leupeptin (20 μg/ml). Control cells were pre-treated with DMSO (vehicle for Chymostatin) at the same concentration for 18 h. Measurements were performed 0 h after UVA treatment. The concentrations of LIP are expressed as the means ± SD (n = 5).
*: Significantly different from the controls, $p < 0.05$.

3.4 The correlation between the level of UVA-induced iron release and the extent of lysosomal membrane damage

After characterisation of the phenomenon of UVA-induced LIP release in both fibroblast and keratinocyte cell lines, an investigation was performed to correlate the level of UVA-induced iron release and the extent of UVA-mediated lysosomal membrane damage in both fibroblasts and keratinoytes following single or repeated exposures to radiation treatment. Four independent assays were used for this purpose, as described below.

3.4.1 Epifluorescence microscopy studies

Epifluoresence microscopy was used in conjunction with an acidotropic fluorescent dye (LysoSensor DND-153) to assess the integrity of lysosomal membranes by monitoring the retention of the proton gradient across the membranes of the acidic vacuolar compartments. LysoSensor DND-153 is a weak base that enters the cells as uncharged species. Then the proton gradient between the cytosol and the lysosomal compartment allow the fluorescent dye to be trapped as protonated species in the acidic organelles. When excited by blue light, the highly concentrated LysoSensor DND-153 in lysosomes will emit a pH-dependent bright orange granular fluorescence (Molecular probes: LysoTracer ^{TM} and LysoSensor ^{TM} Probes). However the same dye when uncharged or diluted in the cytosol will emit a diffuse greenish fluorescence. Therefore the level of retention of this dye in the lysosomal compartment can be used to monitor the extent of UVA-induced lysosomal damage. For this purpose, the cells were first cultured on coverslips to 80% confluency and then irradiated with a range of doses of UVA (i.e. 250 and 500 kJ/m^2). Immediately after irradiation, the irradiation buffer was replaced with fresh media containing the LysoSensor DND-153 and the cells were incubated for 1 to 2

h at 37°C. The integrity of lysosomal organelles was then monitored by epifluorescence microscopy using the appropriate emission/excitation wavelength. The results are summarized below.

3.4.1a Fibroblasts

Dose response

Fig. 3F1 shows the intact lysosomal organelles in non-irradiated (control) cells. The appearance of orange/yellow fluorescent organelles was due to the accumulation of the acidotropic dye in the acidic lysosomal compartments, indicating that the lysosomal membranes were intact and that the proton gradient was not disturbed. Following UVA irradiation of cells with a moderate dose of 250 kJ/m^2 (**Fig. 3F2**), the number of intact orange lysosomal organelles reduced significantly. Instead, the fluorescence of the lysosomal compartment was substantially lower indicating that the proton gradient of he lysosomal membrane was disturbed. Furthermore the loss of fluorescence in the lysosomal compartment was accompanied with the appearance of a diffuse and diluted greenish fluorescence in the cytosol. The latter is known to occur as a result of leakage of the dye from the acidic compartment to the cytosol due to the UVA-mediated damage to the lysosomal membrane. At a high dose of 500 kJ/m^2 (**Fig. 3F3**), the image revealed only very few intact fluorescent lysosomes surrounded by a cytosolic compartment with a highly intense blurred greenish fluorescence. The latter observation indicates that a high dose of UVA could substantially damage the lysosomal membranes resulting in a significant leakage of the fluorescent dye from lysosomal organelles. The same dose-response experiments were also in 1BR3 fibroblasts. The results (**Fig. 3B1-3B3**) showed a similar pattern of lysosomal membrane damage following UVA radiation treatment.

These results confirmed the observations previously made by Pourzand et al (1999) that in FEK4 cells, UVA triggers an immediate and dose-dependent damage to lysosomal membranes. The authors have also provided data showing that with a moderate dose of 250 kJ/m^2, the UVA-mediated immediate lysosomal damage could substantially recover by 6 h post-irradiation time. However at a high dose of 500 kJ/m^2, the damage to lysosomes could only partially recover 24 h following the radiation treatment.

Effect of DFO

DFO is a highly potent hydrophilic chelator. Several studies (e. g. Zdolsek et al., 1993; Cable and Lloyds, 1999) have shown that DFO (as a hydrophilic compound) can enter the cells via endocytosis and is first detected in the lysosomal compartments. Since lysosomal organelles are primarily the organelles that degrade both hemoproteins and ferritin, it is believed that these compartments contain a substantial pool of LIP. Studies from Ollinger and Brunk (1995) suggest that this pool of reactive iron could participate in the formation of highly reactive $OH^{\bullet}$ following treatment of cells with H_2O_2, resulting in an immediate burst of lysosomal membranes. The authors also demonstrated that pre-treatment of cells with DFO prior to H_2O_2 exposure, could substantially protect the cells against the H_2O_2-mediated lysosomal membrane damage. To test the possibility that DFO treatment of fibroblasts prior to UVA irradiation, could also protect the lysosomal membranes against the UVA-mediated damage, the LysoSensor epifluorescence study was performed in FEK4 and 1BR3 cells that were pre-treated with DFO prior to UVA irradiation. The results (**Fig. 3F4-F6** for FEK4 and **Fig. 3B4-3B6** for 1BR3) were in agreement with the findings by Ollinger and Brunk (1997) since DFO pre-treatment significantly protected the lysosomal membrane against UVA-mediated damage in both studies.

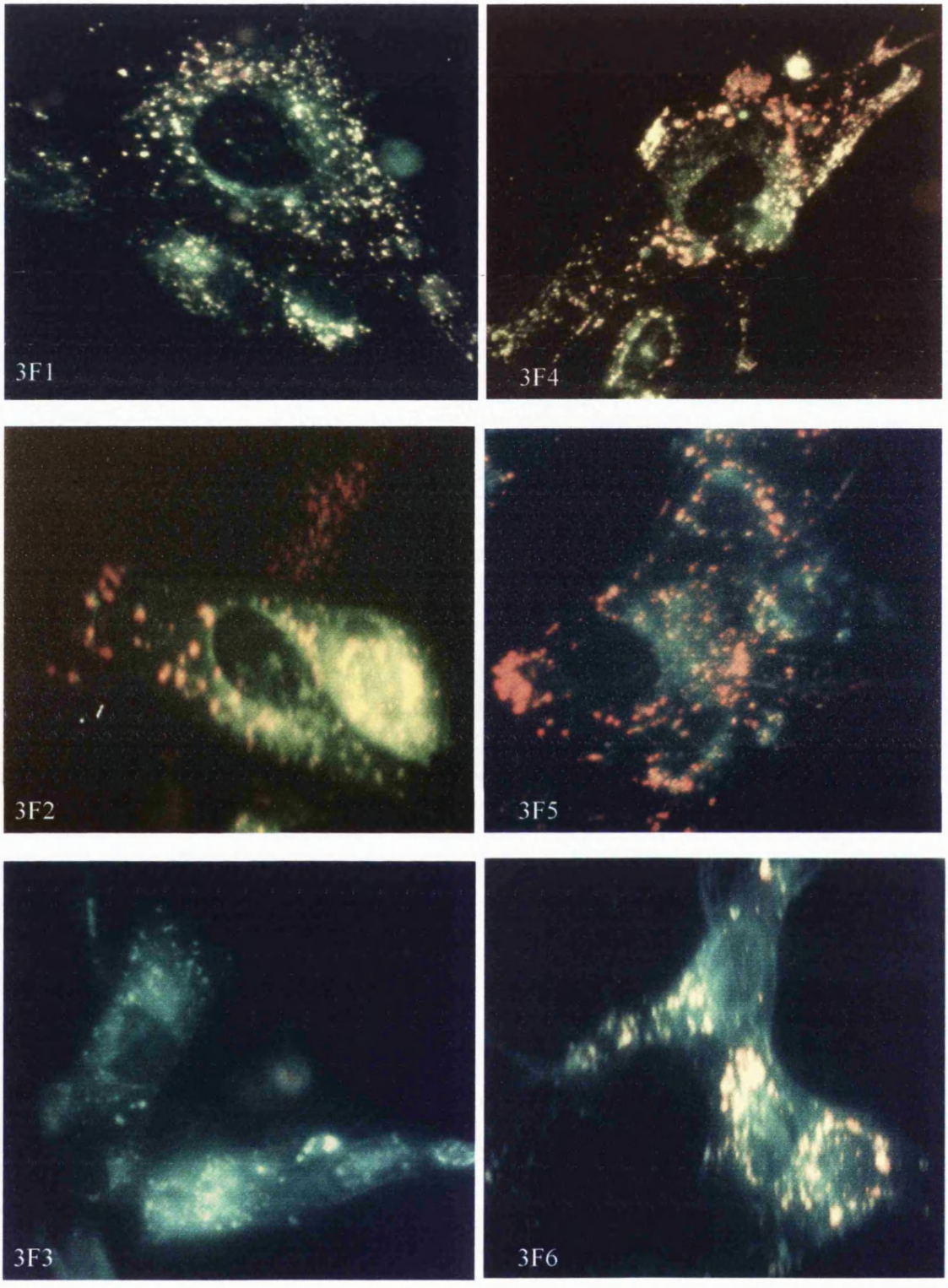

Fig. 3F. Effect of DFO on the UVA-mediated lysosomal damage of FEK4 cells
DFO treated or non-treated FEK4 cells were irradiated with UVA, then loaded with LysoSensor DND-153 for 2 h.
3F1 (0 kJ/m^2), 3F2 (250 kJ/m^2), 3F3 (500 kJ/m^2);
DFO treated 3F4 (0 kJ/m^2), 3F5 (250 kJ/m^2 , 3F6 (500 kJ/m^2)

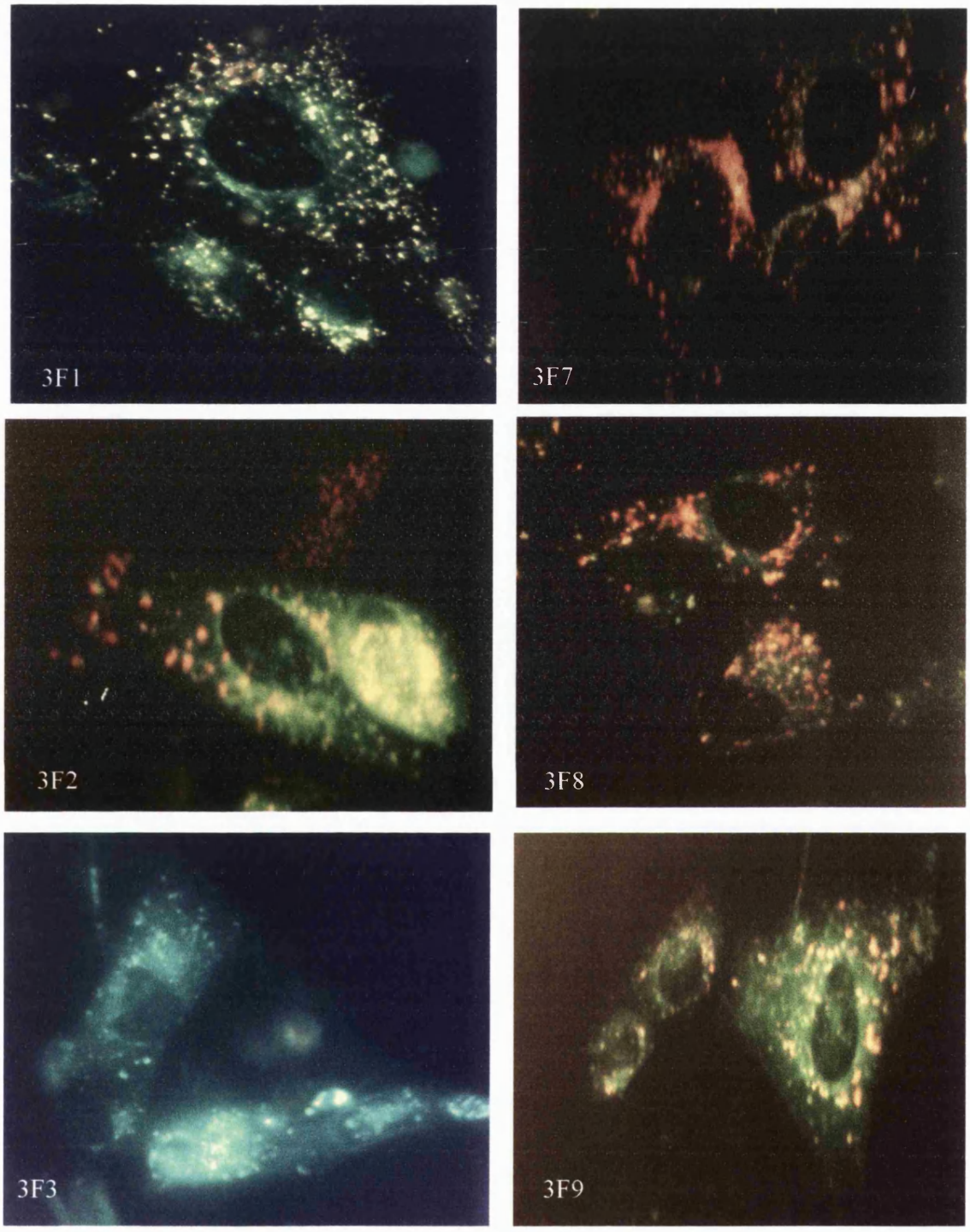

Fig. 3Fb. Effect of BHT on the UVA-mediated lysosomal damage of FEK4 cells
BHT treated or non-treated FEK4 cells were irradiated with UVA, then loaded with LysoSensor DND-153 for 2 h.
3F1 (0 kJ/m^2), 3F2 (250 kL/m^2), 3F3 (500 kJ/m^2);
BHT treated 3F7 (0 kJ/m^2), 3F8 (250 kJ/m^2), 3F9 (500 kJ/m^2)

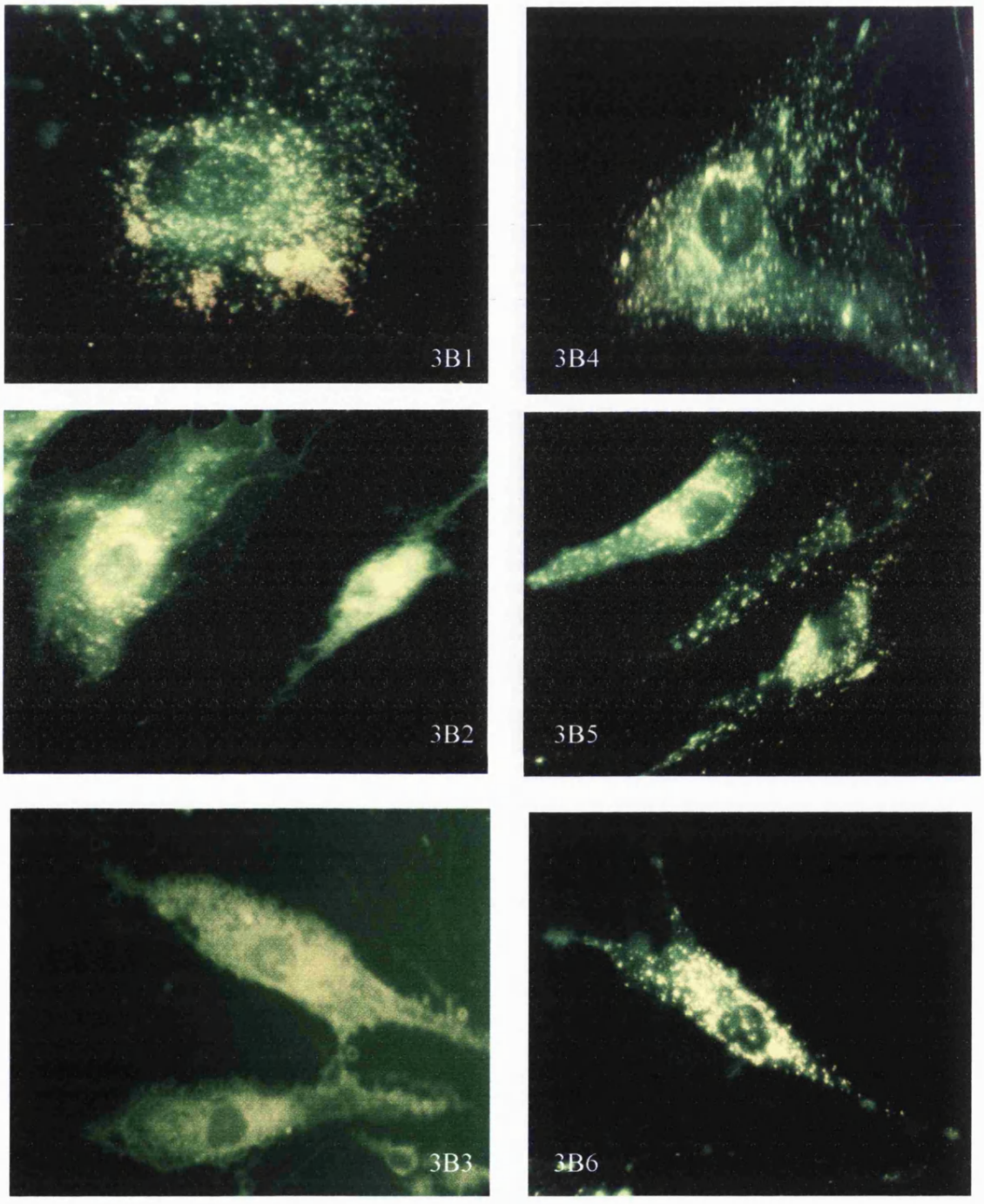

Fig. 3B. Effect of DFO on the UVA-mediated lysosomal damage of 1BR3 cells
DFO-treated or non-treated 1BR3 cells were irradiated with UVA, then loaded with LysoSensor DND-153 for 2 h.
3B1 (0 kJ/m^2), 3B2 (250 kL/m^2), 3B3 (500 kJ/m^2);
DFO treated 3B4 (0 kJ/m^2), 3B5 (250 kJ/m^2), 3B6 (500 kJ/m^2)

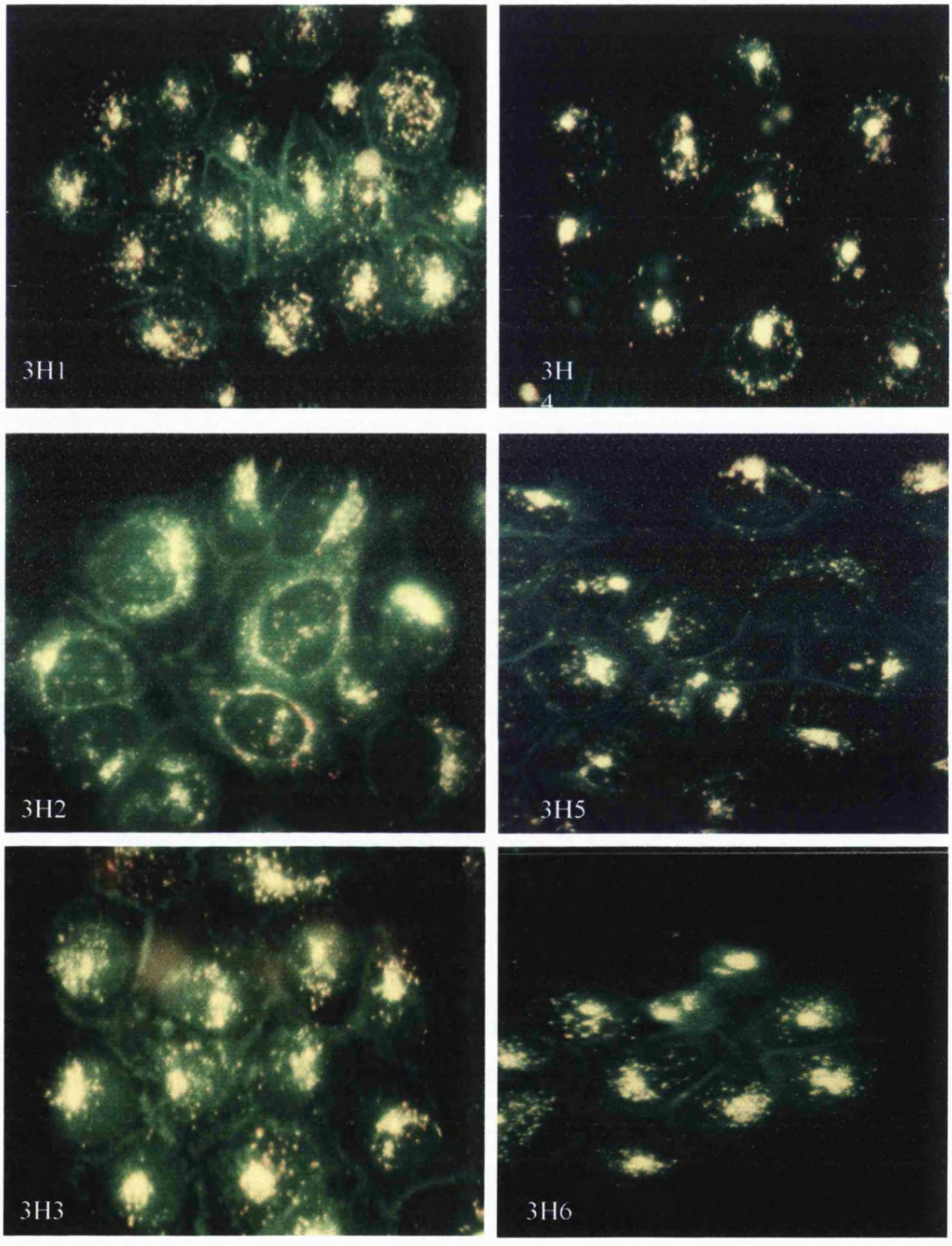

Fig. 3H. Effect of DFO on the UVA-mediated lysosomal damage of HaCaT cells

DFO-treated or non-treated HaCaT cells were irradiated with UVA, then loaded with LysoSensor DND-153 for 2 h.
3H1 (0 kJ/m^2), 3H2 (250 kL/m^2), 3H3 (500 kJ/m^2);
DFO treated 3H4 (0 kJ/m^2), 3H5 (250 kJ/m^2), 3H6 (500 kJ/m^2).

Effect of BHT

BHT is a membrane antioxidant since it has the property to block the lipid peroxidation chain reaction. Ollinger and Brunk (1995) have demonstrated that antioxidant could also protect the cells against H_2O_2-mediated lysosomal membrane damage. To investigate whether BHT could also protect the FEK4 cells against the UVA-induced lysosomal membrane damage, the LysoSensor epifluorescence study was performed in FEK4 cells that were pre-treated with BHT prior to UVA irradiation. The results (**Fig. 3Fb(7-9)**) demonstrated that in contrast to DFO, BHT could only partially protect the organelles against the UVA-induced damage. The fact that this antioxidant in contrast to DFO could not significantly modulate both the basal and UVA-induced LIP levels (data not shown), strongly suggests that the pool of reactive iron either in lysosomes or at cellular level plays a role in promotion of lysosomal membrane damage by UVA.

3.4.1b Keratinocytes

Dose-response

The UVA dose-response experiments were also carried out with HaCaT cells. The results (**Fig. 3H1-3**) showed that UVA-induced lysosomal damage occurs also in a dose-dependent manner in this cell line. However the extent of lysosomal damage in keratinocytes was not as dramatic as fibroblasts. Indeed at UVA doses of both 250 and 500 kJ/m^2, a substantial number of intact lysosomal organelles could still be detected. Also, it is worthy of note that HaCaT cells contain much fewer lysosomal organelles than fibroblasts.

Effect of DFO

In contrast to fibroblast cells, DFO pre-treatment of HaCaT cells prior to UVA irradiation could only partially recover the UVA-induced lysosomal membrane damage **(Fig. 3H4-6)**.

3.4.2 Cathepsin B ELISA

Lysosomal organelles are rich in proteases since they degrade and recycle several proteins such as ferritin. Cathepsin B (Cath B) belongs to the family of lysosomal cysteine proteases and is expressed at significantly higher concentration under certain pathological conditions such as malignancy. Two independent studies from this laboratory (Pourzand et al, 1999; Waltner et al, unpublished data, this laboratory, unpublished) have demonstrated that UVA-induced damage to lysosomal organelles promotes the leakage of potentially harmful lysosomal proteases into the cytosol. The latter has shown that following irradiation of FEK4 cells with a UVA dose of 250 kJ/m^2, the level of lysosomal Cath B, L and D are increased up to 2.5-fold of the control values in the cytosolic fraction of cells devoid of intact organelles (i.e. cytosolic S100 fraction prepared as Dignam et al, 1983). Also Pourzand et al. (1999a) have shown that in the same cells and following the same dose of UVA, the level of lysosomal protease Chymotrypsin (i.e. the specific lysosomal protease responsible for the degradation of ferritin) is increased up to 2.7-fold of the control values. Therefore the Cath B ELISA kit was used in the present study to monitor the level of UVA-induced lysosomal damage in both fibroblasts and keratinocytes following single or repeated exposures to UVA radiation. The results are summarised below.

3.4.2a Fibroblasts

Cells were first cultured to 80% confluency and then irradiated with UVA doses of 250 and 500 kJ/m^2. Immediately after irradiation, cells were detached from the plates by either mild trypsinization or using a non-enzymatic cell dissociation solution. Then, the outer cell membrane was either broken in a hypotonic buffer by cell homogenisation or alternatively by treatment of cells with a mild detergent (i.e. 0.1% Nonidet-P 40). This step was followed by a low speed centrifugation to pellet the cell membrane debris. The supernatant was then subjected to an ultra centrifugation to pellet the intact organelles and the nucleus. The resulting supernatant called the "Cytosolic S100 fraction" which was devoid of any intact organelle was used for the Cath B ELISA. The results are shown in **Table 3.4.2a**. The basal level of Cath B was similar in both FEK4 and 1BR3 fibroblasts, however following UVA irradiation the level of Cath B increased in both cell lines in a dose-dependent manner up to 2.3-fold of the control values. These results are in agreement with the data obtained by LysoSensor DND-153 epifluorescence microscopy. It was also observed that the increase in Cath B in the cytosolic fraction of cells irradiated with a moderate dose of 250 kJ/m^2 returned to control levels at 24 h post-irradiation time (i.e. 250^{d0} / 0^{d1}). Furthermore, the UVA irradiation of pre-irradiated cells 24 h following the first UVA challenge (i.e. 250^{d0} / 250^{d1}) triggered the leakage of the lysosomal protease Cath B to the cytosol, although to a lesser extent than the first irradiation treatment (i.e. 0^{d0} / 250^{d1}).

DFO pre-treatment of cells prior to UVA irradiation slightly decreased the level of Cath B release, although a statistically significant protection could not be established. These results were in contrast to the previous study performed by LysoSensor DND-153. A possible explanation for this discrepancy is that perhaps during the procedure of

preparation of the cytosolic S-100 fraction the lysosomal organelles were mechanically damaged. This physical damage could cause a contamination of the cytosolic preparations with a residual background Cath B protein and decrease the accuracy of our findings.

Table 3.4.2a UVA-mediated Cath B release in FEK4 and 1BR3 cells

Treatment	FEK4 Cath B (ng/ml)	IBR3 Cath B (ng/ml)
0^{0h}	8.96±4.2	11.2±1.92
250^{0h}	14.84±5.6*	18.48±5.32*
500^{0h}	21.28±5.6*	19.32±4.48*
DFO + 0^{0h}	8.40±5.04	11.2±2.24
DFO + 250^{0h}	13.44±4.48*	18.48±5.60*
DFO + 500^{0h}	18.20±4.48*	19.60±6.16*
250^{d0} / 250^{d1}	12.88± 4.48	16.8±0.56 +
250^{d0} / 0^{d1}	8.12±1.12	9.80±5.04

Cytosolic Cath B levels were measured using an ELISA kit.
Protein extracts were diluted in the incubation buffer to the concentration of 0.06 mg/ml. Cells were treated for 18 h with 100 μM DFO.
Data represent the mean ± SD (n = 3-6).
* Significantly different from the sham-irradiated control (0^{0h}), $p < 0.05$.
+ Significantly different from 250^{d0} / 0^{d1}, $p < 0.05$.

3.4.2b Keratinocytes

HaCaT cells contain less lysosomal organelles than fibroblasts as determined by epifluorescence microscopy. Accordingly the level of cytosolic Cath B in HaCaT cells appeared to be much lower than in FEK4 and 1BR3 fibroblasts, in order to detect the Cath B levels by ELISA in this cell line, a much higher level of protein extract was used. The results (**Table 3.4.2b**) showed that in HaCaT cells, UVA could also trigger

the lysosomal leakage of Cath B to the cytosol in a dose-increase manner. However the level of residual Cath B in non-treated HaCaT cells was substantially lower than in fibroblasts. Surprisingly, the DFO treatment did not affect the level of UVA-induced Cath B release. This result was in contrast to the findings with the LysoSensor epifluorescence study, where DFO pre-treatment could partially protect the HaCaT lysosomal organelles against UVA-induced membrane damage. These findings were similar to the observations made in fibroblasts. It was therefore proposed that, as for fibroblasts, the mechanical damage to lysosomes during the procedure of cytosolic extraction might have contaminated the cytosolic fraction with residual traces of Cath B consequently masking the protection by DFO. To test this hypothesis an *in situ* immunocytochemistry analysis was performed in both fibroblasts and keratinocytes using a polyclonal human Cath B antibody (see section **3.4.3**).

Table 3.4.2b UVA-mediated Cath B release in HaCaT cells

Treatment	Cath B (ng/ml)
0^{0h}	2.07±0.47
250^{0h}	4.59±1.65*
500^{0h}	5.46±2.10*
DFO + 0^{0h}	2.24±0.86
DFO + 250^{0h}	4.98±2.46*
DFO + 500^{0h}	5.94±1.79*

HaCaT Cytosolic Cath B levels were measured using an ELISA kit.
Protein extracts were diluted in the incubation buffer to the concentration of 0.2 mg/ml.
Cells were treated for 18 h with 100 μM DFO.
Data represent the mean ± SD (n = 4-6).
* Significantly different from the sham-irradiated control (0^{0h}), $p < 0.05$.

Total Cath B of skin cells

The immunohistochemistry showed that HaCaT cells has very faint staining and the cytosol S-100 fraction showed that they have much lower level of Cath B. To further support that HaCaT cells have lower level of Cath B, the Cath B ELISA was determined in total protein of cell extracts. Table **3.4.2c** showed that indeed in HaCaT cells have much lower intracellular level of Cath B compared with FEK4 and 1BR3 fibroblasts. In order to detect the Cath B levels by ELISA in this cell line, a much higher level of protein extract was used.

Table 3.4.2c Total Cath B levels of skin cells

Cell line	Cath B (ng/ml)
FEK4	6.55 ±2.10
1BR3	18.90±3.58
HaCaT	24.40±0.70

Note: Cells total Cath B levels were measured using a Cath B ELISA kit. Protein extracts were diluted in the incubation buffer to the concentrations of 0.02 mg/ml for FEK4 and 1BR3 cells and 0.2 mg/ml for HaCaT cells. Data represent the mean ± SD (n = 3-4).

3.4.3 Cath B immunocytochemistry

Cells were grown on coverslips to 80% confluency and then irradiated with a range of doses of UVA (i.e. 250 and 500 kJ/m^2). Following irradiation the cells were fixed with methanol and then incubated firstly with polyclonal rabbit anti-human Cath B antibody and secondly with polyclonal goat anti-rabbit IgG tagged with FITC antibodies. This was followed by epifluorescence microscopy using the appropriate excitation and emission wavelengths. **Fig. 3F10** shows a representative example of a Cath B immunostaining in non-treated FEK4 cells. As you can see the Cath B proteases were mainly localised as bright green dots within the lysosomal organelles. However following UVA irradiation of cells with a dose of 250 kJ/m^2 (**3F11**), a significant delocalisation of the proteases from the lysosomal compartment to the cytosol was observed. At a high dose of 500 kJ/m^2, the delocalisation of the enzyme was even more apparent (**Fig. 3F12**). In 1BR3, the same dose-dependent pattern of Cath B redistribution was observed. In HaCaT cells however the immunostaining was very faint presumably due to the fact that this cell line contained much fewer lysosomal organelles **(data not shown).**

When fibroblasts were pre-treated with DFO and then UVA irradiated (**Fig. 3F13-15 and 3B10-12**) a significant decrease in the redistribution of the Cath B from the lysosomal compartment to the cytosol could be observed, consistent with the notion that DFO has a protective effect on UVA-induced lysosomal membrane damage.

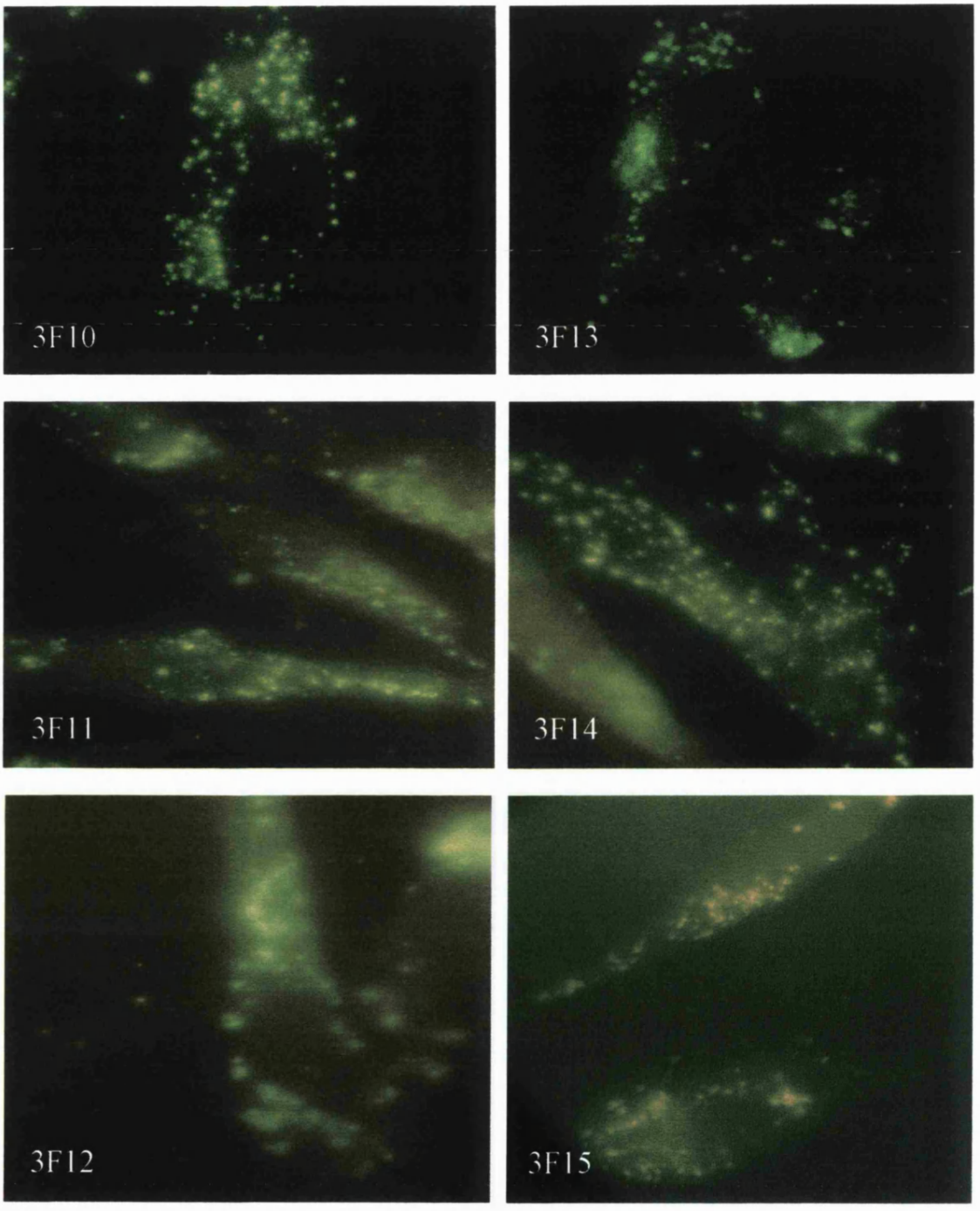

Fig. 3F10-15 Effect of DFO on UVA-mediated delocalisation of lysosomal Cath B in FEK4 cells. Control (3F10), 250 kJ/m^2 (3F11) and 500 kJ/m^2 (3F12); DFO treated control (3F13), 250 kJ/m^2 (3F14) and 500 kJ/m^2 (3F15).

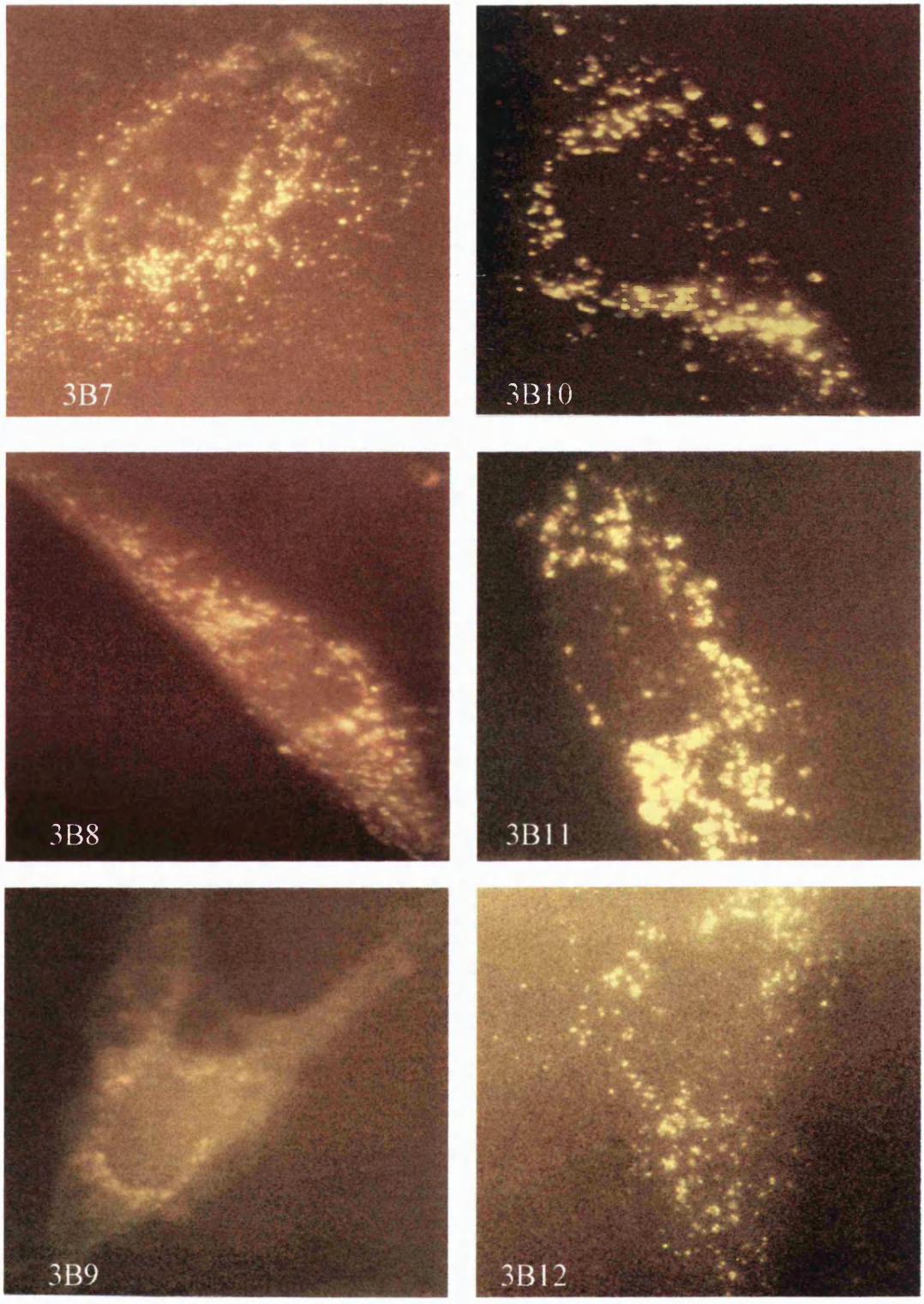

Fig. 3B7-12 Effect of DFO on UVA-mediated delocalisation of lysosomal Cath B in 1BR3 cells. Control (3B7), 250 kJ/m^2 (3B8) and 500 kJ/m^2 (3B9); DFO treated control (3B10), 250 kJ/m^2 (3B11) and 500 kJ/m^2 (3B12).

3.4.4 Neutral red assay

The Neutral red assay was used to further reinforce the data showing that UVA induces dose-dependent lysosomal membrane damage and that DFO pre-treatment protects the organelles against UVA-mediated damage. This assay is based on the uptake of neutral red dye and retention of the dye in the lysosomes of cultured cells. For this purpose FEK4, 1BR3 and HaCaT cells were irradiated with a range of doses of UVA (i.e. 250 and 500 kJ/m^2) and then the cells' ability to retain the neutral red compound were monitored. The results **Fig. 3.4A, B** and **C** (for FEK4, 1BR3 and HaCaT cells, respectively) confirmed that UVA induces a dose-dependent leakage of the dye from the lysosomes and that DFO pre-treatment prior to UVA radiation could significantly increase the retention of neutral red within fibroblast cell lines. However in HaCaT cells, the extent of UVA-induced lysosomal damage was significantly lower than fibroblast cell lines. These results strongly suggested a direct correlation among the level of intracellular LIP, the amount of lysosomal organelles and the extent of UVA-induced lysosomal damage.

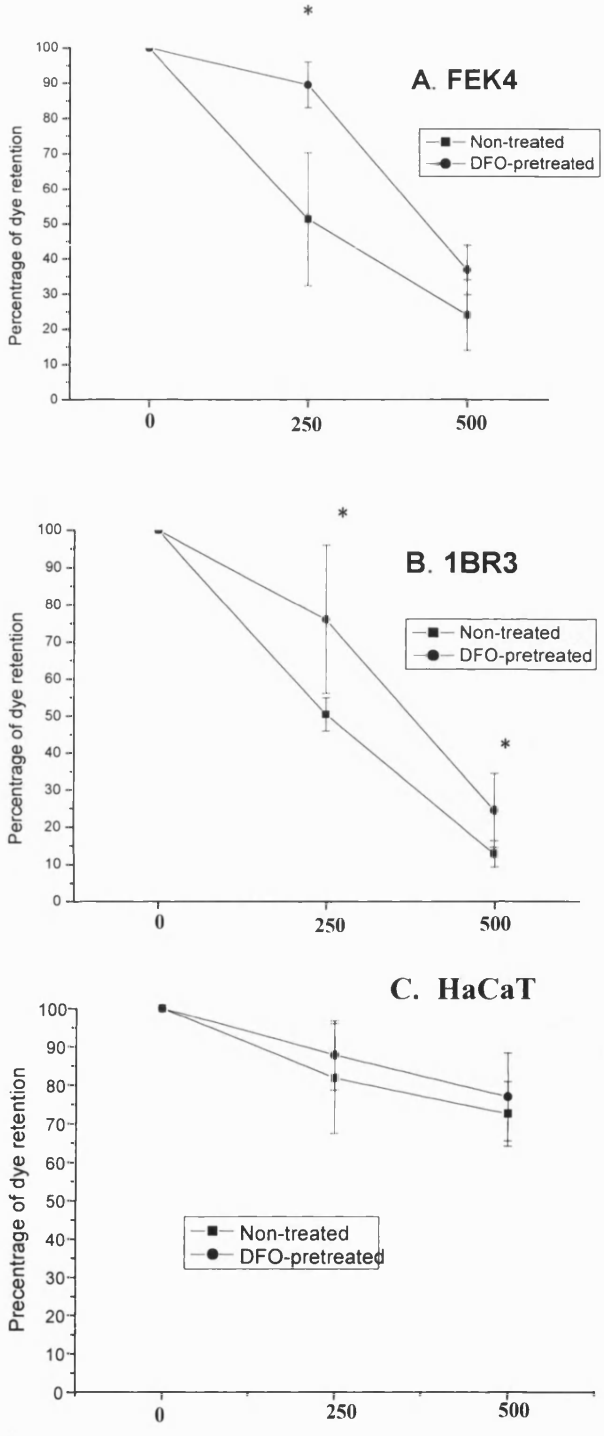

Fig. 3.4 A. B. C. Effect of DFO on UVA-mediated lose of neutral red dye retention of skin cells
Cells were pre-treated or non-treated with DFO, then irradiated at the indicated doses. The uptake of neutral red dye was measured. Data were normalised by taking 100% as the retention of the dye of controls. Values are the mean ± SD of 3-5 independent experiments.
*: Significance level when compared with non-treated sample, $p < 0.05$

3.5 The correlation between the level of UVA-induced iron release and the extent of plasma membrane damage

After characterisation of the phenomenon of UVA-induced lysosomal damage, an attempt was made to correlate the level of UVA-induced iron release with the extent of UVA-mediated plasma membrane damage. For this purpose the level of leakage of intracellular LDH was used as a monitor for plasma membrane damage in both fibroblasts and keratinocytes following single or repeated exposures to UVA radiation. The results are summarised below.

3.5.1 UVA-induced LDH release in FEK4 cells

UVA is a strong membrane-damaging agent. Previous studies from this laboratory (Vile et al, 1994) and others (e. g. Morliere et al., 1991) have shown that UVA triggers lipid peroxidation of cellular membranes as evaluated by the formation of TBARs. Since the peroxidation of lipids in cell membranes will promote the leakage of the intracellular content (notably the cytosolic LDH enzyme), the quantification of the amount of LDH leakage from cells to the extracellular media could be used as a monitor for evaluation of the extent of UVA-induced membrane damage. Indeed in some studies the extent of UVA-induced cell membrane lipid peroxidation also directly correlated with the amount of LDH leakage (e. g. Vile et al, 1994). Using both TBAR and LDH assays, Vile et al (1994) have also demonstrated that UVA pre-irradiated (i.e. 250 kJ/m^2) FEK4 fibroblasts, sustain less membrane damage following a second high dose of UVA radiation (i.e. 750 kJ/m^2) when compared with the corresponding non-pre-irradiated cells. Since UVA induces LIP release following either single or a second challenge dose of UVA, the observed adaptive response was sought in the fibroblasts following UVA irradiation of pre-irradiated cells (i.e. 250 kJ/m^2) with a moderate dose

of 250 kJ/m^2 (i.e. conditions used for LIP measurements). The results (**Table 3.5a**) showed that pre-irradiated cells sustain similar LDH release of the corresponding non-pre-irradiated controls, consistent with the notion that the adaptive response (i.e. observations by Vile et al, 1994) does not occur in the conditions used in this study. Indeed, it appears that the extent of LIP release in the present study directly correlates with the amount of LDH leakage, suggesting that the cell membrane might be a primary target for LIP-mediated damage, since iron is a catalyst of lipid peroxidation.

Table 3.5a UVA-induced LDH release in FEK4 cells

Samples	LDH activity of supernatant	Fold increase compared to control
0^{0h}	0.0362±0.009	1
250^{0h}	0.1049±0.028*	3.0±0.27
$0^{d0}/0^{d1}$	0.039±0.016	1
$0^{d0}/250^{d1}$	0.0710±0.020 *	2.0±0.30
$250^{d0}/250^{d1}$	0.0921±0.071 *	2.8±0.53
$250^{d0}/0^{d1}$	0.0415±0.010	1.2±0.12
$0^{d0}/0^{d2}$	0.0404±0.010	1
$0^{d0}/250^{d2}$	0.0886±0.044 *	2.1±0.22
$250^{d0}/250^{d2}$	0.0980±0.037 *	2.4±0.13
$250^{d0}/0^{d2}$	0.0431±0.021	1.1±0.11

Note: The level of LDH activity was measured in supernatant of cells following UVA treatments. The LDH values of the controls were arbitrary set to 1. Values are mean ± SD of 3 experiments.
* Significantly different from the sham-irradiated control, $p < 0.05$.

Although the total LDH activity of fibroblast cells, when normalized to the cell number was constant between the experiments, it was found that the total LDH of the UVA pre-irradiated samples were always lower than the non-pre-irradiated group. To investigate this phenomenon further, the total LDH activity of cells irradiated with a dose of 250 kJ/m^2 was followed up to 24 h post-irradiation time. The results (**Table 3.5b**) revealed that the total enzymatic activity of LDH decreases gradually following radiation treatment where at 24 h time-point this activity reaches half of its original value. These results strongly suggest that UVA mediates a direct damage to LDH protein resulting in a decrease of its enzymatic activity.

Table 3.5b UVA-mediated damage to LDH in FEK4 cells

Time post UVA (h)	**0**	**3**	**6**	**10**	**16**	**20**	**24**
LDH activity (% of control)	97	90	84	80	75	60	45

Note: LDH activity of the cells was measured at different time points following UVA irradiation. Total LDH activity was compared with relative control (n = 2).

In **Table 3.5a** the level of UVA-induced LDH release to supernatant was calculated relative to the control samples, which was arbitrarily set to 1. However in order to estimate the leakage of LDH in FEK4 cells, the LDH of supernatant this time was expressed as percentage of total LDH (LDH of supernatant + LDH remaining in the cells). This quantification (**Table 3.5c**) revealed that despite the UVA-induced damage to the LDH enzyme, the percentage of LDH leakage in the pre-irradiated sample (i.e. $250^{d0} / 250^{d1}$) is much higher than in the non-pre-irradiated sample (i.e. $0^{d0} / 250^{d1}$)

consistent with the notion that exposure of cells to low split doses of UVA increases the susceptibility of the plasma membrane to UVA-induced damage.

Table 3.5c UVA induced LDH leakage of FEK4 cells

Sample	LDH leakage (%)
$0^{d0} / 0^{d1}$	4.2±1.3
$0^{d0} / 250^{d1}$	8.0±3.1
$250^{d0} / 250^{d1}$	12.6±5.1
$250^{d0} / 0^{d1}$	5.7±2.7

Note: LDH leakage in the supernatant was expressed as a percentage of total LDH (supernatant + cell portion). Values are the mean ± SD of 3 independent experiments.

3.5.2 UVA-induced LDH release in HaCaT cells

The LDH assay was also carried out in HaCaT keratinocytes following either single or second challenge doses of UVA radiation. The results (**Table 3.5d**) showed that UVA also induces LDH release following both single and repeated exposures to UVA. Furthermore, as for fibroblasts, the fold increase in LDH induced in pre-irradiated HaCaT cells was similar to that of non-pre-irradiated cells, consistent with the notion that UVA-induced membrane damage occurs following single or repeated exposures to UVA radiation.

Table 3.5d UVA-induced LDH release in HaCaT cells

Sample	LDH activity of supernatant	Fold increase compared to control
0^{0h}	0.014±0.005	1
250^{0h}	0.027±0.013*	1.9±0.67
$0^{d0} / 0^{d1}$	0.020±0.007	1
$0^{d0} / 250^{d1}$	0.035±0.016*	1.7±0.53
$250^{d0} / 250^{d1}$	0.039±0.014*	2.1±0.82
$250^{d0} / 0^{d1}$	0.024±0.003	1.2±0.28

Note: The level of LDH activity was measured in supernatant of cells following UVA treatments. The LDH values of the controls were arbitrarily set to 1. Values are the mean ± SD of 3 experiments. * Significantly different from the sham-irradiated control, $p < 0.05$.

In **Table 3.5e** the LDH activity of the supernatant was also expressed as percentage of total LDH (LDH of supernatant + LDH remainingin the cells). These results showed that the percentage of LDH leakage in HaCaT cells is significantly lower than in fibroblasts, consistent with the notion that HaCaT keratinocytes are more resistant to UVA-induced membrane damage. Also, as for fibroblasts, the percentage of LDH leakage in the pre-irradiated sample (i.e. $250^{d0} / 250^{d1}$) was significantly higher than for the non-pre-irradiated sample (i.e. $0^{d0} / 250^{d1}$), consistent with the notion that exposure of keratinocytes to low split doses of UVA also increases the susceptibility of plasma membrane to UVA-induced damage. Furthermore the fact that in HaCaT cells, both basal and UVA-induced levels of LIP were significantly lower than in fibroblasts, strongly suggests that the amount of intracellular LIP should play a role in the degree of susceptibility of cells to UVA-induced damage.

Table 3.5e UVA induced LDH leakage in HaCaT cells

Sample	LDH leakage (%)
0^{0h}	1.8±0.5
250^{0h}	3.2±0.5
0^{d0} / 0^{d1}	1.7±0.4
0^{d0} / 250^{d1}	3.1±1.6
250^{d0} / 250^{d1}	6.5±4.1
250^{d0} / 0^{d1}	2.5±1.0

Note: LDH leakage in the supernatant was expressed as a percentage of total LDH (supernatant + cell portion). Values are the mean ± SD of 3 independent experiments.

3.6 Determination of colony-forming ability

It has been shown in this laboratory that UVA mediates dose-dependent inactivation of human skin cells in culture as monitored by colony-forming ability assay (Tyrrell and Pidoux, 1987 and 1988). In order to test whether the LIP is involved in the mechanism of cell killing by UVA radiation, UVA-induced cytotoxicity was determined by colony-forming ability curves for fibroblasts and HaCaT cells that were treated with DFO for 18 h prior to UVA irradiation. The results (**Fig. 3.6A, B** and **C** for FEK4, 1BR3 and HaCaT cells, respectively) showed that DFO pre-treatment does not increase the cell survival, consistent with the notion that UVA-induced LIP release is not involved in long-term UVA-mediated cell killing. Furthermore, HaCaT cells that were much resistant to both UVA-induced lysosomal and plasma membrane damage, were found to loose their ability to form clones following UVA treatment. These results emphasize that the factors involved in short-term effects of UVA should be entirely different from those involved in long-term cell killing. In other words, the UVA-induced LIP release might play a role only in UVA-induced short-term damage.

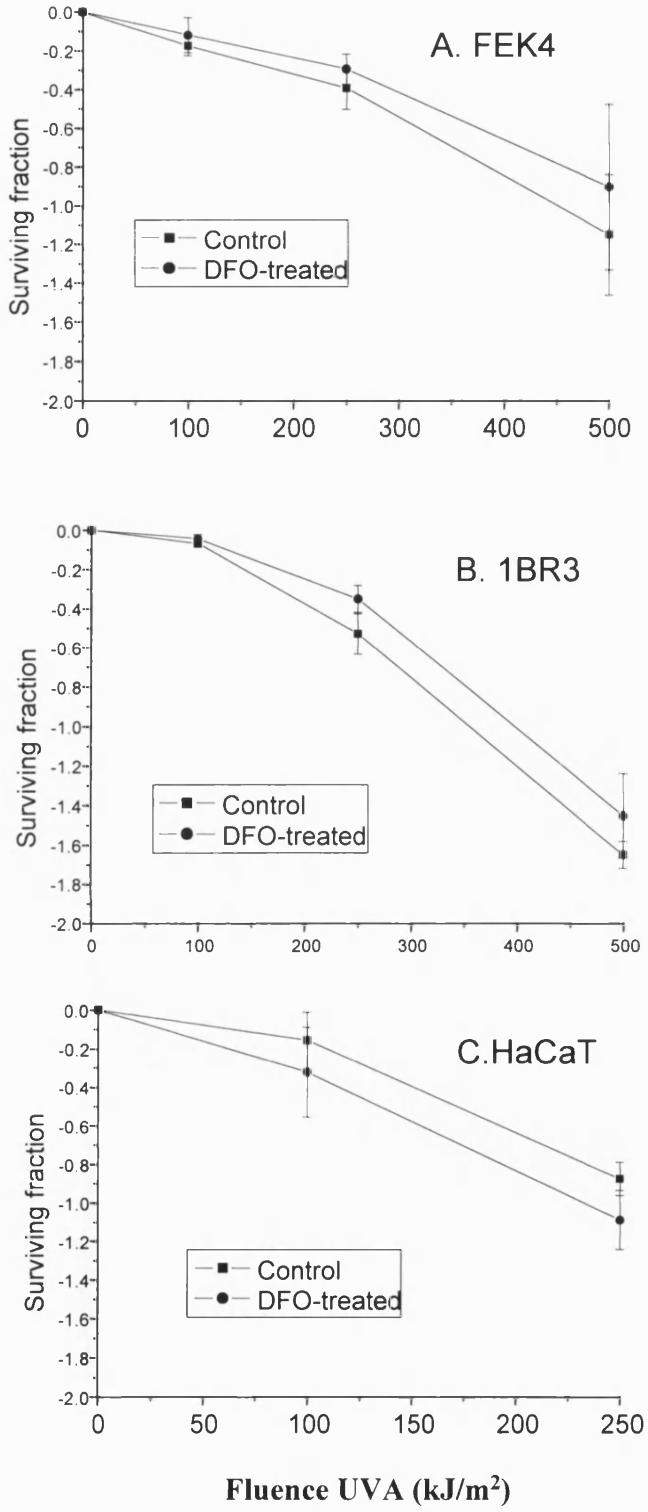

Fig. 3.6A. B. C Survival curves for FEK4, 1BR3 and HaCaT cells.
Inactivation of cells by exposure to UVA at the indicated doses with DFO-treated and non-treated cells.
Data are plotted as fraction of non-irradiated controls (which are taken as 100% survival).
The plating efficiency for FEK4, 1BR3 and HaCaT cells are 30%, 28% and 15%, respectively.
Values are log of mean ± SD of 3 independent experiments.

4. Discussion

4.1 The significance of UVA-mediated labile iron pool (LIP) release in skin cells

Although in humans, excessive exposure to solar ultraviolet radiation has been shown to be associated with increased risk of developing a number of pathologies, ranging from erythema, immunosuppression, hyperplasia, cataract, skin ageing to the development of melanoma and non-melanoma skin cancer, the cellular mechanisms underlying such risks are, at present, not fully understood. It is known that most of these effects are wavelength dependent and usually occur as a result of cumulative solar UV dose. The identification of specific cellular changes following irradiation with either UVA or UVB component of sunlight is therefore likely to provide clues as to the development of such pathologies. Most of the studies in the field of photobiology focus on the effect of acute i.e. single high dose rather than chronic i.e. repeated low doses of UVA and UVB exposures. Since skin is repeatedly exposed to solar UV radiation and long-term photo-damage is a consequence of cumulative UV radiation injury, it is crucial to examine the effects of repetitive exposure of human skin cells to UV radiation in order to obtain clues as to the early alterations that lead to photo-aged skin and ultimately to carcinogenesis. The recent discovery that UVA radiation leads to immediate measurable increase in potentially harmful available iron in human dermal fibroblasts (Pourzand et al., 1999a), prompted us to characterise further this phenomenon in both skin fibroblasts and keratinocytes following single or repeated exposures to UVA irradiation, since iron is a catalyst of biological oxidations. The UVA doses used in this study were 250 and 500 kJ/m^2, which are equivalent to the amount the surface of skin would be exposed to over 70 or 140 min, respectively on a summer day around noon at a northern latitude of 30-35° (Frederick and Albert, 1992), so that these doses mimic normal exposures to sunlight.

The results of this study (**Table 3.2, 3.5 3.10** and **3.12**) clearly demonstrated that LIP release occurs immediately following UVA irradiation of both human skin fibroblasts and keratinocytes following either single or repeated exposure to UVA irradiation. These findings also emphasized the importance of repeated iron release in promoting cumulative UV radiation injury in the skin. Indeed, free iron, due to its bioavailability in biological systems, plays an essential role in the promotion of the prooxidant condition in cells since as a redox-cycling metal, iron catalyses the formation of ROS (see section **1.5**). The release of potentially harmful free 'transit' iron within cells should exacerbate the damaging effects of the UVA-induced oxidative stress and is likely to be of central importance to both the reversible and degenerative damage to skin cells that follows exposure to solar UVA, including the events that lead to skin ageing. Indeed daily exposures at low doses of UVA (50-100 kJ/m^2) have been reported to promote the cumulative morphological alteration as well as 'surburn cells' in human skin as a result of cumulative UVA doses applied (Kumakirim et al., 1977; Lavker et al., 1995). Furthermore Berneburg et al. (1999) have reported that repetitive UVA exposure of human fibroblasts to UVA irradiation (80 kJ/m^2) results in mitochondrial DNA damage, which may contribute to skin ageing. It has also been demonstrated that UVA-induced increase in LIP has the potential role to promote mitochondrial membrane damage (this laboratory, unpublished data). Furthermore UVA induces the rapid proteolytic degradation of ferritin within both skin fibroblasts and keratinocytes (Pourzand et al, 1999a and unpublished data, this laboratory). The lack of this critical iron storage protein ferritin during the first hour that followed irradiation is thought to further exacerbate the consequences of the UVA-induced iron release within human skin cells, since the excess of the highly reactive LIP cannot be withdrawn from the cells. Indeed, in the present study it was found that the UVA-induced immediate increase in LIP is

sustained for at least 2 h following irradiation and only returns to basal levels 6 h following irradiation (**Table 3.3** and **3.11**).

The presence of excess iron has also been demonstrated in a variety of skin disorders such as psoriasis (Molin and Wester, 1973), venous ulceration (Ackerman et al., 1988) and atopic eczema (David et al., 1990), indicating the involvement of iron in the pathology of skin. Furthermore, Bissett and coworkers (1991) have reported that chronic exposure of mice to suberythemal doses of UV radiation led to an increased skin level of non-heme iron after 12 weeks of irradiation presumably as a result of UV-induced increase in vascular permeability. They also observed that there were greater amounts of non-heme iron in sun-exposed sites of human skin biopsies (after sunburn) indicating that similar events occur in man (Bissett et al, 1992). Our *in vitro* findings are in good agreement with the *in vivo* studies of Bissett, suggesting that the phenomenon of UVA-induced iron release may also occur in human skin following exposure to the sunlight.

The findings of UVA-induced iron release in both fibroblasts and keratinocytes is of paramount importance to cancer studies, since iron may play a role in carcinogenesis. Over the past few decades, it has been shown that one of the dangers of iron is its ability to favour neoplastic cell growth (reviewed by Weinberg, 1996). The metal is carcinogenic due to its catalytic effect on the formation of highly reactive hydroxyl radicals, suppression of host defence cells and promotion of cancer cell multiplication. In both animals and humans, primary neoplasms develop at body sites of excessive iron deposits such as the skin. The body has already developed mechanisms to withhold iron from cancer cells via sequestration of the metal into newly formed ferritin. It is clear

that the fast proteolytic degradation of ferritin following UV radiation would have deleterious consequences. Furthermore, since skin is potentially the target of significant oxidative damage due to its constant exposure to high oxygen tensions, frequent exposure to UV light and the presence of considerable amounts of polyunsaturated fatty acids, it is clear that increased deposit of transit iron on the surface of skin will catalyse the formation of highly reactive radicals and could contribute to severe oxidative damage. High dietary iron has also been reported to induce skin cancer in mice (Hann et al., 1988). Taken together, a picture emerges suggesting that repeated exposures to UVA and the consequent mobilisation and deposit of iron might be a major factor in both the photoageing and photocarcinogenesis processes.

4.2 The source of UVA-induced iron release in skin cells

Although the present work clearly demonstrates that UVA radiation rapidly causes the release of free iron within cultured human skin fibroblasts and keratinocytes, the potential source of this transit iron has yet to be identified. This study (see also Pourzand et al., 1999) has shown that ferritin iron is only partially involved in UVA-induced LIP release since neither preventing the UVA-mediated ferritin degradation by protease-inhibitors nor enhancing the level of ferritin by iron-loading (e.g. iron citrate) could substantially modulate the level of UVA-induced LIP release (**Table 3.3.3** and **Table 3.3.4**). Therefore it appears that sources of iron, in addition to ferritin, are responsible for the observed effect. One such source is the heme that is released from microsomal hemoproteins immediately after UVA irradiation of FEK4 cells (Kvam et al., 1999). Although heme itself is not a source of LIP, it is a substrate for heme-catabolizing enzyme heme-oxygenase (HO) which could release the heme iron.

The UVA-induced immediate release of heme within microsomal membranes of skin cells could therefore contribute to the observed increase in LIP.

The other candidate source for LIP is the lysosomal organelles. Indeed, lysosomal organelles that are responsible for the degradation of ferritin and other hemoproteins in the cells are thought to contain significant levels of free iron (Ollinger and Brunk, 1995; Petrat at al., 2001) It therefore follow that the UVA-induced lysosomal membrane damage could release this source of free iron from lysosomal compartments to the cytosol again contributing to the increase in the LIP that is detected by the CA-assay.

Since damage to the lysosomal membrane and the consequent leakage of lysosomal proteases to the cytosol is responsible for the UVA-induced immediate degradation of ferritin, such proteases could also degrade other iron-containing proteins (i.e. hemoproteins) in the cytosol. Mitochondrial cytochrome c has been shown to be released from mitochondrial membrane immediately after UVA irradiation of FEK4 fibroblasts (this laboratory, unpublished data) and could be a substrate for degradation and iron release. It is well known that the total protein content of the cells decreases dramatically and in a dose-dependent manner following UVA irradiation of skin fibroblasts and keratinocytes (this study and also unpublished data from this laboratory), consistent with the notion that several proteins are degraded following radiation treatment.

4.3 The origin of UVA-induced iron release in skin cells

Pourzand et al. (1999) have suggested that the phenomenon of UVA-induced LIP release in fibroblasts originates from the immediate damage to the lysosomal membrane leading to the leakage of potentially harmful proteases in the cytosol, which in turn degrade ferritin in the cytosol and release iron. In this thesis it was also found that the LIP release (see section **4.1**) and damage to plasma membrane (release LDH) occur both in fibroblasts and keratinocytes following single or repeated exposures to UVA radiation (**Table 3.5a and 3.5d**).

Two questions arise from these observations: Firstly what is the mediator of UVA-induced immediate lysosomal membrane damage and secondly is the lysosomal damage the origin of LIP release or is this a consequence of LIP release? Several studies have shown that during cellular injury by oxidative stress, lysosomal membranes could be destabilized through lipid peroxidation promoting lysosomal rupture and release of potent hydrolytic enzymes to the cytosol. It has been suggested that during oxidative injury, the presence of abundant redox active iron in lysosomes along with H_2O_2 generation within the vicinity of such organelles could yield the formation of highly reactive hydroxyl radical leading to lysosomal rupture and cell damage (Ollinger and Brunk, 1995; Roberg and Ollinger, 1998).

Since UVA is a membrane-damaging agent, and it has been shown that iron and singlet oxygen contribute to the peroxidation of human skin fibroblast membranes (Vile & Tyrrell, 1995), it was hypothesized that UVA may also trigger the peroxidation of lysosomal membranes. However the pre-treatment of fibroblasts with membrane

antioxidants BHT (**Fig. 3F7-9**) and α-Tocopherol succinate (unpublished data, this laboratory) could only partially protect the lysosomal membranes against UVA-induced damage, suggesting that membrane peroxidation is not the major mediator of UVA-mediated lysosomal damage. Furthermore the same treatment failed to modulate the level of UVA-induced LIP release (**Table 3.2e**) consistent with the notion that UVA-induced iron release is not related to peroxidation of lysosomal membrane.

To further ascertain that UVA-induced LIP release is not a consequence of UVA-mediated lipid peroxidation in cell membranes, the role of ROS in this process was investigated. Singlet oxygen has been shown to contribute to UVA inactivation of human skin FEK4 cells (Vile and Tyrrell, 1995) and is the primary effector in the UVA induction of HO in FEK4 cells (Basu-Modak et al., 1993). This reactive oxygen intermediate can also abstract hydrogen and initiate the lipid peroxidation in cell membranes. Also H_2O_2 appears to be generated in cultured human skin fibroblasts at micro-molar (μM) concentrations during UVA radiation (Peak et al., 1990a; Vile and Tyrrell, 1995) and is thought to participate in Fenton chemistry to yield the highly reactive hydroxyl radical, which is a known mediator of cell membrane damage. The results (**Table 3.2d** and **3.2c**) demonstrated that neither enhancing $^1O_2$ half-life by deuterium oxide (D_2O) nor increasing the level of UVA-induced endogenous H_2O_2 by the catalase inhibitor amino-triazole, could significantly enhance the level of UVA-mediated LIP release in FEK4 cells, consistent with the notion that these reactive oxygen intermediates do not play a key role in UVA-induced lysosomal damage and LIP release.

It appears that UVA-induced lysosomal damage is a consequence of LIP release and not the primary mediator of it. In addition to LIP, early release of lysosomal enzymes might activate feedback processes that cause further lysosomal rupture. Such feedback processes may be either LIP-mediated and/or due to activation of lytic cytosolic pro-enzymes such as caspases.

The lysosomal membrane damage that occurs upon irradiation could also be due to the interaction of UVA radiation with an unknown chromophore present within lysosomal organelles that leads to an immediate burst of these organelles. The candidate chromophore could be a partially degraded hemoprotein with a protoporphyrin-IX-type structure. Further investigations are required to address such issues.

4.4 The link between intracellular LIP and the susceptibility of skin cells to the UVA-mediated oxidative damage

Although UVA promotes rapid release of potentially harmful free iron in both human fibroblasts and keratinocytes, it was observed that both the basal and UVA-induced levels of LIP were 2-4 fold higher in human skin fibroblasts when compared with keratinocytes. Since iron plays a crucial role in propagation of lipid peroxidation in cellular membranes, we hypothesised that the low level of LIP in keratinocytes could be responsible for the higher resistance of keratinocytes to UVA-induced membrane damage. The investigation of the correlation between the amount of UVA-mediated LIP release and the rate of membrane damage in different cellular organelles i.e. plasma (**Table 3.5a** and **3.5d**), lysosomes (**Fig. 3F1-15**,) and mitochondria (unpublished data, this laboratory) demonstrated that UVA promotes membrane damage in both

keratinocytes and fibroblasts, however the extent of damage in keratinocytes is not as dramatic as in fibroblasts.

In fibroblasts, DFO treatment, which is known to abolish the UVA-induced LIP release significantly, protected the cells from lysosomal membrane damage. Similarly, It has been shown that DFO treatment can also substantially protect the fibroblasts against both the mitochondrial membrane damage and the necrotic cell death (i.e. loss of cell membrane integrity: recent unpublished data, this laboratory) consistent with the notion that UVA-induced LIP release plays a key role in UVA-mediated membrane damage. Furthermore, based on the finding that hemin-loading of cells prior to radiation could increase the level of UVA-induced LIP release (**Table 3.3.3**), it has been shown that hemin treatment of FEK4 cells could dramatically increase the level of UVA-induced peroxidative damage in lysosomal, mitochondrial and plasma membranes (this laboratory, unpublished data). Taken together, these data indicate that the level of UVA-induced LIP release in fibroblasts is directly related to the extent of UVA-mediated membrane damage.

In the present study, DFO treatment of keratinocytes that have low LIP levels only partially protect them against UVA-mediated damage (**Fig. 3H1-6**). It also did not significantly protect cells against the effect of UVA irradiation by clone-forming ability (Fig. 3.6A,B,C). So in the long term, the starvation of cells by DFO may not protect UVA-mediated cell killing.

Comparison of the fibroblast data with the keratinocyte data reveals that in addition to the lower basal level of LIP, keratinocytes have 5 times lower ferritin level, far fewer

lysosomal organelles and lower lysosomal Cath B level (**Table 3.2, 3.10, 3.21** and **3.4.2**). We propose that a combination of low basal and UVA-induced intracellular LIP, low basal level of ferritin and low lysosomal organelle and low lysosomal Cath B content will all contribute to the higher resistance of keratinocytes to UVA-induced membrane damage.

Overall, the results demonstrate that UVA-mediated release of reactive iron immediate following radiation treatments plays a key role in the increased susceptibility of cells to UVA-induced damage and will almost certainly act to exacerbate damage caused by further exposure. UVA also liberates heme within microsomal membranes of skin cells. This will sensitise cells to further exposure to UVA. Although cells have mechanisms to remove iron (i.e. long-term increase in ferritin) and heme (heme-oxygenase activation within hours), these defence mechanisms develop over several hours and days. Therefore it appears that high intensity short-term exposures to UVA radiation are the most likely to be damaging. This is precisely the situation for exposure to sunlamps where people tend to expose themselves habitually for short high intensity periods. A clear role for iron in exacerbating UVA damage suggests potential pathways to protection through iron chelation or natural antioxidants with iron chelating properties (e.g. polyphenols found in most fruits and vegetables).

5. Future projects

In the present study, the phenomenon of UVA-induced LIP release has been characterized in two cultured human skin fibroblasts and keratinocytes. However in order to gain insight into the *in vivo* relevance of such studies, it is necessary to measure the same phenomenon either in animal models (e.g. hairless mice) or in human skin biopsies (e.g. after sunburn). Also, the present study has only focussed on the effect of UVA component of sunlight, but it is clear that such investigations should also be monitored following UVB component of sunlight. As mentioned before, most of the effects of sunlight are wavelength dependent, so it is of particularly importance to investigate whether UVB also promotes LIP release both *in vitro* in cultured skin cells and *in vivo* in animal or human skin. Such studies will complement our knowledge about the immediate cellular effect of solar UV radiation and will therefore provide information pertinent to develop strategies for the delay of/or protection against UV-mediated damage to the skin.

5. References

Abok, K., Hirth, T., Ericsson, J. L., Brunk, U. (1983) Effect of iron on the stability of macrophage lysosomes. Virchows Arch. B Cell Pathol. *Incl. Mol. Pathol.* 43, 85-101

Ackerman, Z., Seidenbaum, M., Loewenthal, E., Rubinow, A. (1988) Overload of iron in the skin of patients with varicose ulcers. Possible contributing role of iron accumulation in progression of the disease. *Arch Dermatol.* 124, 1376-8

Amstad, P., Peskin, A., Shah, G., Mirault, M. E., Moret, R., Zbinden, I., Geriutti P. (1991) The balance between Cu, Zn-SOD and catalase affects the sensitivity of mouse epidermal cells to oxidative stress. *Biochemistry* 30, 9305-13

Ansari, K. N. (1997) The free radicals- the hidden culprits-an update. Indian J. Med. Sci. 51(9), 319-36

Applegate, L. A., Scaletta, C., Labidi, F., Vile, G., Frenk, E. (1990) Susceptibility of human melanoma cells to oxidative stress including UVA radiation. E. *Mol. Cell Biol.* 10, 4967-9

Applegate, L. A., Lautier, D., Frenk, E., Tyrrell, R. M. (1992) Endogenous glutathione levels modulate the frequency of both spontaneous and long wavelength ultraviolet induced mutations in human cells. *Carcinogenesis.* 13, 1557-60

Applegate, L. A., Frenk, E., Gibbs, N., Johnson, B., Ferguson, J., Tyrrell, R. M. (1994) Cellular sensitivity to oxidative stress in the photosensitivity dermatitis/actinic reticuloid syndrome. *J. Invest. Dermatol.* 102, 762-767

Applegate, L. A., Noel, A., Vile, G., Frenk, E., Tyrrell, R. M. (1995) Two genes contribute to different extents to the heme oxygenase enzyme activity measured in cultured human skin fibroblasts and keratinocytes: implications for protection against oxidant stress. *Photochem. Photobiol.* 61, 85-91

Applegate, L. A, Frenk, E. (1996) Oxidative defense in cultured human skin fibroblasts and keratinocytes from sun-exposed and non-exposed skin. *Photodermatol Photoimmunol Photomed.* 11, 95-101

Applegate, L. A., Scaletta, C., Panizzon, R., Frenk, E. (1998) Evidence that ferritin is UV inducible in human skin: part of a putative defense mechanism. *J. Invest. Dermatol.* 111, 159-163

Aubailly, M., Santus, R., Salmon, S. (1991) Ferrous ion release from ferritin by ultraviolet-A radiations. *Photochem. Photobiol.* 54, 769-773

Aubailly, M., Salmon, S., Haigle, J., Bazin, J. C., Maziere, J. C., Santus, R. (1994) Peroxidation of model lipoprotein solution sensitized by photoreduction of ferritin by 365 nm radiation. *Photochem. Photobiol. B: Biol.* 26, 185-191

Aulleta, M., Ganeg, R. W., Tan, O. T., Matzinger, E. (1986) Effect of cutaneous hypoxia upon erythema and pigment response to UVA, UVB and OUVA (8-MOP + UVA) in human skin. *J. Invest. Dermatol.* 86, 649-652

Aust, S. D., Morehouse, L. A., Tomas, C. E. (1985) Role of metals in oxygen radical reactions. *Free Radic. Biol. Med.* 1, 3-25

Aust, S. D. (1995) Ferritin as a source of iron and protection from iron-induced toxicities. *Toxicol. Lett.* 82-83, 941-4

Baader, S. L., Bruchelt, G., Garmine, T. C., Lode, H. N., Rieth, A. G., Niethammer, D. (1994) Ascorbic acid-mediated iron release from cellular ferritin and its relation to the formation of DNA strand breaks in neuroblastoma cells. *J. Cancer Res. Clin. Oncol.* 120, 415-421

Babior, B. M. (1999) NADPH oxidase: an update. *Blood.* 93, 1464-1476

Baker, M. S, Gebicki, J. M. (1986) The effect of pH on yields of hydroxyl radicals produced from superoxide by potential biological iron chelators. *Arch Biochem Biophys.* 246, 581-8

Balla, G., Jacob, H. S., Balla, J., Rosenberg, M., Nath, K., Apple, F., Eaton, J. W., Vercellotti, G. M. (1992) Ferritin: a cytoprotective antioxidant stratagem of endothelium. *J. Biol. Chem.* 267, 18148-53

Balla, J., Jacob, H. S., Balla, G., Nath, K., Vercellotti, G. M. (1992) Endothelial cell heme oxygenase and ferritin induction by heme proteins: a possible mechanism limiting shock damage. *Trans. Assoc. Am. Physicians.* 105, 1-6

Balla, J., Jacob, H. S., Balla, G., Nath, K., Eaton, J. W., Vercellotti, G. M. (1993) Endothelial-cell heme uptake from heme proteins: induction of sensitization and desensitization to oxidant damage. *Proc. Natl. Acad. Sci. USA.* 90, 9285-9

Basu-Modak, S., Tyrrell, R. M. (1993) Singlet oxygen: a primary effector in the ultraviolet A/near-visible light induction of the human heme oxygenase gene. *Cancer Res.* 53, 4505-10

Berg, R. J., van Kranen, H. J., Rebel, H. G., de Vries, A., van Volten, W. A., van Kreijl, C. F., van der Leun, J. C., de Grijil, F. R. (1996) Early p53 alterations in mouse skin carcinogensis by UVB radiation:

immunohistochemical detection of mutant p53 protein in clusters of preneoplastic epidermal cells. *Proc. Natl. Acad. Sci. USA. 93,* 274-278

Berneburg, M., Grether-Bcek, S., Kurten, V., Ruzicka, T., Briviba, K., Sies, H., Krutmann, J. (1999) Singlet oxygen mediates the UVA-induced generation of the photoageing associated mitochondrial common deletion. *J. Biol. Chem.* 274, 15345-9

Berneburg, M., Plettenberg, H., Krutmann, J. (2000). Photoaging of human skin. *Photodermatol. Photoimmunol. Photomed.* 16, 239-244

Bernerd, F., Asselineau, D. (1998) UVA exposure of human skin reconstructed in vitro induces apoptosis of dermal fibroblasts: subsequent connective tissue repair and implication in photoaging. *Cell Death Differ.* 5, 792-802

Bertling, C. J., Lin, F., Girotti, A. W. (1996) Role of hydrogen peroxide in the cytotoxic effects of UVA/B radiation on mammalian cells. *Photochem. Photobiol.* 64, 137-142

Bestak, R., Halliday, G. M. (1996) Chronic low-dose UVA irradiation induces local suppression of contact hypersensitivity, Langerhans cell depletion and suppressor cell activation in C3H/HeJ mice. *Photochem. Photobiol.* 64, 969-974

Biemond, P., Swaak, A. J., van Eijk, H. G. and Koster, J. F. (1988) Superoxide dependent iron release from ferritin in inflammatory diseases. *Free Radic. Biol. Med.* 4, 185-198

Bissett, D. L., Chatterjee, R., Hannon, D. P. (1990) Photoprotective effect of superoxide-scavenging antioxidants against ultraviolet radiation-induced chronic skin damage in the hairless mouse. *Photodermol. Photoimmunol. Photomed.* 7, 56-62

Bissett, D. L., Chatterjee, R., Hannon, D. P. (1991) Chronic ultraviolet radiation-induced increase in skin iron and the photoprotective effect of topical applied iron chelators. *Photochem. Photobiol.* 54, 215-223

Bissett, D. L., Hannon, D. P., McBride, J. F., Patrick, L. F. (1992) Photoaging of skin by UVA. In: Biological Responses to ultraviolet A Radiation, Urbach F. Ed., pp. 181-188, *Valdenmar Publishing Company, Overland park, KS*

Black, H. S., Lenger, W. A., Gerguis, J. and Thornby J. I. (1985) Relation of antioxidants and level of dietary lipid to epidermal lipid peroxidation and ultraviolet carciniogenesis. *Cancer Res.* 45, 6254-9

Black, H. S. (1987) Potential involvement of free radical reaction in ultraviolet light mediated cutaneous damage. *Photochem. Photobiol.* 46, 213-221

Black, H. S., de Gruijl, F. R., Forbes, P. D., Cleaver, J. E., Anathaswamy, H. N, de Fabo, E. C, Ullrich, S. E., Tyrrell, R. M. (1997) Photocarcinogenesis: an overview. *J. Photochem. Photobiol. B.* 40, 29-47

Bolann, B. J. and Ulvik, R. J. (1990) On the limited ability of superoxide to release iron form ferritin. *Eu. J. Biochem.* 193, 899-904

Bose, B., Agarwal, S., Chatterjee, S. N. (1989) UV-A induced lipid peroxidation in liposomal membrane. *Radiat. Environ. Biophys.* 28, 59-65

Bose, B., Agarwal, S., Chatterjee, S. N. (1990) Membrane lipid peroxidation by UV-A: mechanism and implications. *Biotechnol. Appl. Biochem.* 12, 557-561

Bose, B., Soriani, M., Tyrrell, R. M. (1999) Activation of expression of the c-fos oncogene by UVA irradiation in cultured human skin fibroblasts. *Photochem. Photobiol.* 69, 489-493

Boukamp, P., Petrussevska, R. T., Breikreutz, D., Hoenung, J., Markham, A., Fusenig N. E. (1988). Normal keratinisation in a spontaneously immortalized aneuploid human keratinocyte cell line. *J. Cell Biol.* 106, 761-771

Bradford, M. M. (1976) A rapid and sensitive method for the quantitation of microgram quantities of protein utilizing the principle of protein-dye binding. *Anal. Biochem.* 72, 248-254

Brash, D. E., Rudolph, J. A., Simon, J. A., Lin, A., McKenna, G. I., Baden, H. P., Halperin, A. J., Ponten, J. (1991) A role for sunlight in skin cancer: UV-induced p53 mutations in squamous cell carcinoma. *Proc. Natl. Acad. Sci. USA.* 88, 10124-8

Breuer, W., Epsztejn, S., Canbantchik, Z. I. (1995) Iron acquired from transferrin by K562 cells is delivered into a cytoplasmic pool of chelatable iron (II). *J. Biol. Chem.* 270, 24209-15

Breuer, W., Epsztejn, S., Millgram, P., Cabantchik, Z. I. (1995a) Transport of iron and other transition metals into cells as revealed by fluorescent probe. *Am. J. physiol.* 268, C1354-C1361

Breuer, W., Epsztejn, S., Cabantchik, Z. I. (1996) Dynamics of the cytosolic chelatable iron pool of K562 cells. *FEBS Lett.* 382, 304-308

Breuer, W., Greenberg, E., Cabantchik, Z. I. (1997) Newly delivered transferrin iron and oxidative cell injury. *FEBS Lett.* 403, 213-219

Bruls, W. A., Slaper, H., van de Leun, J. C., Berrens, L. (1984) Transmission of human epidermis and stratum corneum as function of thickness in the ultraviolet and visible wavelengths. *Photochem. Photobiol.* 40, 485-494

Brunk, U. T., Zhang, H., Dalen, H., Ollinger, K. (1995) Exposure of cells to nonlethal concentractions of hydrogen peroxide induces degeneration-repair mechanisms involving lysosomal destablization. *Free Radic. Biol. Med.* 19, 813-822

Brunk, U. T., Dalen, H., Roberg, K., Hellquist H. B. (1997) Photo-oxidative disruption of lysosomal membrane causes apoptosis of cultured human skin fibroblasts. *Free Radic. Biol. Med* 23, 616-626

Brunk, U. T., Svensson, I. (1999) Oxidative stress, growth factor starvation and Fas activation may all cause apoptosis through lysosomal leak. *Redox Report.* 4, 3-11

Bucala, R. (1996) Lipid and lipoprotein oxidation: basic mechanisms and unsolved questions in vivo. *Redox Report.* 2(50), 291-307

Burren, R., Scalatta, C., Frenk, E., Panizzon, R. G., Applegate, L. A. (1998) Sunlight and carcinogensis: expression of p53 and pyrimidine dimers in human skin following UVA I, UVAI+II and solar simulating radiations. *Int. J. Cancer* 76, 201-206

Cabantchik, Z. I., Glickstein, H., Milgram, P., Breuer, W. (1996) A fluorescence assay for assessing chelation of intracellular iron in a membrane model system and mammalian cells. *Anal. Biochem.* 233, 221-227

Cabantchik, Z. I., Moody-Haupt, S., Gordeuk, V. R. (1999) Iron chelators as anti-infectives; malaria as a paradigm. *FEMS Immunol. Med. Microbiol.* 26, 289-298

Cable, H. and Lloyd, J. B. (1999) Cellular uptake and release of two contrasting iron chelators. *Pharm. Pharmacol.* 51, 131-134

Cadenas, H. (1989) Biochemistry of oxygen toxicity. *Annu. Rev. Biochem.* 58, 79-110

Campbell, D. L., Fisher, M. E., Johnson, J. G., Rossi, F. M., Campling, B. G., Pottier, R. H., Kennedy, J. C. (1996) Flow cytometric technique for quantitating cytotoxic response to photodynamic therapy *Photochem. Photobiol.* 63, 111-116

Carbonare, D. M., Pathak, M. A. (1992) Skin photosensitizing and the role of reactive oxygen species in photoaging. *J. Photochem. Photobiol. B:Boil.* 14, 105-124

Cario, G., Tacchini, L., Pogliaghi, G., Anzon, E., Tomas, A., Bernelli-Zazzera, A. (1995) Induction of ferritin synthesis by oxidative stress. Transcriptional and post-transcriptional regulation by expansion of the 'free' iron pool. *J. Biol. Chem.* 270, 700-703

Cairo, G., Gastrusini, E., Minotti, G., Bernelli-Zazzera, A. (1996) Superoxide and hydrogen peroxide-dependent inhibition of iron regulatory protein activity: a protective stratagem against oxidative injury. *FASEB J.* 10, 1326-35

Cairo, G., Tacchini, L., Recalcati, S., Azzimonti, B., Minotti, G., Bernelli-Zazzera, A. (1998) Effect of reactive species on iron regulatory protein activity. *Ann. N. Y Acad. Sci.* 851, 179-186

Cairo, G. and Pietrangelo, A. (2000) Iron regulatory proteins in pathobiology. *Biochem. J.* 352, 241-250

Cazzola, M., Beguin, Y., Bergamaschi, G., Guarnone, R., Cerani, P., Barella, S., Cao, A., Galanello, R. (1999) Soluble transferrin receptor as a potential determinant of iron loading in congenital anaemias due to ineffective erythropoiesis. *Br. J. Haematol.* 106, 752-755

Cheeseman, K. H. (1993) Mechanisms and effects of lipid peroxidation. *Mol. Aspects Med.* 14, 191-197

Chou, P. T., Khan, A. U. (1983) L-ascorbic acid quenching of single delta molecular oxygen in aqueous media: generalized antioxidant property of vitamin C. *Biochem. Biophys. Res. Commun.* 115, 932-937

Clement-Lacroix, P., Michel, L., Moysan, A., Morliere, P., Dubertret, L. (1996) UVA-induced immune suppression in human skin: protective effect of vitamin E in human epidermal cells in vitro. *Br. J. Dermatol.* 134, 77-84

Connor, M. J. and Wheeler, L. A (1987) Depletion of cutaneous glutathione by ultraviolet radiation. *Photochem Photobiol.* 46, 239-245

Conrad, M. E., Umbreit, J. N, Moore, E. G (1999) Iron absorption and transport. *Am. J. Med. Sci.* 318, 213-229

Conrad M. F., Umbreit, J. N., Moore, E. G., Hainsworth L. N., Porubcin, M., Simovich, M. J., Nakada, M. T., Dolan. K., Garrick M. D (2000) Separate pathways for cellular uptake of ferric and ferrous iron. *Am. J. Physiol. Gastrointest. Liver Physiol.* 279, G767-774

Cook, J. A. and Mitchell, J. B. (1989) Viability measurement in mammalian cell systems. *Anal. Chem.* 179, 1-7

Cooper, K. D., Obrehelman, L., Hamilton, T. A., Daadsgaard, O., Terhune, M., LeVee, G., Anderson, T. (1992) UV exposure reduces immunization rates and promotes tolerance to epicutaneous antigens in humans: ralationship to dose, CD1a-DR^+ epidermal macrophage induction, and langerhans cell depletion. *Proc. Natl. Acad. Sci. USA.* 89, 8497-8501

Coulomb, B., Lebreton, C., Mathieu, N., Morliere, P. (1996) UVA-induced oxidative damage in fibroblasts cultured in a 3-dimensional collagen matrix. *Exp. Dermatol.* 5, 161-167

Crawford, D. R. and Davies, K. J. (1994) Adaptive response and oxidative stress. *Environ. Health Prospect Suppl.* 10, 25-28

Crichton, R. R. and Charloteaux-Wanters, M. (1987) Iron transport and storage. *Eur. J. Biochem.* 164, 485-506

Crichton, R. R. and Ward, R. J. (1992) Structure and molecular biology of iron binding proteins and the regulation of 'free' iron pools. In: Lauffer, R. B. (ed): Iron and human disease. *CRC Press Inc., Florida, USA,* pp. 23-75

Cunningham, M. L., Johnson, J. S., Giovanazzi, S. M., Peak, M. J. (1985) Photosensitized production of superoxide anion by monochromatic (290-405nm) ultravoilet radiation of NADH and NADPH coenzymes. *Photochem. Photobiol.* 42, 125-128

Cunningham, M. L., Krinsky, N. I., Giovanazzi, S. M., Peak, M. J. (1985a) Superoxide anion is generated from cellular metabolites by solar radiation and its compounds. *Free Radic. Biol. Med.* 1, 381-385

Czochralska, B., Kawczynski, W., Bartosz, G., Shugar, D. (1984) Oxidation of excited-state NADH and NAD dimer in aqueous medium involvement of O_2^- as a mediator in the presence of oxygen. *Biochim. Biophys. Acta.* 801, 403-409

Danpure, H. J. and Tyrrell, R. M. (1976) Oxygen dependence of near-UV (365 nm) lethality and the interaction of near-UV and X-rays in two mammalian cell lines. *Photochem. Photobiol.* 23, 171-177

Darr, D., Combs, S., Dunston, S., Manning, T., Pinnell, S. (1992) Topical vitamin C protects porcine skin from ultraviolet radiation-induced damage. *Br. J. Dermatol.* 127(3), 247-253

David, T. J., Wells, F. E., Sharpe, T. C., Gibbs, A. C., Devlin, J. (1990) Serum levels of trace metals in children with atopic eczema. *Br. J. Dermatol.* 122, 485-489

de Gruijl, F. R., Sterenborg, H. J., Forbes, P. D., Davis, R. E., Cole, C., Kelfkens, G., van Weelden, H., Slaper, H., van der Leun, J. C. (1993) Wavelength dependent of skin cancer induction by ultraviolet irradiation of albino hairless mice. *Cancer Res.* 53, 53-60

de Gruijl, F. R. (1999) Skin cancer and solar UV radiation. *Eur. J. Cancer.* 35, 2003-9

de Gruijl, F. R. (2000) Photocarcinogenesis: UVA vs UVB. *Methods Enzymol.* 319, 359-366

de Laat, A., van Tilburg, M., van der, Leun J. C., van Vloten, W. A., de Gruijl, F. R. (1996) Cell cycle kinetics following UVA irradiation in comparison to UVB & UVC irradiation. *Photochem. Photobiol.* 63, 492-497

de Laat, A., van de Leun, J. C., de Rruijl, F. R. (1997) Carcinogenesis induced by UVA (365-nm) radiation: the dose-time dependence of tumour formation in hairless mice. *Carcinogenesis.* 18, 1013-20

Dignam, J. D., Lebovitz, R. M., Roeder, R. G. (1983) Accurate transcription initiation by RNA polymerase II in a soluble extract isolated mammalian nuclei. *Nucleic Acid. Res.* 11, 1475-89

Djavaheri-Mergny, M., Maziere J. C., Santus, R., Mora, L., Maziere, C., Auclair, M., Dubertret L. (1993) Exposure to long wavelength ultraviolet radiation decreases processing of low density lipoprotein by cultured human fibroblasts. *Photochem. Photobiol.* 57, 302-305

Duthie, M. S., Kimber, J., Norval, M. (1999) The effect of Ultraviolet A radiation on the human immune system. *Br. J. Dermatol.* 140, 995-1009

Eisenstein, R. S. and Munro, H. N. (1990) Translational regulation of ferritin synthesis by iron. *Enzyme.* 44, 42-58

Eisenstein, R. S., Garcia-Mayol, D., Pettingell, W., Munro, H. N. (1991) Regulation of ferritin and heme oxygenase synthesis in rat fibroblasts by different from of iron. *Proc. Natl. Acad. Sci. USA.* 88, 688-692

Eisenstein, R. S. and Blemings, K. P. (1998) Iron regulatory proteins, iron responsive elements and iron homeostasis. *J. Nutr.* 128, 2295-8

Eisentark, A. and Perrot, G. (1987) Catalase has only a minor role in protection against near ultraviolet radiation damage in bacteria. *Mol. Gen. Genet.* 207, 68-72

Elbirt, K. K. and Bonkovsky, H. L. (1999) Heme oxygenase: recent advances in understanding its regulation and role. *Proc. Assoc. Am. Physicians* 111, 438-447

Emonent, N., Leccia, M. T., Favier, A., Beani, J. C., Richard, M. J. (1997) Thiols and selenium: protective effect on human skin fibroblasts exposed to UVA radiation. *Photochem. Photobiol. B.* 40, 84-90

Epe, B. (1991) Genotoxicity of singlet oxygen. *Chem. Biol. Interact.* 80, 239-260

Epstein, J. H. (1977) Effects of beta-carotene on ultraviolet induced cancer formation in the hairless mouse skin. *Photochem. Photobiol.* 25, 211-213

Epsztejn, S., Kakhlon, O., Glickstein, H., Breuer, W., Cabantchik, Z. I. (1997) Fluorescence analysis of the labile iron pool of mammalian cells. *Anal. Biochem.* 248, 31-40

Epsztejn, S., Glickstein, H., Picard, V., Slotki, I. N., Breuer, W., Beaumont, C. and Cabantchik, Z. I. (1999) H-ferritin subunit overexpression in erythroid cells reduces the oxidative stress response and induces multidrug resistance properties. *Blood.* 94, 3593-3603

Farber, J. L. (1994) Mechanisms of cell injury by activated oxygen species. *Environ. Health Prospect Suppl.* 10, 17-24

Feder, J. N., Penny, D. M., Irrinki, A., Lee, V. K., Lebron, J. A., Watson, N., Tsuchihashi, Z., Sigal, E., Bjorkman, P. J., Schatzman, R. C. (1998) The hemochromatosis gene product complexes with the transferrin receptor and lowers its affinity for ligand binding. *Proc Natl Acad Sci USA.* 95, 1472-7

Fenton, H. J. H. (1894) *J. Chem. Soc. (London)* 65, 899-910

Ferris, C. D., Jaffrey, S. R., Sawa, A., Takahashi, M., Brady, S. D., Barrow, R. K., Tysoe, S. A., Wolosker, H., Baranano, D. E., Dpre, S., Poss, K. D., Snyder, S. H. (1999) Heme oxygenase-1 prevent cell death by regulating cellular iron. *Nat. Cell. Biol.* 1, 152-157

Fischer-Nielsen, A., Poulsen, H. E., Loft, S. (1992) 8-Hydroxydeoxyguanosine in vitro: effects of glutathione, ascorbate and 5-aminosalicylic acid. *Free Radic. Biol. Med.* 12, 121-126

Fischer-Nielsen A, Loft, S., Jensen, K. G. (1993) Effect of ascorbate and 5-aminosalicylic acid on light-induced 8-hydroxydeoxyguanosine formation in V79 Chinese hamster cells. *Carcinogenesis.* 14, 2431-2433

Foote, C. S. (1991) Definition of Type I and Type II photosensitized oxidation. *Photochem. Photobiol.* 54, 659-673

Frederick, J. E., Snell, H. E., Haywood, E. K. (1989) Solar ultraviolet at the earth's surface. *Photochem. Photobiol.* 50, 443-450

Frederick, J. E. and Alberts, A. D. (1992) The natural UVA radiation enviroment. In: Urbach, F., ed. Biological responses to ultraviolet A radiation. *Kansas: Valdenmar Publishing Company.* 7-18

Frederiksen, S., Nielsen, P. E., Hoyer, P. E. (1989) Lysosomes: a possible target for psoralen photodamage. *Photochem. Photobiol B.* 3, 437-447

Freeman, S. E., Hacham, H., Gange, R. W., Maytum, D. J., Sutherland, J. C., Sutherland, B. M. (1989) Wavelength dependence of pyrimidine dimer formation in DNA of human skin irradiated in situ with ultraviolet light. *Proc. Natl. Acid. Sci. USA.* 86(14), 5605-9

Fridovich, I. (1978) Superoxide radicals, superoxide dismutases and the aerobic lifestyle. *Photochem. Photobiol.* 28, 733-741

Fridovich, I. (1995) Superoxide radical and superoxide dismutases. *Annu. Rev. Biochem.* 64, 97-112

Fryer, M. J. (1993) Evidence for the photoprotective effects of vitamin E. *Photochem. Photobiol.* 58, 304-312

Fuchs, J., Huflejt, M. E., Rothfuss, L. M., Wilson, D. S., Carcano, G., Packer, L. (1989) Acute effects of near ultraviolet and visible light on the cutaneous antioxidant defense system. *Photochem. Photobiol.* 50, 739-744

Fuchs, J. and Packer, L. (1990) Ultraviolet irradiation and the skin antioxidant system. *Photodermatol. Photoimmunol. Photomed.* 7, 90-92

Gaboriau, F., Morliere, P., Marquis, I., Moysan, A., Geze, W., Dubertret, L. (1993) Membrane damage induced in culture human skin fibroblasts by UVA irradiation. *Photochem. Photobiol.* 58, 515-520

Gaboriau, F., Demoulins-Giacca, N., Tirache, I., Morliere, P. (1995) Involvement of singlet oxygen in ultraviolet A-induced lipid peroxidation in cultured human skin fibroblasts. *Arch. Dermatol. Res.* 287, 338-340

Garate, M. A., Nunez, M. T. (2000) Overexpression of the ferritin iron-responsive element decreases the labile iron pool and abolishes the regulation of iron absorption by intestinal epithelial (Caco-2) cells. *J. Biol. Chem.* 275, 1651-5

Gardner, P. R., Raineri, I., Epstein, L. B., White, C. W. (1995) Superoxide radical and iron modulate aconitase activity in mammalian cells. *J. Biol. Chem.* 270, 13399-13405

Garner, B., Li, W., Roberg, K., Brunk, U. T. (1997) On the cytoprotective role of ferritin in macrophages and its ability to enhance lysosomal stability. *Free Radic. Res.* 27, 487-500

Gasparro, F. P., Mitchnick, M., Nash, J. F. (1998) A review of sunscreen safety and efficacy. *Photochem. Photobiol.* 68, 243-256

Geze, M., Morliere, P., Maziere, J. C., Smith, K. M., Santus, R. (1993) Lysosomes, a key target of hydrophobic photosensitizers proposed for photochemotheraputic applications. *J. Photochem. Photobiol. B:Biol.* 20, 22-35

Giordani, A., Morliere, P., Aubailly, M., Santus, R. (1997) Photoinactivation of cellular catalase by ultraviolet radiation. *Redox. Report.* 3, 49-55

Giordani, A., Morliere, P., djavaheri-Mergny, M., Santus, R. (1998) Ultraviolet A-dependent inhibition of cytoplasmic aconitase activity of iron regulatory protein-1 in NCTC 2544 keratinocytes. *Photochem. Photobiol.* 68, 309-313

Giordani, A., Martin, M. E, Beaumont, C., Santus, R., Morliere, P. (2000) Inactivation of iron responsive element-binding capacity and aconitase function of iron regulatory protein-1 of skin cells by ultraviolet A. *Photochem. Photobiol.* 72, 746-52

Girotti, A. W. (1990) Photodynamic lipid peroxidation in biological systems. *Photochem. Photobiol.* 51, 497-509

Godar, D. E., Thomas, D. P., Miller, S. A., Lee, W. (1993) Long-wavelength UVA radiation induces oxidative stress, cytoskeletal damage and hemolysis. *Photochem. Photobiol.* 57, 1018-26

Greene, M. I., Sy, M. S., Kripke, M., Benacerraf, B. (1979) Impairment of antigen-presenting cell function by ultraviolet radiation. *Proc. Natl. Acad. Sci. USA.* 76, 6591-5

Grether-Beck, S., Buetter, R., Krutmann, J. (1997) Ultraviolet radiation-induced expression of human genes: molecular and photobiological mechanism. *Biol. Chem.* 378, 1231-6

Grewe, M., Gyufko, K., Krutmann, J. (1995) Interleukin-10 production by cultured human keratinocytes: regulation by ultraviolet B and ultraviolet A1 radiation. *J. Invest. Dermatol.* 104, 3-6

Griffiths, H. R., Mistry, P., Herbert, K. E., Lunec, J. (1998) Molecular and cellular effects of ultraviolet light-induced genotoxicity. *Crit. Rev. Clin. Lab Sci.* 35, 189-237

Gurguerira, S. A. and Meneghini. R. (1996) An ATP-dependent iron transport system in isolated rat liver nuclei. *J. Biol. Chem. 271, 13616-20*

Guyton, K. Z. and Kensler, T. W. (1993) Oxidative mechanisms in carcinogenesis. *Br. Med. Bull.* 49, 523-544

Haile, D. J. (1999) Regulation of genes of iron metabolism by the iron–response proteins. *Am. J. Med. Sci.* 318, 230-40

Halliwell, B., Gutteridge, J. M. C. (1999*) Free radicals in biology and medicine. 3rd ed, Oxford University Press, Oxford, UK*

Hann, H. W., Stahlhut, M. W., Blumberg, B. S. (1988) Iron nutrition and tumor growth: decreased tumor growth in iron-deficient mice. *Cancer Res.* 48, 4168-70

Hanson, D. L. and deLeo, V. A. (1989) Long wave ultraviolet radiation stimulates arachidonic acid release and cyclooxgenase activity in mammalian cells in culture. *Photochem. Photobiol.* 49, 423-30

Hanson, D. L. and deLeo, V. A. (1990) Long wave ultraviolet light induces phospholipase activation in cultured human skin keratinocytes. *J. Invest. Dermatol.* 95, 158-163

Harber, F. and Weiss, J. (1934) *Proc. R. Soc. London, Ser. A.* 147, 332-351

Harrison, P. M., Arosio, P. (1996) The ferritins: molecular properties, iron storage function cellular regulation. *Biochim. Biophys. Acta.* 1275, 161-203

Hayes, J. D. and McLellan, L. I. (1999) Glutathione and glutathione-dependent enzymes represent a co-ordinary regulated defence against oxidative stress. *Free Radic. Res.* 31, 273-300

Hentze, M. W., Kuhn, L. C. (1996) Molecular control of vertebrate iron metabolism: mRNA based regulatory circuits operated by iron, nitric oxide, and oxidative stress. *Proc. Natl. Acad. Sci. USA.* 93, 8175-82

Hoerter, J., Pierce, A., Troupe, C., Epperson, J., Eisenstark, A. (1996) Role of enterobactin and intracellular iron in cell lethality during near-UV irradiation in *E. coli.* 64, 537-541

Hu, M. L. and Tappel, A. L. (1992) Potentiation of oxidative damage to proteins by UVA and protection by antioxidants. *Photochem. Photobiol.* 56, 357-363

Ito, A. and Ito, T. (1983) Visible involvement of membrane damage in the inactivation by broad-band near-UV radiation in *Saccharomyces cerevisiae* cells. *Photochem. Photobiol.* 37, 395-401

Jacobs, A. (1976) An intracellular transit iron pool. *Ciba Found Sym.* 7-9, 91-106

Jacobs, A. (1977) Low molecular weight intracellular iron transport compounds. *Blood.* 50, 433-9

Jornot, L. and Junod, A. F. (1993) Variable glutathione levels and expression of antioxidant enzymes in human endothelial cells. *Am. J. Physiol.* 264, L482-L489

Jurkiewicz, B. A. and Buettner, G. R. (1994) Ultraviolet light induced free radical formation in skin: An electron paramagnetic resonance study. *Photochem. Photobiol.* 59, 1-4

Jurkiewicz, B. A., Bissett, D. L., Buettner, G. R. (1995) Effect of topically applied tocopherol on ultraviolet radiation-mediated free radical damage in skin. *J. Invest. Dermatol.* 104, 484-458

Jurkiewicz, B. A., Buettner, G. R. (1996) EPR detection of free radicals in UV-irradiated skin: mouse versus human. *Photochem. Photobiol.* 64, 918-22

Kakhlon, O., Gruenbaum, Y. and Cabantchik, Z. I. (2001) Repression of ferritin expression increases the labile iron pool, oxidative stress, and short-term growth of human erythroleukemia cells. *Red cells.* 97, 2863-71

Kasid, U. N., Dritschilo, A., Rhim, J. S. (1987) Human epidermal keratinocytes retain radiation resistance following in vitro immortalization and malignant transformation. *Radial. Res.* 111, 567-571

Kelfkens, G., de Guijl, F. R., vander Leun, J. C. (1992) The influence of ventral UVA exposure on subsequent tumorigenesis in mice by UVA or UVB irradiation. *Carcinogenesis.* 13, 2169-74

Keyse, S. M. and Tyrrell, R. M. (1989) Heme oxygenase is the major 32-kDa stress protein induced in human skin fibroblasts by UVA radiation, hydrogen peroxide, and sodium arsenite. *Proc. Natl. Acad. Sci. USA.* 86, 99-103

Keyse, S. M. and Tyrrell, R. M. (1989a) Induction of the heme oxygenase gene in human skin fibroblasts by hydrogen peroxide and UVA (365 nm) radiation: evidence for the involvement of the hydroxyl radical. *Carcinogenesis.* 11, 787-791

Keyse, S. M., Applegate, L. A., Tromvoukis, Y., Tyrrell, R. M. (1990) Oxidant stress leads to transcriptional activation of the human heme oxygenase gene in cultured skin fibroblasts. *Mol. Cell Biol.* 10, 4967-9

Keyse, S. M. and Emslie, E. A. (1992) Oxidative stress and heat shock induce a human gene encoding a protein-tyrosine phosphatase. *Nature.* 359, 644-647

Klausner, R. D., Ronault, T. A., Harford, J. B. (1993) Regulation the fate of mRNA: The control of cellular iron metabolism. *Cell.* 72, 19-28

Konijn, A. M., Glickstein, H., Vaisman, B., Meyron-Holtz, E. G., Slotki, I. N., Cabantchik, Z. I. (1999) The cellular labile iron pool and intracellular ferritin in K562 cells. *Blood.* 94, 2128-34

Kozlov, A. V., Yegorov, D. Y., Vladimirov, Y. A., Azizova, O. A. (1992) Intracellular free iron in liver tissue and liver homogenate: studies with electric paramagnetic resonance on the formation of paramagnetic complexs with desferal and nitric oxide. *Free Radic. Biol. Med.* 13, 9-16

Kralli, A. and Moss. S. H. (1987) The sensitivity of an actinic reticuloid cell strain to near-ultraviolet radiation and its modification by trolox-C, a vitamin E analogue. *Br. J. Dermatol.* 116, 761-772

Kramer, G. F., Ames, B. N. (1987) Oxidative mechanisms of toxicity of low-intensity near-UV in Salmonella typhimurium. *J. Bacteriol* 169, 2259-66

Krinsky, N. I. and Deneke, S. M. (1982) Interaction of oxygen and oxy-radicals with carotinoids. *J. Natl. Cancer Inst.* 69(1), 205-210

Kripke, M. L. (1974) Antigenicity of murine skin tumors induced by ultraviolet light. *J. Natl. Cancer Inst.* 53, 1333-6

Kripke, M. L., Cox, P. A., Alas, L. G., Yarosh, D. B. (1992) Pyrimidine dimer in DNA initiates systemic immunosuppression in UV-irradiated mice. *Proc. Natl. Acad. Sci. USA.* 89, 7516-7520

Krutmann, J. and Grewe, M. (1995) Involvement of cytokines, DNA damage, and reactive oxygen intermediates in ultraviolet radiation-induced modulation of intercellular adhesion molecule-1 expression. *J. Invest. Dermatol.* 105, 67S-70S

Krutmann, J. (1998) Ultraviolet A radiation-induced immunomodulation: molecular and photobiological mechanism. *Eur. J. Dermatol.* 8, 200-202

Kuhn, L. C. (1994) Molecular regulation of iron proteins. *Baillieres Clin. Haematol.* 7, 763-785

Kuhn, L. C. (1998) Iron and gene expression: molecular mechanisms regulating cellular iron homeostasis. *Nutr. Rev.* 56, S11-S19

Kuhn, A., Fehsel, K, Lehmann, P., Krutmann, J., Ruzicka, T., Kolb-Bachofen, V. (1998) Aberrant timing in epidermal expression of inducible nitric oxide synthesis after UV irradiation in cutaneous lupus erythematosus. *J. Invset. Dermatol.* 111, 149-153

Kumakiri, M., Hashimoto, K., Willis, I. (1977) Biologic changes due to long-wave ultraviolet irradiation on human skin: ultrastructural study. *J. Invest. Dermatol.* 69, 392-400

Kvam, E. and Tyrrell, R. M. (1997) Induction of oxidative DNA damage in human skin cells by UV and near visible radiation. *Carcinogenesis.* 18, 2379-84

Kvam, E., Noel, A., Basu-Modak, S., Tyrrell, R. M. (1999) Cyclooxygenase dependent release of heme from microsomal hemeproteins correlates with induction of heme oxygenase 1 transcription in human fibroblasts. *Free Radic. Biol. Med.* 26, 511-7

Kvam, E., Hejmadi, V., Ryter, S., Pourzand, C., Tyrrell, R. M. (2000) Heme oxygenase activity causes transient hypersensitivity to oxidative ultraviolet A radiation that depends on release of iron from heme. *Free Radic. Biol. Med. 28, 1191-1196*

Laval, J. (1996) Role of DNA repair enzymes in the cellular resistance to oxidative stress. *Pathol. Biol.* 44, 14-24

Lautier, D., Luscher, P., Tyrrell, R. M. (1992) Endogenous glutathione levels modulate both constitutive and UVA radiation/hydrogen peroxide inducible expression of the human heme oxygenase gene. *Carcinogenesis.* 3, 227-32

Lavker, R. M., Gerberick, G. F., Veres, D., Irwin, C. J., Kaidbey, K. H. (1995a) Cumulative effects from repeated exposures to suberythemal doses of UVB and UVA in human skin. *J. Am. Acad. Dermatol.* 32, 53062

Lavker, R. M., Veres, D. A., Irwin, C. J., Kaidbey, K. H. (1995) Quantitative assessment of cumulative damage from repetitive exposures to suberythemogenic doses of UVA in human skin. *Photochem. Photobiol.* 62, 348-352

Leccia, M. T., Richard, M. J., Beani, J. C., Faure, H., Monjo, A. M., Cadet, J., Amblard, P., Favier, A. (1993) Protective effect of selenium and zinc on UVA damage in human skin fibroblasts. *Photochem. Photobiol.* 58, 548-53

Leccia, M. T., Richard, M. J., Joanny-Crisci, F., Beani, J. C. (1998) UV-A1 cytotoxicity and antioxidant defence in keratinocytes and fibroblasts. *Eur. J. Dermatol.* 8, 478-82

Leccia, M. T., Richard, M. J., Favier, A., Beani, J. C. (1999) Zinc protects against ultraviolet A1-induced DNA damage and apoptosis in cultured human fibroblasts. *Biol. Trace Elem. Res.* 69, 177-190

Levi, S., Yewdall, S. J., Harrison, P. M., Santambrogio, P., Cozzi, A., Rovida, E., Albertini, A., Arosio, P. (1992) Evidence of H- and L-chains have co-operative roles in the iron-uptake mechanism of human ferritin. *Biochem. J.* 288, 591-596

Ley, R. D., Applegate, L. A., Fry, R. J., Sanchez, A. B. (1991) Photoreactivation of ultraviolet radiation-induced skin and eye tumors of Monodelphis domestica. *Cancer Res.* 51, 6539-6542

Lieu, P. T., Heiskala, M., Peterson, P. A., Yang, Y. (2001) The roles of iron in health and disease. *Mol Aspects Med.* 22, 1-87

Lin, F. and Girotti, A. W. (1997) Elevated ferritin production, iron containment, and oxidant resistance in hemin-treated leukemia cells. *Arch. Biochem. Biophys.* 346, 131-141

Lloyd, J. B., Cable, H., Rice-Evans, C. (1991) Evidence that desferrioxamine cannot enter cells by passive diffusion. *Biochem. Pharmcol.* 14, 1361-3

Luy, H., Frenk, E., Applegate, L. A. (1994) Ultraviolet A-induced cellular membrane damage in the photosensitivity dermatitis/actinic reticuloid syndrome. *Photodermatol Photoimmunol Photomed.* 10, 126-133

Lytton, S. D., Mester, B., Libman, J., Shanzer, A., Cabantchik, Z. I. (1992) Monitoring of iron (III) removal from biological sources using a fluorescent siderphore. *Anal. Biochem.* 205, 326-33

Mathews-Roth M. M. (1982) Photosensitization by porphyrins and prevention of photosensitization by carotenoids. *J. Natl. Cancer Inst.* 69, 279-285

Mathews-Roth, M. M, Krinsky, N. I. (1987) Carotenoids affect development of UV-B induced skin cancer. *Photochem. Photobiol.* 46, 507-509

Matsui, M. S. and DeLeo, V. A. (1991) Longwave ultraviolet radiation and promotion of skin cancer. *Cancer cells.* 3, 8-12.

McCormick, J. P., Fisher, J. R., Pachlark, A., Eisenstark, A. (1976) Characterzation of a cell-lethal product from the photooxidation of tryptophan: hydrogen peroxide. *Science.* 191, 468-469

Meewes, C., Brenneisen, P., Wenk, P., Kuhr, L., Ma, W., Alikoski, J., Poswig, A., Krieg, T., Scharffetter-Kochanek, K. (2001) Adaptive antioxidant response protects dermal fibroblasts from UVA-induced phototoxicity. *Free Radical Biol. Med.* 30, 238-241

Meyron-Holtz, E. G., Vaisman, B., Cabantchik, Z. I., Fibach, E., Rouault, T. A., Hershko, C., Konijn, A. M. (1999) Regulation of intracellular iron metabolism in human erythroid precursors by internalized extracellular ferritin. *Blood.* 94, 3205-11

Mildner, M., Weninger, W., Trautinger, F., Ban, J., Tschachler, E. (1999) UVA and UVB radiation differentially regulate vascular endothelial growth factor expression in keratinocyte-derived cell lines and in human keratinocytes. *Photochem. Photobiol.* 70, 674-679

Moan, J., Dahlback, A., Setlow, R. B. (1999) Epidermiological support for a hypothesis for melanoma induction indicating a role for UVA radiation. *Photochem. Photobiol.* 70, 243-247

Molin, L. and Wester, P. O. (1973) Iron content in normal and psoriatic epidermis. *Acta Derm Venereol.* 53, 473-6

Morita, A., Grewe, M., Grether-Beck, S., Olaizola-Horn, S., Krutmann, J. (1997) Induction of proinflammatory cytokines in human epidermoid carcinoma cells by in vitro ultraviolet A1 irradiation. *Photochem. Photobiol* 65, 630-635

Morliere, P., Moysan, A., Santus, R., Huppe, G., Maziere, J. C., Dubertert, L. (1991) UVA-induced lipid peroxidation in cultured human fibroblasts. *Biochim. Biophys. Acta.* 1084, 261-268

Morliere, P., Salmon, S., Aubailly, M., Risler, A., Santus, R. (1997) Sensitization of skin fibroblasts to UVA by excess iron. *Biochim. Biophys. Acta.* 1334, 283-290

Moysan, A., Marquis, I., Gaboriau, F., Santus, R., Dubertret, L., Morliere, P. (1993) Ultraviolet A-induced lipid peroxidation and antioxidant defense systems in cultured human skin fibroblasts. *J. Invest. Dermatol.* 100, 692-698

Moysan, A., Clement-Lacroix, P., Michel, L., Dubertret, L., Morliere, P. (1996) Effect of UVA and antioxidant defense in cultured fibroblasts and keratinocytes. *Photodermatol. Photoimmunol. Photomed.* 11, 192-7

McCoubrey, W. K., Huang, T. J., Maines, M. D. (1997) Isolation and characterisation of a cDNA from the rat brain that encodes hemeprotein heme oxygenase-3. *Eur. J. Biochem.* 247, 725-732

Nappi, A. J. and Vass, E. (1998) Hydroxyl radical formation resulting from the interaction of nitric oxide and hydrogen peroxide. *Biochim. Biophys. Acta.* 380, 55-63

Niki. E (1987) Lipid antioxidants: how they may act in biological systems. *Br. J. Cancer Suppl.* 8, 153-157

Njus, D., Kelley, P. M. (1991) Vitamins C and E donate single hydrogen atoms in vivo. *FEBS Lett*; 284), 147-51

Noel. A. and Tyrrell, R. M. (1997) Development of refractoriness of induced human heme oxygenase-1 gene expression to reinduction by UVA irradiation and hemin. *Photochem. Photobiol.* 66, 456-63

Ollinger, K. and Brunk, U. T. (1995) Cellular injury induced by oxidative stress is mediated through lysosomal damage. *Free Radic. Biol. Med.* 19, 565-574

Ollinger, K. and Roberg, K. (1997) Nutrient deprivation of cultured rat hepatocytes increases the desferrioxamine-available iron pool and augments the sensitivity to hydrogen peroxide. *J. Biol. Chem.* 272, 23707-11

Ouedraogo, G., Morliere, P., Bazin, M., Santus, R., Kratzer, B., Miranda, M. A., Castell, J. V. (1999) Lysosomes are sites of fluoroquinolone photosensitization in human skin fibroblasts: a microspectrofluorometric approach. *Photochem. Photobiol.* 70, 123-9

Pantopoulos, K., Mueller, S., Atzberger, A., Ansorge, W., Stremmel, W., Hentze, M. W. (1997) Differences in the regulation of iron regulatory protein-1 (IRP-1) by extra- and intracellular oxidative stress. *J. Biol. Chem.* 272, 9802-8

Pantopoulos, K., Hentze, M. W. (1998) Activation of iron regulatory protein-1 by oxidative stress in vitro. *Proc. Natl. Acad. Sci. USA.* 95, 10559-63

Parat, M. O., Richard. M. J, Leccia, M. T., Amblard, P., Favier, A., Beani, J. C. (1995) Does manganese protect cultured human skin fibroblasts against oxidative injury by UVA, dithranol and hydrogen peroxide? *Free Radic. Res.* 23, 339-351

Parish, C. R (1999) Fluorescence dyes for lymphocyte migration and proliferation studies. *Immunology and cell Biology.* 77, 499-508

Park, K. C, Jung, H. C, Hwang, J. H., Youn, S. W, Ahn, J. S., Park, S. B., Kim, K. H., Chung, J. H., Youn, J. I. (1997) GM-CSF production by epithelial cell line: upregulation by ultraviolet A. *Photodermatol Photoimmunol Photomed.* 13, 133-8

Parkinson, E. K. and Newbold, R. F. (1980) Benzo(a) pyrene metabolism and DNZ adduct formation in serially cultivated strains of human epidermal keratinocytes. *Int. J. cancer.* 26, 289-299

Pathak, M. A., (1997) Photoprotection against harmful effects of solar UVB and UVA radiation: an update. In Lowe, N. J. Shaath, N. A., Pathak, M. A. (eds): Sunscreens development, evaluation, and regulatory aspects. *Marcel Decker, Inc., N. Y., USA,* pp, 117-137

Peak, M. J., Peak, J. G. (1990) Hydroxyl radical quenching agents protect against DNA breakage caused by both 365-nm UVA and by gamma radiation. *Photochem. Photobiol.* 51, 649-652

Peak MJ, Jones CA, Sedita BA, Dudek EJ, Spitz DR, Peak JG. (1990a) Evidence that hydrogen peroxide generated by 365-nm UVA radiation is not important in mammalian cell killing. *Ridiat. Res.* 123, 220-223.

Peak, J. G., Pilas, B., Dudek, E. J., Peak, M. J. (1991) DNA breaks caused by monochromatic 365-nm ultraviolet or hydrogen peroxide and their repair in human epithelioid and xeroderma pigmentatosum cells. *Photochem. Photobiol.* 54, 197-203

Pearse, A. D., Gaskell, S. A., Marks, R. (1987) Epidermal changes in human skin following irradiation with either UVB or UVA. *J. Invest. Dermatol.* 88, 83-87

Petrat, F., de Groot, H., Rauen, U. (2001) Subcellular distribution of chelatable iron: a laser scanning microscopic study in isolated hepatocytes and liver endothelial cells. *Biochem. J.* 356, 61-69

Picard, V., Epsztejn, S., Santambrogio, P., Cabantchik, Z. I., Beaumont, C. (1998) Role of ferritin in the control of the labile iron pool in murine erythroleukemia cells. *J. Biol. Chem.* 273, 15382-6

Picard, V., Govoni, G., Jabado, N., Gros, P. (2000) Nramp2 (DCT1/DMT1) expressed at the plasma membrane transports iron and other divalent cation into a calcein-accessible cytoplasmic pool. *J. Biol. Chem.* 275, 35735-45

Podda, M., Traber, M. G., Weber, C., Yun, L. J. and Packer, L. (1998) UV-irradiation depletes antioxidants and causes oxidative damage in a model of human skin. *Free Radic. Biol. Med.* 24, 55-65

Ponka, P., Grady, R. W., Wilczynska, A., Schulman, H. M. (1984) The effect of various chelating agents on the mobilization of iron from reticulocytes in the presence and absence of pyridoxal isonicotinoyl hydrazone. *Biochem. Biophys Acta.* 802, 477-489

Ponka, P., Beaumont, C., Richardson, D. R. (1998) Function and regulation of transferrin and ferritin. *Semin. Hematol.* 35, 35-54

Ponka, P. and Lok, C. N. (1999) The transferrin receptor: role in health and disease. *Int. J. Boichem. cell Biol.* 31, 1111-37

Ponka, P. (1999) Cellular iron metabolism. *Kidney. Int. Suppl.* 69, S2-11

Poss, K. D and Tonegawa, S. (1997) Heme oxygenase 1 is required for mammalian iron reutilization. *Proc Natl Acad Sci USA.* 94, 10919-24

Poswig, A., Wenk, J., Brenneisen, P., Wlaschek, M., Hommel, C., Quel, G., Faiss K., Dissemond, J., Briviba, K., Krieg, T., Scharffetter-Kochanek, K. (1999) Adaptive antioxidant response of manganase-superoxide dismutase following repetitive UVA irradiation. *J. Invest. Dermatol.* 112, 13-18

Pourzand, C., Watkin, R. D., Brown, J. E., Tyrrell, R. M. (1999a) Ultraviolet A radiation induces immediate release of iron in human primary skin fibroblasts: the role of ferritin. *Proc. Natl. Acad. Sci. USA.* 96, 6751-6

Pourzand, C., Reelfs, O., Kvam, E., Tyrrell, R. M (1999b) The iron regulatory protein can determine the effectiveness of 5-aminolevulinic acid in inducing protoporphyrin IX in human primary skin fibroblasts. *J. Invest. Dermatol.* 112(4), 419-25

Punnonen, K., Jansen, C. T., Puntala, A., Ahotupa, M. (1991a) Effects of in vitro UVA irradiation and PUVA treatment on membrane fatty acids and activities of antioxidant enzymes in human keratinocytes. *J. Invest. Dermatol.* 96(2), 255-9

Punnonen, K., Puntala, A., Ahotupa, M. (1991) Effcets of UVA and UVB irradiation on lipid peroxidation and activity of the antioxidant enzymes in keratinocytes in culture. *Photodermatol. Photoimmunol. Photomed.* 8(1), 3-6

Quiec, D., Mazeiere, C., Santus, R., Andre P., Redziniak, G., Chevy, F., Wolf, C., Driss, F., Dubertret, L., Maziere, J. C. (1995) Polyunsaturated fatty acid enrichment increase ultraviolet A-induced lipid peroxidation in NCTC 2544 human keratinocytes. *J. Invest. Dermatol.* 104, 964-969

Radisky, D. C. and Kaplan, J. (1998) Iron in cytosolic ferritin can be recycled through lysosomal degradation in human skin fibroblasts. *Biochem. J.* 336, 201-205

Reeve, V. E. and Tyrrell, R. M. (1999) Heme oxygenase induction mediates the photoimmunoprotection activity of UVA radiation in the mouse. *Proc. Natl. Acad. Sci.* 96, 9317-21

Reif, D. W. (1992) Ferritin: a source of iron for oxidative damage. *Free Radic. Biol. Med.* 12, 417-27

Richard, M. J., Guiraud, P., Leccia, M. T., Beani, J. C., Favier, A. (1993) Effect of zinc supplemention on resistance of cultured human skin fibroblasts toward oxidative stress. *Biol. Trace Elem. Res.* 37, 187-199

Richardson, D. R. and Ponka, P. (1997) The molecular mechanisms of the metabolism and transport of iron in normal and neoplastic cells. *Biochim. Biophys. Acta.* 1331, 1-40

Richardson, D. R. and Ponka P. (1998) Development of iron chelators to treat iron overload disease and their use as experimental tools to probe intracellular iron metabolism. *Am. J. Hematol.* 58, 299-305

Riedel, H. D., Muckenthaler, M. U., Gehrke, S. G., Mohr, I., Brennan, K., Herrmann, T., Fitscher, B. A., Hentze, M. W., Stremmel, W. (1999) HFE downregulates iron uptake from transferrin and induces iron-regulatory protein activity in stably transfected cells. *Blood.* 94, 3915-21

Riley, P. A. (1994) Free radicals in biology: oxidative stress and the effects of ionizing radiation. *Int. J. Radiat. Biol.* 65, 27-33

Roberg, K. and Ollinger, K. (1998) Oxidative stress causes relocation of the lysosomal enzyme cathepsin D with ensuring apoptosis in neonatal rat cardiomyocytes. *Am. J. Pathol.* 152, 1151-6

Rorsman, H. and Tegner, E (1988) Biochemical observations in UV-induced pigmentation. *Photodermatol.* 5, 30-38

Rothman, R. J., Serroni, A., Farber, J. (1992) Cellular pool of transient ferric iron, chelatable by desferoxamine and distinct from ferritin, that is involved in oxidative cell injury. *Mol. Pharmacol.* 42, 703-710

Runger, T. M. (1999) Role of UVA in the pathogenesis of melanoma and non-melanoma skin cancer. A short review. *Photodermatol. Photoimmunol. Photomed.* 15, 212-216

Ryter, S. W. and Tyrrell, R. M. (1998) Singlet oxygen ($^1O2$): A possible effector of eukaryotic gene expression. *Free Radic. Biol. Med.* 24, 1520-1534

Ryter, S. W., Tyrrell, R. M. (2000) The heme synthesis and degradation pathways: role in oxidant sensitivity. Heme oxygenase has both pro- and antioxidant properties. *Free Radic. Biol. Med.* 28, 289-309

Santus, R., Perdrix, L., Haigle, J., Morliere, P., Maziere, J. C., Maziere, C., Labrid. C. (1991) Daflon as a cellular antioxidant and a membrane-stabilizing agent in human fibroblasts irradiated by ultraviolet A radiation. *Photodermatol. Photoimmunol. Photomed.* 8, 200-205

Schallreuter, K. U., Wood, J. M. (1986) The role of thioredoxin reductase in the reduction of free radicals at the surface of the epidermis. *Biochem. Biophys. Res. Commun.* 136, 630-7

Schallreuter, K. U. and Wood, J. M (1989) Free radical reduction in the human epidermis. *Free Radic. Biol. Med.* 6, 519-532

Schmitz, S., Garbe, C., Jinbow, K., Wulff, A., Daniels, H., Eberle, J., Orfanos, C. E. (1995) Photodynamic action of UVA: induction of cellular hydroperoxides. *Recent Results cancer Res.* 139, 43-55

Setlow, R. B., Grist, E., Thompson, K., Woodhead, A. D. (1993) Wavelengths effective in induction of malignant melanoma. *Proc. Natl. Acad. Sci. USA.* 90, 6666-70

Setlow, R. B. (1999) Spectral regions contributing to melanoma: a personal view. *J. Investig. Dermatol Symp. Proc.* 4(1), 46-49

Shigenaga, M. K., Hagen, T. M., Ames, B. N. (1994) Oxidative damage and mitochondrial decay in ageing. *Proc. Natl. Acad. Sci. USA.* 91, 10771-8

Shibutani. S., Takeshita. M., Grollman, A. P. (1991) Insertion of specific bases during DNA synthesis past the oxidation-damage of base 8-oxodG. *Nature.* 349, 431-434

Shindo, Y., Witt, E., Packer, L. (1993) Antioxidant defense mechanism in murine epidermis and dermis and their responses to ultraviolet light. *J. Dermatol.* 100, 260-5

Shindo, Y, Witt, E., Han, D., Epstein, W., Packer, L. (1994) Enzymic and non-enzymic antioxidants in epidermis and dermis of human skin. *J. Invest. Dermatol.* 102, 122-4

Shindo. Y., Hashimoto, T. (1997) Time course of changes in antioxidant enzymes in human skin fibroblasts after UVA irradiation. *J. Dermatol. Sci.* 14, 225-322

Skoog, M. L., Ollinger, K., Skogh, M. (1997) Microfluorometry using fluorescein diacetate reflects the integrity of the plasma membrane in UVA-irradiated cultured skin cells. *Photodermatol. Photoimmunol. Photomed.* 13, 37-42

Stacey. M., Thacker, S., Taylor, A. M. (1989) Cultured skin keratinocytes from both normal individuals and basal cell naevus syndrome patients are more resistant to gamma-rays and UV light compared with cultured skin fibroblasts. *Int.J. Radiat. Biol.* 56, 45-58

Stadtman, E. R. (1990) Metal ion-catalyzed oxidation of proteins: biochemical mechanism and biological consequences. *Free Radic. Biol. Med.* 9, 315-325

Steenvoorden, D. P. and van Henegouwen, G. M. (1997) The use of antioxidants to improve photoprotection. *Photochem. Photobiol. B.* 41, 1-10

Sterenborg, H. J. and van de Leun, J. C. (1990) Tumorigenesis by a long wavelength UVA source. *Photochem. Photobiol.* 51, 324-30

Stewart, M. S., Cameron, G. S., Pence, B. C. (1996) Antioxidant nutrients protect against UVB-induced oxidative damage to DNA of mouse keratinocytes in culture. *J. Invest. Dermatol.* 106, 1086-9

Stocker, R., Yamamoto, Y., McDonagh, A. F., Glazer, A. N., Ames, B. N. (1987) Bilirubin is an antioxidant of possible physiological importance. *Science.* 235, 1043-6

Suzuki, Y., Nomura, J., Koyama, J., Horii, I. (1994) The role of proteases in stratum corneum: involvement in stratum corneum desquamation. *Arch. Dermatol. Res.* 286, 249-253

Tebbe, B., Geilen, C. C., Eberle, J., Kodelja, V., Orfanos, C. E. (1997) L-ascorbic acid inhibits UVA-induced lipid peroxidation and secretion of IL-1 alpha and IL-6 in cultured human keratinocytes in vitro. *J. Invest. Dermatol.* 108, 302-306

Tenger, E., Rorsman, H., Rosengren, E. (1983) 5-S-cysteinyldopa and pigment response to UVA light. *Acta Derm. Venereol.* 63, 21-25

Thiele, J. J., Traber, M. G., Polefka, T. G., Cross, C. E., Packer, L. (1997) Ozone-exposure depletes vitamin E and induces lipid peroxidation in murine stratum corneum. *J. Invest. Dermatol.* 108,753-7

Thiele, J. J., Traber, M. G., Podda, M., Tsang, K., Cross, C. E., Packer, L. (1997a) Ozone depelets tocopherols and tocotrienols topically applied to murine skin. *FEBS Lett.* 401,167-170

Tirache, I. and Morliere, P. (1995) Hydrogen peroxide and catalase in UVA-induced lipid peroxidation in cultured fibroblasts. *Redox Report.* 1, 105-111

Tobi, S. E., Paul, N., McMillan, T. J. (2000) Glutathione modulates the level of free radicals produced in UVA-irradiated cells. *J. Photochem. Photobiol. B.* 57, 102-112

Toyokuni, S. (1996) Iron-induced carcinogenesis: The role of redox regulation. *Free Radic. Biol. Med.* 20, 553-66

Toth, I. and Bridge, K. R. (1995) Ascorbate acid enhances ferritin mRNA translation by an IRP/aconitase switch. *J. Biol. Chem.* 270, 19540-4

Trenam, C. W., Blake, D. R., Morris, C. J. (1992a) Skin inflammation: Reactive oxygen species and the role of iron. *J. Invest. Dermatol. 99, 675-682*

Trenam, C. W., Dabbagh, A. J., Blake, D. R., Morris, C. J. (1992) The role of iron in an acute model of skin inflammation induced by reactive oxygen species. *Br. J. Dermatol.* 126(3), 250-6

Trevithick, J. R., Xiong, H., Lee, S., Shum, D. T., Sanford, S. E., karlik, S. J., Norly, C., Dailworth, G. R. (1992) Topical tocopherol acetate reduces post-UVB, sunburn-associated erythema, edema, and skin sensitivity in hairless mice. *Arch. Biochem. Biophys.* 296, 575-582

Tyrrell, R. M. (1984) Mutagenic action of monochromatic UV radiation on the solar range on human skin cells. *Mutat. Res.* 129, 103-110

Tyrrell, R. M. (1985) A common pathway to protection of bacteria against damage by solar UVA (334 nm, 365 nm) and an oxidising agent (H_2O_2). *Mutat. Res.* 145, 129-136

Tyrrell, R. M. and Pidoux, M. (1986) Endogenous glutathione protects human skin fibroblasts against the cytotoxic action of UVB, UVA and near-visible radiations. *Photochem. Photobiol.* 44, 561-4

Tyrrell, R. M. and Pidoux, M. (1986a) Quantitative differences in host cell reactivation of ultraviolet-damaged virus in human skin fibroblasts and epidermal keratinocytes cultured from the same foreskin biopsy. *Cancer Res.* 46, 2665-9

Tyrrell, R. M. and Pidoux, M. (1987) Action spectra for human skin cells: estimates of the relative cytotoxicity of the middle ultraviolet, near ultraviolet, and violet regions of sunlight on epidermal keratinocytes. *Cancer Res.* 47, 1825-9

Tyrrell, R. M. and Pidoux, M. (1988) Correlation between endogenous glutathione content and sensitivity of cultured human skin cells to radiation at defined wavelengths in the solar ultraviolet range. *Photochem. Photobiol.* 47, 405-12

Tyrrell, R. M. and Pidoux, M. (1989) Singlet oxygen involvement in the inactivation of cultured human fibroblasts by UVA (334 nm, 365 nm) and near-visible (405 nm) radiations. *Photochem. Photobiol.* 49, 407-12

Tyrrell, R. M. and Keyse, S. M. (1990) New trends in photobiology: The interaction of UVA radiation with cultured cells. *Photochem. Photobiol. B.* 4, 349-361

Tyrrell, R. M., Keyse, S. M., Moraes, E. C. (1991a) Cellular defence against UVA (320-380nm) and UVB (290-320nm) radiations. In photobiology (Edited by E. Riklis), pp.861-871. *Plenum Press, New York*

Tyrrell, R. M. (1991) UVA (320-380 nm) radiation as an oxidative stress. In: oxidative stress: oxidants and antioxidants (ed. H. Sies), pp57-83. *Academic Press, London*

Tyrrell, R. M. (1994) The molecular and cellular pathology of solar UVA radiation. *Mol. Aspects Med. (H sies, Eds)* 15(1), 1-77 Review

Vessey, D. A. and Lee, K. H. (1993) Inactivation of enzymes of the glutathione antioxidant system by treatment of cultured human keratinocytes with peroxides. *J. Invest. Dermatol.* 100, 829-833

Tyrrell, R. M. (1995) Ultraviolet radiation and free radical damage to skin. *Biochem. Soc. Symp.* 61, 47-53

Tyrrell, R. M. (1996) UV activation of mammalian stress proteins. *EXS.* 77, 255-71

Tyrrell, R. M. (1997) Approaches to define pathways of redox regulation of a eukaryotic gene: the heme oxygenase 1 example. *Methods.* 11, 313-8

Tyrrell, R. M. (1999) Redox regulation and oxidant activation of heme oxygenase-1. *Free Radic. Res.* 31, 335-340

Ullrich, S. E. (1995) Modulation of immunity by ultraviolet radiation: key effects on antigen presentation. *J. Invest. Dermatol.* 105, 30S-36S

van Weelden, H., de Grujil, F. R., van der Putte, S. C., Toonstra, J., van der Leun, J. C. (1988) The carcinogenic risk of modern tanning equipment: is UVA safer than UVB? *Arch. Dermatol. Res.* 280, 300-7

Vaisman, B., Fibach, F. and Konijn, A. (1997) Utilization of intracellular ferritin iron for hemoglobin synthesis in developing human erythroid precursors. *Blood.* 909, 831-8

Vessey, D. A., Lee, K., Bayer, T. D. (1995) Differentiation-induced enhancement of the ability of cultured human keratinocytes to suppress oxidative stress. *J. Invest. Dermatol.* 104, 355-8

Vile, G. F. and Winterbourn, C. C. (1988) Microsomal reduction of low-molecular-weight Fe^{3+}chelates and ferritin enhancement by adriamycin, paraquat, menadione, and anthraquinone 2-sulfonate and inhibition by oxygen. *Arch. Biochem. Biophys. 267, 606-613*

Vile, G. F., Tyrrell, R. M. (1993) Oxidative stress resulting from ultraviolet A irradiation of human skin fibroblasts leads to a heme oxygenase-dependent increase in ferritin. *J. Biol. Chem.* 268, 14678-81

Vile, G. F., Basu-Modak, S., Waltner, C., Tyrrell, R. M. (1994) Heme oxygenase 1 mediates an adaptive response to oxidative stress in human skin fibroblasts. *Proc. Natl. Acad. Sci. USA.* 91, 2607-10

Vile, G. F., Tyrrell, R. M. (1995) UVA radiation-induced oxidative damage to lipids and proteins in vitro and in human skin fibroblasts is dependent on iron and singlet oxygen. *Free Radic. Biol. Med.* 18, 721-730

Weaver, J. and Pollack, S. (1989) Low-Mr iron isolated from guinea pig reticulocytes as AMP-Fe and ATP-Fe complexes. *Biochem. J.* 261, 787-792

Webb, R. B. (1977) Lethal and mutagenic effects of near-UV irradiation. *Photochem. Photobiol. Rev.* 2, 169-261

Weinberg, E. D. (1996) The role of iron in cancer. *Eur. J. Cancer Prev.* 5, 19-36

White, G. P., Bailey-Wood, R., Jacobs, A. (1976) The effect of chelating agents on cellular iron metabolism. *Clin. Sci. Mol. Med.* 50, 145-152

White, G. P. and Jacob, A. (1978) Iron uptake by Chang cells from transferrin, nitriloacetate and citrate complex: the effect of iron-loading and chelation with desferrioxamine. *Biochim. Biophys Acta.* 543, 217-225

Yohn, J. J., Norris, D. A., Yrastorza, D. G., Buno, L. J., Leff, J. A., Hake, S. S., Repine, J. E. (1991) Disparate antioxidant enzyme activities in cultured human cutaneous fibroblasts, keratinocytes, and melanocytes. *J. Invest. Dermatol.* 97, 405-9

Yarosh, D., Alas, L. G., Yee, V., Oberyszyn, A., Kibitel, J.T., Mitchell, D., Rosenstein R., Spinowitz, A., and Citron, M. (1992) Pyrimidine dimer removal enhanced by DNA repair lipsosomes reduces the incidence of UV skin cancer in mice. *Cancer Res.* 52, 4227-31

Yarosh, D., Zhang, X., Rosenstein, B. S., Wang, Y., Lebwohl, M., Mitchell, D. M., Wei, H. (1997) Induction of 8-oxo-7,8-dioxyguanosine by ultraviolet radiation in calf thymus DNA and Hela cells. *Photochem. Photobiol.* 65, 119-124

Yasui, H. and Sakurai, H. (2000) Chemiluminescent detection and imaging of reactive oxygen species in live mouse skin exposed to UVA. *Biochem. Biophys Res. Commun.* 269, 131-136

Zanninelli, G., Glickstein, H., Breuer, W., Milgram, P., Brissot, P., Hider, R. C., Konijn, A. M., Libman, J., Shanzer, A. and Cabantchik. (1997) Chelation and mobilization of cellular iron by different classes of chelators. *Mol. Pharmacol.* 51, 842-852

Zdolsek, J., Zhong, H., Roberg, K., Brunk, U. (1993) H_2O_2-mediated damage to lysosomal membrane of J-774 cells. *Free Radic. Res. Commun.* 18, 71-85

Ziboh, V. A., Chapkin, R. S (1988) Metabolism and function of skin lipids. *Prog Lipid Res.* 27, 81-105

Ziegler, A., Leffell, D. J., Kunala, S., Sharma, H. W., Gailani, M., Simon, J. A., Halperin, A. J., Baden, H. P., Shapiro, P. E., Bale, A. E. (1993) Mutation hotspots due to sunlight in the p53 gene of nonmelanoma skin cancers. *Proc. Natl. Acad. Sci. USA.* 90, 4216-20